EDITORIAL STAFF

Cecil V. King, Editor
Norman Hackerman, Technical Editor
Ruth G. Sterns, Managing Editor
U. B. Thomas, News Editor
Natalie Michalski, Assistant Editor
Eleanor Blair, Assistant Editor

DIVISIONAL EDITORS

W. C. Vosburgh, Battery
J. E. Draley, Corrosion
John J. Chessman, Electric Insulation
Abner Brenner, Electrodeposition
H. C. Froelich, Electronics
D. H. Baird, Electronics—Semiconductors
Sherlock Swann, Jr., Electro-Organic
John M. Blocher, Jr., Electrothermics and Metallurgy, I
A. U. Seybolt, Electrothermics and Metallurgy, II
W. C. Gardiner, Industrial Electrolytic
C. W. Tobias, Theoretical Electrochemistry

REGIONAL EDITORS

Howard T. Francis, Chicago
Joseph Schulein, Pacific Northwest
J. C. Schumacher, Los Angeles
G. W. Heise, Cleveland
G. H. Fetterley, Niagara Falls
Oliver Osborn, Houston
Earl A. Gulbransen, Pittsburgh
A. C. Holm, Canada
J. W. Cuthbertson, Great Britain
T. L. Rama Char, India

ADVERTISING OFFICE

Jack Bain, Advertising Manager
545 Fifth Avenue, New York 17, N. Y.

ECS OFFICERS

Hans Thurnauer, President
Minnesota Mining & Mfg. Co., St. Paul, Minn.

Norman Hackerman, Vice-President
University of Texas, Austin, Texas

Sherlock Swann, Jr., Vice-President
University of Illinois, Urbana, Ill.

W. C. Gardiner, Vice-President
Olin Mathieson Chemical Corp., Niagara Falls, N. Y.

Lyle I. Gilbertson, Treasurer
Air Reduction Co., Murray Hill, N. J.

Henry B. Linford, Secretary
Columbia University, New York, N. Y.

Journal of the

Electrochemical Society

APRIL 1957 **VOL. 104 • NO. 4**

CONTENTS

Editorial

Mad Scramble for Graduates 89C

Technical Papers

The Gassing of Dry Cells. *E. M. Otto and W. G. Eicke, Jr.* 199

Lead Storage Battery Oxides with Metallic Additions. *B. Agruss, E. H. Herrmann, and F. B. Finan* 204

A Reproducible and Stable Silver-Silver Oxide Electrode. *W. J. Hamer and D. N. Craig* 206

Effect of Ultraviolet Irradiation on the Growth of Anodic Ta_2O_5 Films. *D. A. Vermilyea* 212

Oxidation of 50 Weight Per Cent Uranium-Zirconium Alloy. *S. Barnartt, R. G. Charles, and E. A. Gulbransen* 218

Silicon Diffused Junction "Avalanche" Diodes. *H. S. Veloric and K. D. Smith* 222

Electroless Nickel Plating for Making Ohmic Contacts to Silicon. *M. V. Sullivan and J. H. Eigler* 226

Anodic Formation of Oxide Films on Silicon. *P. F. Schmidt and W. Michel* 230

Semiconducting Properties of Some Vanadate Glasses. *P. L. Baynton, H. Rawson, and J. E. Stanworth* 237

Zone Melting of Uranium. *C. I. Whitman, V. Compton, and R. B. Holden* 240

The Kinetics and Mechanism of Formation of Anode Films on Single-Crystal InSb. *J. F. Dewald* 244

Density and Electrical Conductance in the System KCl-$ZnCl_2$. *F. R. Duke and R. A. Fleming* 251

Technical Feature

The Potential of an Electrode of a Voltaic Cell; A New Definition with Justification for the Use of Two Sign Conventions. *J. B. Ramsey* 255

Current Affairs

Hackerman and Schaefer to Take Office in Washington 92C
Plans Now Complete for Washington Meeting 92C
Highlights of the Board of Directors' Meeting 93C
Gordon Research Conferences 95C

Division News 96C
Section News 97C
New Members 99C
Personals 100C
News Items 101C
Book Review 104C
Announcements from Publishers 104C
Meetings of Other Organizations 104C

Published monthly by The Electrochemical Society, Inc., Manchester, N. H., combining the JOURNAL and TRANSACTIONS OF THE ELECTROCHEMICAL SOCIETY. Editorial offices: 216 West 102nd Street, New York 25, N. Y. Statements and opinions given in articles and papers in the JOURNAL OF THE ELECTROCHEMICAL SOCIETY are those of the contributors, and The Electrochemical Society assumes no responsibility for them. Nondeductible subscription to members $5:00; subscription to nonmembers $18.00. Single copies $1.25 to members, $1.75 to nonmembers.

Copyright 1957 by The Electrochemical Society, Inc.

Entered as second-class matter at the Post Office at Manchester, N. H., under the act of August 24, 1912.

SARGENT POLAROGRAPH

Trademark Reg. U.S. Pat. Off.

MODEL XXI Visible Chart Recording

Indispensable Chemical Facility

Many Uses . . . Many Users

In 1937, eleven Polarographs were known to be located in the United States. Today there are many hundreds of Sargent Polarographs in use—employed for a wide variety of purposes.

From Australia to Sweden, and all over America, Sargent Polarographs are constantly at work for the progress of science.

Dozens of users have more than one Sargent Polarograph working for them. One industrial firm alone has already obtained sixteen.

Of the hundred universities, colleges and research institutes employing Sargent Polarographs, one operates seven and over twenty universities use two or more. The United States Government has already placed more than forty in service.

The Sargent Polarograph's uses are varied and many . . . . . .

1. For the routine analysis of non-ferrous alloys and ores when determining minor constituents including copper, lead, cadmium, zinc, manganese, iron and cobalt.
2. For the routine determination of lead, copper, nickel, manganese and cobalt in ferrous alloys.
3. For the analytical control of plating baths, notably in the field of precious metals.
4. For trace metal measurements in food products, in body fluids and in petroleum products.
5. For the analysis of source materials and processed products for a variety of hormones and vitamins.
6. For the identification and estimation of numerous substances of nutritional and biological regulatory function, supporting or replacing biological assay..
7. For the determination of halides and sulfate groups by titration with a polarized electrode.
8. For the analytical measurement of innumerable organic compounds containing reducible groups.
9. For specific industrial controls such as the estimation of aldehydes in alcoholic products, the quantitative differentiation of sugars and the control of aging quality in sugars.
10. For the measurement of dissolved oxygen, oxygen demand and metal ions in water and sewage.
11. For many uncommon analyses for which classical procedures are unavailable, less accurate and slower.
12. For the investigation and control of commercial reduction processes.
13. For thermodynamic investigations relating to states of ionic aggregations, mobilities and diffusion rates, solubilities, reaction rates and equilibrium constants.

For a complete description of the Sargent Polarograph Model XXI, write today.

S-29303 POLAROGRAPH—Model XXI Visible Chart Recording, Sargent. For operation from 115 Volt 50/60 cycle circuits.....**$2275.00**

SARGENT

SCIENTIFIC LABORATORY INSTRUMENTS • APPARATUS • SUPPLIES • CHEMICALS

Catalog No. 100 Now Available

E. H. SARGENT & COMPANY, 4647 W. FOSTER AVE., CHICAGO 30, ILLINOIS
MICHIGAN DIVISION, 8560 WEST CHICAGO AVENUE, DETROIT 4, MICHIGAN
SOUTHWESTERN DIVISION, 5915 PEELER STREET, DALLAS 35, TEXAS
SOUTHEASTERN DIVISION, 3125 SEVENTH AVE., N., BIRMINGHAM 4, ALA.

Editorial

Mad Scramble for Graduates

SINCE last September the mad scramble has been under way to interview, entice, and hire the coming crop of engineering and science degree candidates. One company after another is building a new plant and laboratory; needs 50, 100, 200 new technicians, engineers, chemists, physicists, metallurgists "immediately." Even students who will not finish (or Commence) before February 1958 have been cheerfully interviewed, cordially invited to come and visit with expenses paid. Open House for less advanced students, with inspection trips, lunch, and dinner "with members of our staff," is intended to pave the way for future years.

Most of the companies concerned hesitate to outbid each other openly with respect to starting salaries, realizing that there are not enough beginners to go around. Nevertheless, the salary scale has been "telescoped" a great deal compared to past years. In a report on unionization among engineers released last December, the National Industrial Conference Board, Inc., pointed out that in 1929 the median salary of engineers with ten years of experience was about three times the starting salary. By 1954 this ratio was less than two to one, and appears to be falling still. This levelling of the salary scale is cited as one cause of dissatisfaction and of lack of good will between management and professional employees.

To many companies the problem has then become, how can we, without upsetting the salary scale further, impress these young upstarts, and get them on the payroll? Fringe benefits, excellent working and living conditions, insurance, health, and retirement schemes are emphasized. The "young upstart" is royally entertained, housed in the best hotel, given an extra travel allowance, even offered a "starting salary" during his last few months of school.

Fortunately, nearly all of these "young upstarts" are very sensible young men. Naturally they are pleased and flattered by the attention they receive. At the same time, they have certain uncomfortable thoughts: just how long will this last, is industrial employment really like this, what will I be expected to produce on the job, what will my salary be ten years from now? Most young scientists, we believe, would prefer definite assurance of reward for faithful work and a good living standard in the future, to an extra thousand now and some vagueness about the future.

Part of the starting salary dilemma has been ascribed to certain "cost-plus defense contractors," who in some cases may be willing to spend as much as the government agents can be induced to allow in building up engineering and research staffs, regardless of economy or efficiency. This has been the subject of a Congressional Subcommittee investigation. Certainly the defense agencies should watch very carefully the use to which their funds are put. The Nation can afford a great deal of money for effective defense measures, but it cannot afford wasteful expenditures or inefficient use of its limited scientific manpower.

We are in an era of "exploding scientific industry," and the shortage of well-trained technicians and researchers will persist for a long time if the national economy continues to expand. Current efforts of considerable magnitude are directed toward training a generation of science-minded young people, and to assist the best ones through school. It has been suggested that the shortage problem would solve itself in a few years if salaries for all scientific work, including teaching, were suddenly doubled. It is true that good income is the greatest single inducement in any field of employment. To be attractive, professional salaries should not be too far behind professional nonsalaried incomes in comparable fields, and should maintain a favorable relation to the income of wage-earners. If the beginner in science is worth what he is being offered today, he must be entering a field where merit should be well recognized financially as well as in other ways.

—CVK

Choose from 4 grades of high purity magnesium

Now in volume—pig and ingot for production of titanium, uranium, zirconium, beryllium

Now—even purer grades of Dow magnesium are available in quantity lots to supplement Dow high purity (99.8%) magnesium. Magnesium pig and ingot of 99.9% purity and above are currently being produced in four different grades:

Grade mg 2, low manganese—(maximum .01% Mn)
Grade mg 3, low aluminum—(maximum .004% Al)
Grade mg 4, extra-low aluminum—(maximum .002% Al)
Grade mg 5, low iron—(maximum .003% Fe)

These specialized grades of high purity magnesium were developed for use in the manufacture of priority defense metals. They can be used in the reduction of titanium, uranium, zirconium and beryllium halides. Further information and data on maximum allowable impurities for the four grades are available on request. Contact the nearest Dow sales office or write THE DOW CHEMICAL COMPANY, Midland, Michigan, Department MA1437QQ.

YOU CAN DEPEND ON DOW

The Gassing of Dry Cells

Earl M. Otto and Woodward G. Eicke, Jr.

National Bureau of Standards, Washington, D. C.

ABSTRACT

A satisfactory method and suitable apparatus for determining the rate of gassing of dry cells are described. Gassing rates for undischarged D-size cells were found to range between 0.02 ml/day as the minimum at +21°C and 8 ml/day as the maximum at +55°C. Rates were independent of the age of the cells. Initial capacity of dry cells is not a function of gassing rate. Retention of capacity also is not a function of gassing rate, but is a function of the total volume of gas evolved before cell discharge.

Although considerable work has been done to prevent gas evolution from the Leclanché type of dry cell, little has been published on the measurement of the actual rate of gassing. Hamer and associates (1) investigated gassing at +130°F while studying packaging methods for cells and batteries for high temperature storage, and Boyer (2) measured gas evolution while studying methods of preventing explosions in closed battery containers. There are references (3, 4) to the study of gas evolution from Zn strips immersed in dry-cell electrolytes, but the paste wall, the bobbin or method of construction of the dry cell might well affect the corrosion of Zn in dry cells. Therefore, it was deemed advisable to develop an accurate method for measuring the gassing rate of completely assembled dry cells.

The chemical reaction which is responsible for the production of useful current does not include the formation of gaseous end products except when the cell is on heavy discharge and ammonia is produced. Likewise, the consumption of oxygen does not enter into the main cell action. The production of H_2 has been accounted for by a reaction of the anodic material resulting in the self-discharge of the dry cell (5)

$$Zn + 2NH_4Cl \rightarrow ZnCl_2 \cdot 2NH_3 + H_2$$

Oxygen may be consumed in the reaction (1)

$$\tfrac{1}{2} O_2 + Zn + H_2O \rightarrow Zn(OH)_2$$

Jennings and Vosburgh (6) have offered an explanation of one self-discharge process by proposing the mechanism of oxygen be liberated from the MnO_2 and deposited on C, with subsequent desorption of the oxygen and reaction with Zn.

Since dry-cell reactions involving evolution of H_2 and the consumption of atmospheric oxygen promote self-discharge of the dry cell, it is assumed that cells with less tendency to evolve or to consume gas should have longer shelf life. Hence, the gas study method should be a useful tool for evaluating dry cells. More specifically, a comparison of gassing rates of cells of different ages or states of discharge might afford a nondestructive way of evaluating these cells and estimating the remaining life in cells which have been in storage or partly discharged. The present investigation is directed toward the measurement of gases evolved under different conditions and the determination of the composition of representative gas samples.

Two methods of measuring the amount of gas evolved by the dry cell were considered, one involving a determination of the change in pressure of the constant volume of the atmosphere confining the cell, and the other involving a determination of the change in volume at a constant pressure. The latter method was finally adopted as the one having the lesser difficulties. Under the conditions of the experiment, gas evolved into a fixed volume, but measurement was accomplished by reducing the pressure to its original value.

Experimental

A sketch of the apparatus is given in Fig. 1. The gasometer consists of four main parts: cell container [5], Hg reservoir [6], manometer [4], and the reference reservoir [11]. In operation the reser-

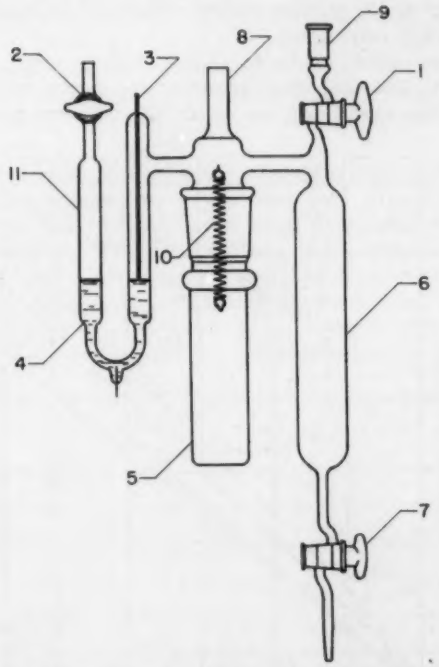

Fig. 1. Diagrammatic sketch of gasometer. Principal parts are cell container [5], Hg reservoir [6], the manometer [4], and reference reservoir [11].

voir [6] is nearly filled with Hg and Hg is injected by hypodermic syringe into the manometer at stopcock [2] until it just touches the Pt-tipped W lead-in wire [3]. The cell being studied is placed in the cell cup [5], which is held to the gasometer proper by means of springs. All ground-glass joints are lubricated and sealed with Apiezon T grease. When an atmosphere other than air is used, a vacuum pump is attached to positions [2] and [9] and, after evacuation, the desired gas is admitted. (In preliminary work, air was used, but for the most part an inert atmosphere of N has been used.) The gasometer is then brought to thermal equilibrium at a selected temperature in an oven.

In order to have a reference volume of gas at known pressure, stopcock [2] is opened. If the Hg in the right arm of the manometer is far below the Pt tip, gas is allowed to escape at [9] until the gap is less than ¼ in. If the Hg is already touching the Pt, more gas is added at [1] or Hg at [7]. After thermal equilibrium is re-established, Hg is removed at [7] until electrical contact is just established between the Pt tip and the Hg of the manometer. This is observed by means of a neon bulb in series with a source of current and the two lead-in wires. As soon as this balance is established, stopcock [2] is closed, thereby trapping a reference quantity of gas at the constant temperature of the oven and at the barometric pressure prevailing at the time of the closure. The gasometer is allowed to stand at the constant temperature until the Pt tip and Hg are separated by about ¼ in. Hg is withdrawn at [7] until electrical contact is re-established. In most cases this contact-making is sensitive to as little change in pressure as 0.01 ml of Hg. From the weight of Hg withdrawn the volume of evolved gas is readily calculated.

Runs were made at +21°, +35°, +45°, and +55°C because these temperatures were used in shelf-life studies of dry cells. The cell cup used at the two lower temperatures was long enough to accommodate two cells.

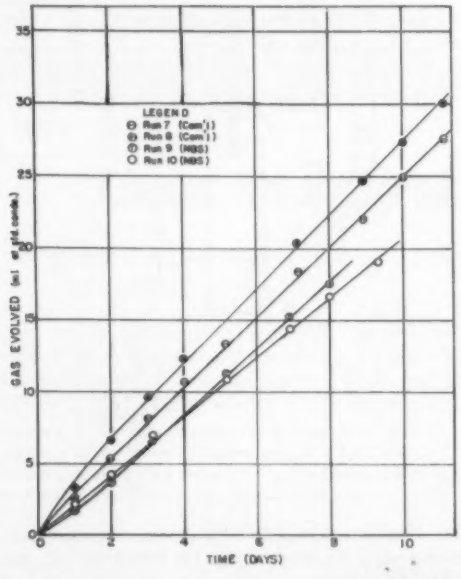

Fig. 2. Evolution of gas from four dry cells stored in an atmosphere of N at +45°C.

Table I. Composition of gas at completion of run*

Component	Oxygen atmosphere	Nitrogen atmosphere
	mole %	mole %
H_2	44	45.5
O_2	14	0.04
CO_2	39	12.1
A	0.17	0.01
N_2	2.0	42
CO	0.6	0.2
Net vol. gas produced	47.9 ml	59.9 ml

* Both runs were made at +55°C for 8.9 days before the gas samples were taken. Analysis by mass spectrometry.

Results

Fig. 2 shows typical gassing curves. Straight lines are obtained after the first day, when an inert gas, such as N_2, is the surrounding atmosphere. With air a straight line is not obtained in less than about 15 days. When the oxygen of the air within the gasometer has been exhausted, the volume increases at a constant rate.

Analysis of the residual gases after a run in oxygen and one in N_2 are shown in Table I. Approximately equal volumes of H_2 and high percentages of CO_2 were obtained regardless of the atmosphere initially surrounding the cells. Based on earlier investigations that MnO_2 oxidizes cornstarch (7) and that dry cells evolve CO_2 (1) the following calculations were made from data on the gasometer which initially contained pure oxygen.

	ml
Volume of O_2 initially in gasometer	40
Volume of gas in gasometer after 8.9 days	87.9
Oxygen content of final volume	12.3
Hence oxygen consumed by cell	27.7
Volume of CO_2 produced by MnO_2 on paste*	12.1
Volume of CO produced by MnO_2 on paste*	0.2
Volume of CO_2 assumed produced by oxygen gas	22.2
Volume of CO assumed produced by oxygen gas	0.4
Volume of O_2 required to produce CO_2 and CO	22.4
Oxygen unaccounted for†	5.3

* This figure is taken from results of run in N_2 atmosphere. It is assumed that MnO_2 acts the same in O_2 as in N_2.
† This oxygen probably may be accounted for in accord with Ref. (1).

Fig. 3 shows the gassing rates of four commercial brands of dry cells at different temperatures. These show the large temperature effect on gassing rates of dry cells.

Fig. 4 gives a plot of performance on the BA-30 test[1] against the calculated volume of gas evolved prior to the discharge. (For convenience the square root of the volume was used as the abscissa.) In each case the loss in performance is less for a given volume of gas liberated at higher temperatures than at lower. Of course, a much longer time is required at low temperatures to evolve the same volume of gas. Also the slopes steepen, and after the cells lose a certain capacity, independent of temperature but

[1] This test, specification MIL-B-18, consists in discharging a cell through 6.67 ohms resistance 4 min/half hour, 10 hr/day, 5 days/week. Results are given as the number of minutes on discharge to an end voltage of 0.93 v.

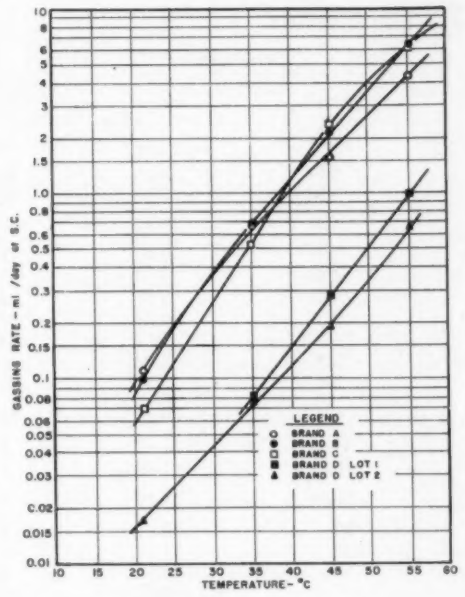

Fig. 3. Effect of temperature on the gassing rates of several brands of dry cells.

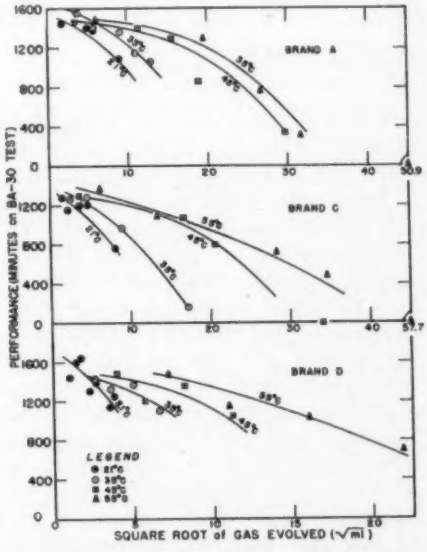

Fig. 4. Effect of gassing during storage at different temperatures on subsequent performance on the BA-30 test.

dependent on type, deterioration progresses at a more rapid rate. Hence, gas producing reactions are not solely responsible for lowering the cell capacity.

Cells on Closed Circuit

Some of the cell cups were modified so that lead wires could pass from the cell in the gasometer to a resistor outside the cell cup. Thus it was possible to determine the gassing rate of a cell on open circuit and then during discharge of the cell. Since five or more days are required to insure that a steady gassing rate has been obtained and since an intermittent type of cell action is not desired, an 83 1/3-ohm continuous discharge test was selected. (This is the BA-8 test adapted to a single cell basis.) On this test two weeks of service were expected, to the end voltage of 1.133 v. To secure appreciable gassing during this period of discharge the temperature was maintained at +55°C.

The predischarge gassing rates on the three cells were determined in five days as described above. Without disturbing the gasometers or the oven, the circuits were closed and the gassing rate determinations continued. Within 0.3 day the first measurements were made, and the gassing rates were found to be less than the predischarge rates; they continued to be less until the voltage of the cell reached about 0.5 v, which is considerably below the usual end voltage, 1.133 v, of the BA-8 test. From 0.5 v to about 0.1 v the gassing rate exceeded the predischarge rate by about 50% (see Fig. 5). Below 0.1 v the gassing rate became much less than the predischarge rate, and it continued at that rate (0.4 ml/day) until the test was stopped on the 173rd day of discharge. Fig. 5 presents graphically the results obtained on one of the three cells, the predischarge gassing rate for this particular cell being 3.5 ml/day at 55°C, which is below the average value found at 55°C.

The curve for gassing during discharge shown in Fig. 5 has three distinct parts: (*a*) that prior to the usual end voltage and down to 0.5 v covering about 23 days, (*b*) that at closed circuit voltages between 0.5 and 0.1 v extending for the next 17 days, and (*c*) that at extremely low voltages or below 0.1 v. The rates found in (*a*) are lower than predischarge rates because the Zn is being used in electrochemical rather than in corrosion reactions. The rates found in (*b*) are higher than predischarge rates probably because the partially reduced MnO_2 is being polarized to the extent that H_2 can readily be discharged from the cathode. The rates found in (*c*) are less than predischarge rates probably because the surface of the Zn is largely covered with corrosion products.

Due to the long duration of this experiment and the limited volume of the reservoir (6), the gas evolved had to be released three times and the Hg replenished. While the gas was being removed the third time, a gas sample was taken from each gasometer for analysis. The analyses showed the gas to

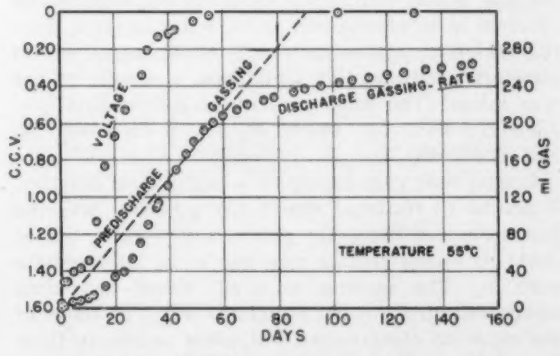

Fig. 5. Effect of 83-1/3-ohm continuous discharge on gassing of cell. Gassing rate is obtained by determining the slope at any desired point on the curve.

Table II. Rates of gassing of intimate mixtures of various thickening agents and MnO_2 in electrolyte*

Temperature	Thickening agent		Kind of MnO_2	Rate of gassing		Length of period
	Kind	Wt		Initial	Avg over period	
°C		g		ml/day	ml/day	days
+45	Wheat flour	1	African	2.68	2.30	13
+45	Cornstarch	2	African	3.97	3.54	13
+45	Wheat flour Cornstarch	1 2	African	3.97	3.12	13
+45	Vulca-60	2	African	2.31	1.82	8
+45	Potato starch	2	African	3.46	2.00	17
+45	Locust bean gum	2	African	4.45	2.91	8
+55	Wheat flour	1	African	4.17	3.34	20
+55	Cornstarch	2	African	4.76	3.57	20
+55	Vulca-60	2	African	5.3	3.28	20
+55	Locust bean gum	2	African	7.7	3.34	20
+55	Wheat flour Cornstarch	1 2	African	6.9	5.3	11
+45	Wheat flour	1	Electrolytic	34.4†	28.6†	2
+45	Cornstarch	2	Electrolytic	45.8†	41.8†	2
+45	Wheat flour Cornstarch	1 2	Electrolytic	39.8†	34.3†	2
+45	Cornstarch	1	Electrolytic	83	52	1.2
+45	Cornstarch	2	Electrolytic	130	91	0.8
+45	Cornstarch	4	Electrolytic	153	132	0.4
+45	Methocel	2	Electrolytic	—	0.61	38
+45	Amylose	2	Electrolytic	97	—	0.3
+45	Amylopectin	2	Electrolytic	83	—	0.3
+55	Separator paper (Coated)	0.48	Electrolytic	0.71	0.51	30

* See footnote to Table III for composition of electrolyte. The weight of MnO_2 used each time was 32 g.
† These values are only relative since the rate was so high and assembled gasometers had been stored over night.

be about 90% H_2 and the balance N_2 with its normal trace of A. Thus it seems that CO and CO_2, if produced at all during discharge, were evolved only in the early stage and then completely flushed out. Further experimental work would be required to furnish evidence as to whether or not oxides of carbon are formed during discharge of a cell.

Cell Components

Gassing studies conducted on dry-cell components (excluding Zn) yielded interesting results. Various thickening agents intimately mixed with MnO_2 and electrolyte were gelatinized in the cup of the gasometer and gassing rates determined at +55° and +45°C. The data are shown in Table II. One sample of gas was analyzed, the gas having resulted from the digestion at +45°C of a mixture of natural African MnO_2, ordinary cornstarch and electrolytic solution in an atmosphere of N_2. After 34 days, during which time the equivalent of 65 ml of gas at standard conditions was produced, a sample of gas was taken. The mole-percentage composition was 1.2% H_2, 3.0% CO, 48.3% N_2, 0.03% O_2, 0.04% A, and 47.4% CO_2.

Locust bean gum appeared to be the most reactive. Vulca 60 (a National Starch Co. product) was the least active of the grain products at +45°C, but at +55° its initial gassing rate was in an intermediate position. The gassing rates of wheat flour-corn starch mixtures do not equal the sums of those of the separate components, but come nearer to their averages. It is quite likely that the MnO_2 is the limiting factor. It was observed that increasing the quantity of corn starch from 1 to 2 and 4 g caused an increase in the gassing rate, but not in proportion to the quantity of starch. Amylose would seem to be more active than amylopectin, but the difference is small. Hence, little would be gained by separating cornstarch into its two components. The ratio of gassing rates obtained on cornstarch with natural African and electrolytic manganese dioxides is about 1-25. At +21°C and lower this would not be of much consequence, but it is evident that cells produced for storage and use at high temperature should not contain starch and such an active MnO_2.

Methocellulose and battery paper are included in Table II because they may be used as separator materials. The gassing rates are about equal, and less than 1% of the rates for starch. In both of these materials glucopyranose units are joined by beta-glucosidic linkages. Starches, however, have alpha glucosidic linkages. Since methyl substitutions in cellulose and starch have little effect, if any, on the gassing rates, it would appear that the two linkages must account for the difference in performance.

Data obtained on the use of bobbins of depolarizer imbedded in paste are given in Table III. Table IV presents data on mixtures which have been assumed to be inactive. It was expected that some would serve as blanks in gassing rate determinations. It is noteworthy that oxygen gas did not oxidize flour or starch when wet with NH_4Cl and $ZnCl_2$ solution, and maintained at +55°C. Natural African MnO_2 apparently oxidized acetylene black, but at a low rate. This rate of 0.43 ml/day was steady over a period of 24 days, during which time ten gassing-rate determinations were made. (The resulting gas was not analyzed, but it was assumed to be CO_2.)

Table III. Rates of gassing of D-size bobbins imbedded in paste*

Temp	Thickening agent: Kind	Thickening agent: Wt	Kind of MnO_2	Rate of gassing: Initial	Rate of gassing: Avg over period	Length of period
°C		g		ml/day	ml/day	days
+45	Wheat flour Cornstarch	1 2	African	1.6	1.6	3.5
+45	Wheat flour Cornstarch	1 2	Electrolytic	9.3	10.2	4.8
+55	Wheat flour Cornstarch	1 2	Electrolytic	42	33	3.7

* The wet mix for the bobbins was made by adding sufficient electrolyte to a mixture of 78.1% African MnO_2, 9.8% acetylene black, and 21.1% NH_4Cl. The electrolyte was composed of 24.4% NH_4Cl, 14.6% $ZnCl_2$, and 61.0% H_2O. The composition of the paste was 22.7% $NHCl_2$, 6.1% $ZnCl_2$, 7.2% wheat flour, 14.4% cornstarch, and 49.6% H_2O.

Table IV. Rates of gassing of supposedly inert mixtures of dry cell components

Temp	Atmosphere	Components of mixture*	Rate of gassing
°C			ml/day
+55	N_2	African MnO_2, electrolyte	0.00
+55	N_2	Acetylene black, water	0.00
+55	N_2	African MnO_2, acetylene black, water	0.43
+55	O_2	Wheat flour, cornstarch, electrolyte	0.00

* The quantity of MnO_2 was 32 g and that of acetylene black was 3.9 g. The composition of the electrolyte is given as a footnote to Table III.

Conclusions

A precise method has been developed for determining the rate of gassing of dry cells. Rates of gassing are greatly affected by temperature, approximately logarithmically. The initial rates of gassing in D-size cells are about 0.1, 0.6, 2.0, and 6.0 ml/day for +21°, +35°, +45°, and +55°C, respectively.

No correlation exists between the rate of gassing and the initial capacity on a BA-30 test. It can be concluded that, prior to discharge on the BA-30 test, evolution of a certain volume of gas during storage of a cell at a high temperature is less detrimental than at a low temperature. However, the time required to produce a given volume at higher temperatures is far less than at lower temperatures. For each temperature and each type of dry cell it is indicated that there is a critical volume of gas a cell may evolve before there is substantial loss in capacity. Once the critical volume has been evolved the cell deteriorates more rapidly. Cells which have lowest gassing rates appear to have best capacity after storage at high temperatures. It appears that, for each brand of a given cell type, a relation exists between the volume of gas evolved during storage at a given temperature and the loss in capacity.

In the early stage of the discharge of a cell gassing continues at a reduced rate. The rate is not constant, but shows trends similar to that shown by the decrease in closed-circuit voltage. Gassing continues long after the cell has no useful life.

Gassing studies conducted with dry cell components have shown that cereal products are definitely oxidized by MnO_2, electrolytic MnO_2 being a much stronger oxidizing agent than natural African MnO_2. Cellulose products such as paper and Methocel are relatively inactive to MnO_2.

Acknowledgments

The authors express their thanks to the Department of the Navy, Bureau of Ships, for granting permission to publish this material. They are indebted to Dr. Walter J. Hamer, who has had such a keen interest in the project and under whose direction the experimental work was performed. Dr. Wm. J. Youden, of the Applied Mathematics Division of the National Bureau of Standards, graciously assisted the authors in the analysis of data and in preparation of graphs.

Manuscript received July 25, 1956. This paper was prepared for delivery before the Boston Meeting, Oct. 3-7, 1954.

Any discussion of this paper will appear in a Discussion Section to be published in the December 1957 issue of the JOURNAL.

REFERENCES

1. W. J. Hamer, J. P. Schrodt, and G. W. Vinal, *Trans. Electrochem. Soc.*, **90**, 449 (1946).
2. M. H. Boyer, Naval Research Laboratory Report P-2315 (1944).
3. C. Drucker, *Z. Elektrochem.*, **29**, 412 (1923).
4. C. K. Morehouse, W. J. Hamer and G. W. Vinal, *J. Research Nat Bur. Standards*, **40**, 151 (1948), RP 1863.
5. N. C. Cahoon, *Trans. Electrochem. Soc.*, **92**, 159 (1947).
6. C. W. Jennings and W. C. Vosburgh, *This Journal*, **99**, 309 (1952).
7. E. M. Otto, C. K. Morehouse, and G. W. Vinal, *Trans. Electrochem. Soc.*, **90**, 419 (1946); unpublished work of E. M. Otto, E. H. Ostrander, and W. G. Eicke, Jr.

Lead Storage Battery Oxides with Metallic Additions

B. Agruss, E. H. Herrmann, and F. B. Finan

Research Laboratories, National Lead Company, Brooklyn, New York

ABSTRACT

Oxides were produced from lead containing various added metals. The concentrations more than covered the range of impurities ordinarily present in primary lead used in manufacturing battery oxides. The influence of these metals, both singly and combined, on battery performance has been studied. Battery capacity and life are unaffected by any of the added metals. Shelf life is unaffected by Bi, Ag, and Cu and is shortened by Ni, Sb, and Te. With the exception of Bi, each of these elements depressed the initial end-of-charge voltage, Te being particularly effective. The effect on end-of-charge voltage is more than additive when several added metals are present.

Data on the effects of impurities on storage battery performance are limited. Gillette (1) has studied the effects of a number of elements while Vinal (2) has carried out tests under rather special conditions. Willihnganz (3) recently evaluated the effects of Fe.

In all of these studies the impurity was added to the electrolyte. Sb which is present in grid metal is anodically corroded and deposits on the negative active material. In the latter state, it may be considered as an impurity and its effects are well understood. Zachlin (4) along with others has shown the part played by the concentration of Sb in the grid metal on the self-discharge rate.

No data are available showing the effects of impurities when present in the Pb from which the oxides are made. Such information is required for a better understanding of the lead-acid battery and this is the reason for the present investigation.

Experimental

This study was confined to the more common elements associated with Pb, viz., Bi, Ag, Cu, Ni, Sb, and Te. Impurities were introduced in concentration ranges which would more than cover the percentages usually found in Pb used for storage battery oxides. With the exception of Te, alloys were made by adding the proper amount of each element to U.S.S. electrolytic Pb. Metals were added singly or in combination with others as required. The alloys were then converted to high metallic litharges in a small size Barton pot. Each oxide was analyzed spectrographically for the added elements. Results were close to the anticipated concentrations.

The oxides containing Te as a single added impurity were prepared by blending TeO_2 with pure oxide made from the electrolytic metal. Oxides were also prepared from alloys consisting of corroding Pb and added Te. Because of the mode of preparation, the results obtained with the Te-bearing oxides are not strictly comparable with results corresponding to the other oxides. However, this does not obviate the validity of the conclusions. Te has been investigated because of its presence in corrosion-resistant grid metal.

Oxides were processed into batteries of the standard height, 100 amp-hr, 15 plate, 6 v automobile type. Both the positive and negative plates in any one battery were made from the same oxide sample. The negative plates contained carbon black, blanc fixe, and a ligneous material as is customary.

TABLE I. Composition of grid and post alloys

Metal	Per cent	
	Grid	Post
Sb	8.4	4.4
Cu	0.028	0.05
As	0.023	0.017
Sn	0.38	0.33
Ag	0.0034	0.0033
Bi	0.017	0.017
Fe	<0.001	—
Ni	<0.001	<0.001
Cd	<0.0005	<0.001
Zn	<0.001	—

All grids were cast from one lot of 8% antimonial lead. The post straps were cast from a single lot of 4% antimonial lead. The composition of these alloys is shown in Table I. Analyses were made spectrographically. Cedar separators were used throughout and these were screened and shuffled.

Three batteries were made from each sample of oxide. This entailed a total of 12 batteries for each element studied since four concentrations were made for each added metal. All 12 batteries were prepared and tested in series and at the same time.

Formations were carried out by the group container method using H_2SO_4 of 1.100 specific gravity as the electrolyte, a rate of 12.5 amp and an input of 290 amp-hr. The conditioning charge input was about 100 amp-hr. Final electrolyte specific gravities were approximately 1.280.

Elements were examined at the end of the forming period. Since all of the plates were substantially cleared of visible lead sulfate, it was concluded that over the concentration ranges studied none of the added impurities had any appreciable retarding action on formation. With regard to the copper series, when concentrations of 0.01 and 0.06% were used a deposit of this metal was distinctly visible on both the negative plates and post straps. When oxides containing 0.005% Cu were used, the deposit was barely visible.

Cell voltages and negative plate to cadmium voltages were determined at the 10 amp rate just prior to termination of the conditioning charge. Since cell voltage variations are entirely attributable to variations in the negative plate voltages, no further mention of the former will be made.

Shortly after completing the conditioning charge, one battery representing each sample of oxide was placed in a constant temperature room operating at 90°F (32°C) for a 28-day shelf test. The drop in the electrolyte specific gravity during this period was determined for each cell and recorded in terms of number of points, one point being equal to 0.001 sp gr. Shelf life is an indirect function of the drop in the specific gravity. Stated another way, the self-discharge rate is a direct function of the specific gravity drop.

At the conclusion of the shelf test, the batteries were fully charged and then tested for capacity and deep cycle life according to S.A.E. specifications (5). Results were averaged with those obtained from S.A.E. capacity and cycle life tests made on two sets of batteries placed on test shortly after the conditioning charge. Over the concentration ranges investigated, neither capacity nor cycle life was affected by any of the elements studied.

Single Elements

The negative plate to cadmium voltage taken toward the end of the conditioning charge is shown in Table II for each oxide tested. This table shows that Bi has no effect in concentrations of up to 0.25% while Ag, Cu, Ni, Sb, and Te serve to decrease the voltage. Of these, Ni and Te are particularly effective.

The change in electrolyte specific gravity during a 28-day open circuit period at 90°F is shown in Table III for each of the oxides tested. These data show that, within the concentration limits studied, shelf life is unaffected by Bi, Ag, and Cu. Ni, Sb, and Te serve to shorten the shelf life.

Combinations of Elements

In the preliminary work with combinations of elements, the desired compositions were obtained by intimately blending oxides containing the individual elements. Later work has shown that the results corresponding to such blends are misleading. The effects are much less pronounced than when the additions are made to the base Pb. For this reason, work reported here is confined to oxides prepared from metal containing the added elements.

TABLE II. Negative plate to cadmium voltages on conditioning charge at 10 amp

%	Bi	Ag	Cu	Ni	Sb	Te
0.0000	−0.24	−0.24	−0.23	−0.23	−0.27	−0.24
0.0001	—	—	—	—	—	−0.24
0.0005	—	—	—	—	—	−0.21
0.0010	—	—	—	−0.15	—	−0.20
0.0050	−0.24	−0.24	−0.23	−0.05	−0.27	−0.13
0.0100	—	—	−0.20	—	—	—
0.0350	—	—	—	—	—	—
0.0500	−0.25	−0.20	—	−0.02	−0.24	—
0.0600	—	—	−0.15	—	—	—
0.1000	—	—	—	—	−0.11	—
0.2500	−0.26	−0.12	—	—	—	—

TABLE III. Drop in electrolyte specific gravity 28-day open circuit period

%	Points Drop					
	Bi	Ag	Cu	Ni	Sb	Te
0.0000	24	31	28	28	27	28
0.0010				27		
0.0050	27	31	27	36	28	40
0.0350				53		
0.0500	25	34			32	
0.0600			26			
0.1000					44	
0.2500	27	30	27			

TABLE IV. Impurities combined negative cadmium voltages drop in electrolyte specific gravity

No.	Per cent					
	Ag	Cu	Bi	Sb	Ni	Te
1	no added impurity					
2	0.01	0.009	0.27	0.05	0.0004	—
3	0.0034	0.0036	0.04	—	0.0038	—
4	<0.0006	<0.0008	0.016	<0.001	—	0.0002
5	<0.0006	<0.0008	0.016	<0.001	—	0.0003
6	<0.0006	<0.0008	0.016	<0.001	—	0.0004

No.	Negative to cadmium Volts		Electrolyte sp gr Points Drop	
	Computed	Actual	Computed	Actual
1	—	−0.24	—	29
2	−0.17	−0.10	32	47
3	−0.18	−0.09	27	26
4	—	−0.09	—	34
5	—	−0.09	—	—
6	—	−0.10	—	36

Data covering oxides containing more than one added element are shown in Table IV. Computed negative plate charge voltages as well as computed electrolyte specific gravity drops represent summations of the effects of the individual added metals. These effects were picked off from curves representing the data shown in Tables II and III. Comparisons are made with the results of actual determinations.

Based on the data for single elements, one would expect the negative plate voltage corresponding to oxide 2 to be influenced primarily by Ni with Sb also making a small contribution. The computed voltage is −0.17. Since the actual voltage is −0.10, it is obvious that with this particular combination the effects on voltage are considerably more than additive. The same situation applies to oxide 3 which contains no added Sb.

Reference to the last two columns of Table IV shows that the elements present in sample 2 serve to increase the open circuit electrolyte specific gravity drop to a marked degree. The actual drop was 47 points as compared to a computed drop of 32 points. The impurities in oxide 3 have no effect on the specific gravity drop and this is to be expected from computations. The only essential difference in the composition of the two oxides is the presence of antimony in oxide 2. From this, it follows that Sb exerts a synergistic effect on shelf life.

Te in concentrations of 0.0002, 0.0003, and 0.0004% is represented by samples 4, 5, and 6, respectively. All of these samples contain 0.016% Bi and only very small concentrations of other elements. Te is

the only impurity present which would be expected to have any effects. No computed values are shown since there are no data at hand covering the effects produced by Te when present as a single impurity added to the Pb used in producing oxide. Nevertheless, its depressing action on the negative plate voltage is obvious. Table IV shows a voltage of about −0.10 corresponding to the three Te-bearing oxides as compared to a voltage of −0.24 when no impurity is present. Similarly, the impurities in these oxides bring about a moderate increase in the open-circuit electrolyte specific gravity drop.

Discussion

Bi, Ag, Cu, Ni, Sb, and Te have been added to the base Pb from which both positive and negative battery oxides have been produced. The metals were added singly and in combination. The oxides have been processed into batteries and tested.

None of the added metals affects battery capacity or life, nor is the positive plate voltage affected.

When added as single elements, Bi, Ag, and Cu have no effect on shelf life. Ni, Sb, and Te serve to shorten shelf life. When present with other metals, Sb has a synergistic action on the self-discharge rate.

With the exception of Bi, each of the elements studied depresses the end of charge voltage, the most outstanding effect being produced by Te. As little as 0.0002% of this element introduced by way of corroding Pb depresses the voltage to a marked degree. When a number of added metals is present in an oxide, the effect on the end of charge voltage is more than additive.

Since the grid metal used in this work contained Sb in the concentration commonly present in automotive batteries, it is felt that conclusions based on the findings of this report are generally applicable to this type of battery. Batteries such as the L.D. type and those made from calcium-lead grids may not be affected in the same manner.

The findings justify the conclusion that no change should be made for the present in the long established practice of using only high purity Pb for making storage battery oxide.

Acknowledgment

The authors take pleasure in acknowledging the direction, suggestions and assistance of Dr. J. A. Orsino during the course of the work and in the preparation of this paper. They express their thanks also to the management of the National Lead Company for permission to publish this paper.

Manuscript received July 7, 1955. This paper was prepared for delivery before the Boston Meeting, Oct. 3-7, 1954.

Any discussion of this paper will appear in a Discussion Section to be published in the December 1957 JOURNAL.

REFERENCES

1. H. Gillette, *Trans. Am. Electrochem. Soc.*, **41**, 217 (1922).
2. G. W. Vinal, "Storage Batteries," p. 135, John Wiley & Sons, Inc., New York (1940).
3. E. Willihnganz, *This Journal*, **100**, 527 (1953).
4. A. C. Zachlin, *ibid.*, **92**, 259 (1947).
5. Hand Book, Society of Automotive Engineers, 29 West 39th St., New York, N. Y. (1952).

A Reproducible and Stable Silver-Silver Oxide Electrode

Walter J. Hamer and D. Norman Craig

National Bureau of Standards, Washington, D. C.

ABSTRACT

A method is described for the preparation of silver-silver oxide electrodes which are stable and reproducible. When used in cells of the type Hg(l), HgO(s) | NaOH, aq. | Ag_2O(s), Ag(s) the silver-silver oxide electrodes give stable potentials over periods of 38 days. No evidence was found that Ag, Ag_2O electrodes evolve oxygen, that Ag_2O exists in different forms in aqueous solutions at normal temperatures, that Ag_2O reverts to a lower oxide, or that imperfections exist in the Ag_2O crystal. The free energy and entropy changes for the reaction in the above cell are −11254 cal. and −9.12 e.u., respectively, at 25°C. These values are reasonably consistent with the best available thermodynamic data. The standard electrode potential of the Ag, Ag_2O electrode is found to be −0.342 v at 25°C.

The literature states that silver-silver oxide (Ag_2O) electrodes cannot be prepared in a reproducible or stable condition. Luther and Pokorny (1) and Buehrer [reported by Lewis and Randall (2)] investigated the cell:

$$Pt, H_2(g) \mid KOH, aq. \mid Ag_2O(s), Ag(s) \quad [A]$$

and reported that the emf decreased with time. The former concluded that the decrease was due to the formation of Ag_4O; the latter also attributed the decrease to the formation of a lower oxide of silver but did not speculate on its composition. Furthermore both obtained emf's which differed by many millivolts from the one calculated from thermodynamic data.

Fried (3) also found variable and uncertain results at 0°, 23.5°, and 58°C for the cell:

$$Hg(l), HgO(s) \mid NaOH, aq. \mid Ag_2O(s), Ag(s) \quad [B]$$

Reasoning that the fall of emf was caused by the re-

lease of oxygen from the Ag_2O, he subjected his silver oxide to prolonged heating at 200°C. Even so, his heated oxides gave potentials that first increased with time and attained a fairly constant value only for a short time. Also, two different samples of his oxide gave free energy changes for the reaction of cell [*B*] which were lower by about 10 and 14%, respectively, than from the best thermodynamic data (4). Furthermore, he obtained +0.000182 v/°C and +0.000195 v/°C for the emf-temperature coefficient. A positive emf-temperature coefficient, however, corresponds to a positive entropy change for the cell reaction whereas the best thermodynamic data (4) give a negative value of −0.00020 v/°C.

Rördan (5) believed that he found evidence for two forms of Ag_2O having free energies of formation of −2420 and −3980 cal mole, but Kelley and Anderson (6) stated that there is no real proof of the existence at room temperature of two forms. Also, Pitzer and Smith (7) in their heat-capacity measurements of Ag_2O found no evidence of two forms, although they did find anomalies in the heat capacity from 15° to 50°K. Kobayashi (8) found that the heat capacity of Ag_2O depended on the treatment given the oxide. He concluded that Ag_2O undergoes a change in physical structure when heated between 100° and 200°C, this change not being one of lattice transition, as Fried also considered unlikely, but rather one associated with the melting of the "freezing in" of the imperfections in the crystal produced by the dehydration of Ag_2O precipitated below 100°C. This fact may account in part for the "hump" observed by Pitzer and Smith in their capacity curve as their sample of oxide was heated only to 110°C.

Kobayashi found that the heat change for the transformation

$$Ag_2O \text{ (precipitated below 100°C)} = Ag_2O \text{ (heated above 100°C)}$$

was −315 cal/mole, which would correspond to 6.8 mv assuming an entropy change of zero. (This instability would manifest itself as a decrease in the potential of Ag, Ag_2O electrodes.) Kobayashi further believed that the instability of the Ag, Ag_2O electrode could cause emf variations greater than 6.8 mv owing to the nature of the Ag_2O surface.

In view of the above inconsistencies, especially the difference in sign for the entropy change between the best thermodynamic data and Fried's results, it was deemed advisable to reinvestigate the behavior of Ag, Ag_2O electrodes. This paper gives some results of such a reinvestigation. The most significant result pertains to a method of preparing stable and reproducible Ag, Ag_2O electrodes whose potentials are reasonably consistent with most recent thermodynamic data.

Experimental

In this study of Ag, Ag_2O electrodes, cells of type [*B*] were used. Although there is some uncertainty in the standard potential of Hg, HgO electrodes, they were used nevertheless as reference electrodes so that the potentials of the Ag, Ag_2O electrodes could be measured conveniently over long periods of time. The uncertainty in the potentials of the Hg, HgO electrodes has been attributed to a difference in the particle size and solubility of the red and yellow forms of HgO. The potential difference between the red and yellow forms has been reported to be only 0.685 mv at 25°C (9) and to decrease with time, the decrease being about 0.3 mv in 15 days (10). The uncertainties in the potential Hg, HgO electrodes were, however, of little moment in these initial studies, consequently a sample of HgO designated as red was used. It is recognized, however, that this is not an adequate description of HgO and ultimately H_2 electrodes should be employed to establish the most accurate value of the standard potential of Ag, Ag_2O electrodes.

The Ag_2O and HgO used in making the electrodes were of certified reagent grade. Both were digested for prolonged periods in distilled water on a steam bath and the water was frequently poured off and replaced with a fresh portion. Simple H-type Pyrex glass containers were used in assembling the cells. The legs were 1 in. in diameter and 5 in. long and were connected near the top by a cross tube 2 in. long and 0.5 in. in diameter. One leg contained two Ag, Ag_2O electrodes and the other leg two Hg, HgO electrodes. One of the Hg, HgO electrodes, made in the usual way, was at the bottom of the respective leg and the other was in a glass cup suspended in the same leg by a glass tube which was sealed to the cup and protruded through a rubber stopper at the top of the leg. The electrode at the bottom of the leg is referred to as electrode No. 1 and the suspended or upper electrode is referred to as electrode No. 2. Purified Hg was used in preparing these electrodes and the HgO was well washed with successive portions of the NaOH solution to be used in filling the cells. The silver oxide electrodes were prepared by two methods.

Method No. 1.—The first Ag, Ag_2O electrodes were prepared as follows: Ag_2O was washed repeatedly with the NaOH solution to be used in filling the cell and was then placed in one leg of the cell. In this slurry were placed two small Pt helices completely covered with Ag and sealed in the end of soft glass tubes. These tubes were supported in the leg of the cell by a rubber stopper. The Pt helices were covered with Ag by a process similar to that used in preparing silver for Ag-AgCl electrodes of the Harned (11) type. Ag thus prepared is considered to be superior to the electrolytic Ag because the removal of the electrolyzing solution from the interstices of the electrolytic Ag is known to be most difficult, if not impossible. The cell was then carefully filled with NaOH solution.

Method No. 2.—These Ag, Ag_2O electrodes consisted of pieces of Pt gauze 1.5 cm x 1.5 cm welded to Pt wires 2.5 cm long sealed into a soft glass tube. The lower portion of the Pt gauze was folded up thereby making a small v-shaped trough suitable for holding Ag_2O. The platinum trough was filled with moist Ag_2O, slowly dried over a hot plate, and repeatedly pasted until the Pt was totally incased in dry Ag_2O. The electrodes were then mounted in a glass reduction tube and the Ag_2O partially reduced at 60°C to Ag by passing H_2 through the tube. It is

necessary to avoid too rapid a rate of reduction otherwise the heat liberated by the reaction

$$H_2(g) + Ag_2O(s) \rightarrow 2\ Ag(s) + H_2O(g) \qquad (I)$$

will flash the electrodes and the reaction will go to completion. When the Ag_2O was sufficiently reduced as judged by the gray color of the electrodes, the reduction tube was cooled to room temperature and the electrodes were transferred quickly to an H-cell containing two Hg, HgO electrodes and the requisite amount of NaOH solution. Ag, Ag_2O electrodes can be prepared by this method without the necessity of repeatedly washing them to free them of objectionable electrolytic impurities. Furthermore, the Ag should be free from occluded or adsorbed oxygen and be intimately mixed and in close contact with the Ag_2O.

Results

Cells Containing Ag, Ag_2O *Electrodes Prepared by Method No. 1*

Results obtained with electrodes prepared by method No. 1 confirmed results of Luther and Pokorny (1), Buehrer (2), and Fried (3) in that the potentials decreased with time as shown in Fig. 1 for a 15% NaOH solution. Similar results were also obtained for 5-40% NaOH solutions. During these measurements no evidence of O_2 evolution was obtained and all attempts by x-ray analysis failed to indicate lower oxides of Ag. However, two phenomena were observed, not reported by the above authors, namely: (*a*) the decline in emf, approximating 0.01 v in 17 days, was accompanied by a decrease in the reproducibility of the electrodes and the sensitivity of the measurements, and (*b*) if the Ag were removed from the Ag_2O slurry, after 17 days, and replaced by new Ag the emf's returned to their original high values and again exhibited high sensitivity, after which the potential and sensitivity of the electrodes again declined (*see* Fig. 1). These facts proved conclusively that the abnormal behavior observed by the authors cannot be attributed to changes in Ag_2O.

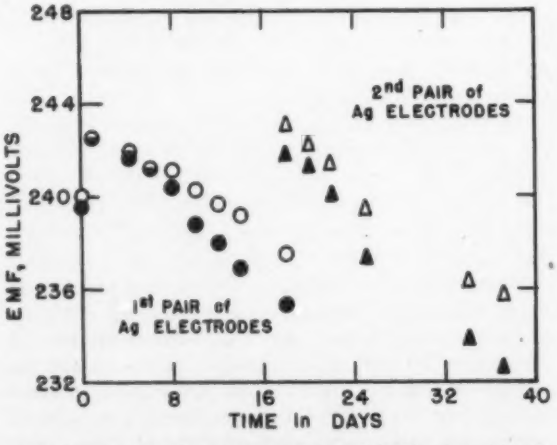

Fig. 1. Emf at 25°C of a Hg, HgO/NaOH (15% solution)/Ag_2O, Ag cell containing two Ag, Ag_2O electrodes prepared by Method No. 1 and two Hg, HgO electrodes. Each indicated value is an average value for each Ag, Ag_2O electrode against the two Hg, HgO electrodes.

It was also observed that the decline in potential and sensitivity was more rapid when small Ag foils were used instead of the Ag-covered helices. This suggested that the abnormal behavior of the electrodes is caused by a surface phenomena which is a function of the relative amounts of free oxygen in the cell and the surface area of the Ag. This is supported by the fact that the temperature coefficient of the emf of the cells when first assembled is about −0.2 mv/°C which leads to an entropy change for the cell reaction which approximates the thermodynamic value.

One might postulate that the exposed Pt of the electrodes caused the observed abnormalities, but exposed Pt does not cause Ag, AgCl electrodes to behave abnormally; data presented later in this paper do not support such a postulation. One might suspect that oxygen adsorbed on the Ag or Ag_2O or dissolved in the electrolyte might give rise to the high initial values and as it was dissipated the potential of the electrodes would fall and the higher potentials would again be observed when new Ag electrodes were placed in the cell. Two facts tend to contradict such an explanation, viz., (*a*) it does not explain the decrease in the sensitivity or reproducibility of the measurements with respect to the age of the electrodes, (*b*) the lower emf values do not agree within a few 0.01 of a volt with those calculated from thermodynamic data for the cell reaction. Benton and Drake (12) have reported that oxygen reacts with Ag at room temperature to form chemabsorbed films of nonstoichiometric composition. Conceivably such films could be of a passive nature and their effectiveness and rate of formation could be a function of the available oxygen and the area of the Ag surface thereby accounting for the more pronounced abnormalities observed with the small Ag foil electrodes. Such considerations prompted the authors to make cells with Ag, Ag_2O electrodes prepared by method No. 2.

Cells Containing Ag, Ag_2O *Electrodes Prepared by Method No. 2*

Results obtained with cells containing Ag, Ag_2O electrodes prepared by method No. 2 are given in Table I.[1] These cells are definitely superior and with respect to time are relatively free of the difficulties encountered in the earlier experiments discussed above. It is evident from Table I that the electrodes attained equilibrium in about ½ day and that Ag, Ag_2O electrodes prepared by method No. 2 do give steady and reproducible potentials to within a millivolt for periods of 14-38 days.

The emf's of Table I show a slight concentration dependence. Although, theoretically, the emf should be independent of alkali concentration, the observed dependence may be real and of the type found in Ni-Fe alkaline batteries. Until such is established, a total average value (averaging all values) are taken which is 0.2440 ± 0.0005 v for cell [*B*] at 25°C. Using

[1] An extended version of Table I has been deposited as Document 5109 with the ADI Auxiliary Publications Project Photoduplication Service, Library of Congress, Washington 5, D. C. A copy may be secured by citing the Document number and by remitting $1.25 for a photoprint or for a 35-mm microfilm. Advance payment is required. Make check payable to: Chief, Photoduplication Service, Library of Congress.

TABLE I. Electromotive forces at 25°C of the cell Hg, HgO | NaOH (aq.) | Ag_2O, Ag

	Weight % NaOH										
	30		20		15		10		5		
Time	HgO(1)*	HgO(2)*	HgO(1)	HgO(2)	HgO(1)	HgO(2)	HgO(1)	HgO(2)	HgO(1)	HgO(2)	Avg
(days)	(v)	(v)	(v)	(v)	(v)	(v)	(v)	(v)	(v)	(v)	(v)
0.5	0.2445	0.2444	0.2442	0.2444	0.2439	0.2438	0.2438	0.2440	0.2429	0.2429	0.2439
1	0.2446	0.2445	0.2445	0.2444	0.2438	0.2438	0.2431	0.2438	0.2430	0.2430	0.2439
5	0.2450	0.2449	0.2438	0.2445	0.2434	0.2437	0.2431	0.2439	0.2430	0.2426	0.2438
10	0.2451	0.2451	0.2436	0.2445	0.2435	0.2437	0.2434	0.2442	0.2434	0.2432	0.2440
14	0.2450	0.2451	0.2439	0.2444	0.2434	0.2437	0.2439	0.2442	0.2435	0.2431	0.2440
35			0.2436	0.2444	0.2427	0.2433					
38			0.2435	0.2439	0.2426	0.2432					

* Electrode (1) means lower Hg, HgO electrode; electrode (2) means upper Hg, HgO electrode.

TABLE II. Electromotive forces of the cell Hg, HgO | NaOH (aq.) | Ag_2O, Ag at various temperatures in the order of observation

Wt % NaOH							
30		20		10		5	
t°C	E (v)	t°C	E (v)	t°C	E (v)	t°C	E (v)
22.70	0.24556	22.90	0.24452	22.60	0.24429	22.80	0.24382
0.00	0.24963	0.00	0.24899	12.30	0.24641	0.00	0.24770
23.90	0.24528	23.10	0.24459	0.00	0.24870	23.10	0.24372
24.80	0.24506	51.75	0.23863	12.05	0.24654	51.75	0.23733
46.90	0.24018	46.75	0.23975	36.80	0.24122	46.85	0.23834
41.85	0.24124	75.45	0.23420	21.70	0.24468	23.90	0.24347
25.00	0.24463	69.20	0.23539	54.50	0.23771	75.70	0.23282
11.15	0.24745	25.10	0.24421	70.55	0.23466	69.15	0.23402
13.86	0.24698			69.55	0.23495	24.10	0.24186
25.10	0.24469			55.10	0.23791		
				22.40	0.24495		
				90.50	0.23061		
25.00*	0.24487	25.00*	0.24410	25.00*	0.24388	25.00*	0.24278
(dE/dT) 25°C	−0.0002035		−0.0001951		−0.0001958		−0.0001967

* Calculated.

23,060.5 cal/abs. volt g-equiv. (4) for F, the free energy change for the reaction of cell [*B*] is −11,254 ± 24 cal at 25°C.

The effect of temperature on the emf of the cell is given in Table II. Observations for each cell covered a period of from 3 to 6 days and no appreciable emf temperature hysteresis was noted. The emf-temperature coefficients at 25°C obtained from the emf at the various temperatures by the method of least squares are listed in the last row of the table. The noteworthy fact observed in these studies is that the temperature coefficient is negative and not positive as reported by Fried. The authors have no explanation for the positive temperature coefficient observed by Fried (3), except that he probably either was not dealing with Ag_2O or was working in the range of electrode insensitivity. The average value for the coefficient at 25°C is −0.0001978 ± 0.0000029 which gives −9.12 ± 0.14 e.u. for ΔS at 25°C, since $\Delta S = nF\ (dE/dT)$. Then ΔH, the heat of the reaction is −13.973 ± 69 cal at 25°C since $\Delta H = \Delta F + T\Delta S$.

It remains to be seen if the above values for ΔF and ΔS are reasonably consistent with the thermodynamic data reported in the literature for Ag_2O.

Thermodynamic Considerations

The free energy change of the reaction for cell [*B*] is equal to the difference between the free energies of formation of HgO and Ag_2O. The former may be calculated from the free energy of formation of liquid water, which value (−56,690 cal) is well known (4) and the free energy change for the reaction:

$$H_2\ (g) + HgO\ (s) = Hg\ (1) + H_2O\ (1) \quad (II)$$

given by the cell:

Pt, H_2(g) | NaOH or KOH, aq. | HgO (s), Hg (l) [*C*]

The emf of this cell has been measured at 25°C by Brönsted (13), Chow (14), Miyamoto (15), Fried (3), Ishikawa and Kimura (10), Shibata and Murata (16), Shibata, Kobahashi, and Furukawa (17), and Kobayashi and Wang (18). Their results are brought together in Table III. Using only those values corrected to infinite dilution, and assuming all experimenters used the correct international volt, −13,977 cal is the free energy of formation of HgO. When this value is combined with that found for the free energy of the cell reaction, −2723 cal is the free energy of formation of Ag_2O.

TABLE III. Entropy and free energy changes for the reaction $H_2(g) + HgO(s) = Hg(l) + H_2O(l)$

Experimenter	Emf (25°C)	(dE/dT) 25°C	$\Delta F°$ (25°C) cell reaction	$\Delta S°$ (25°C) cell reaction	$\Delta F°$ (25°C) formation HgO	$S°$ HgO
	(v) [b]	(v) [b]/deg	cal	e.u.	cal	e.u.
Brönsted*	0.9261[c]	—0.0002791	—42727	—12.88	—13963	16.89
Chow	0.9264	—	—42741	—	—13949	—
Mujamoto	0.9268	—	—42759	—	—13931	—
Fried	0.92598[c]	—0.0002918	—42721	—13.46	—13979	17.47
Ishikawa and Kimura	0.92565[c]	—0.0002949	—42706	—13.61	—13984	17.62
Shibata and Murata	0.92558	—0.000284	—42703	—13.10	—13987	17.11
Shibata, Kobayashi, and Furukawa	0.92445	—0.000281	—42697	—12.96	—13993	16.97
Kobayashi and Wang	0.925495[c]	—0.0002854	—42699	—13.17	—13991	17.18
Avg.	0.92593	0.0002860	—42719	—13.19	—13971	17.21
Avg†	0.92581	0.0002878	—42713	—13.27	—13977	17.29

* At the time of his measurements Brönsted used an international volt which was 0.03% too high; the above value includes a correction for this.
[c] Corrected to infinite dilution.
[b] International volt.
† Average of only those corrected to infinite dilution.

Pitzer and Smith (7) obtained the free energy of formation of Ag_2O at 25°C from heat capacity measurements from 12.9 to 285.3°K and the free energies of dissociation of Ag_2O as calculated from the equilibrium data of Lewis (19), Keyes and Hara (20), and Benton and Drake (12) for the temperature range 446.1-773.1°K, and an assumed heat capacity curve for Ag_2O from 285.3 to 773.1°K. [Kobayashi's subsequent heat capacity measurements at high temperatures (8) showed their assumed curve to be reliable.] By this procedure, Pitzer and Smith (7) calculated a value of —2585 cal for the formation of Ag_2O at 25°C. This value is 135 cal lower than that found in this investigation.

However, Pitzer and Smith in their determinations of the heat capacity of Ag_2O observed an anomalous "hump" in their curve of C_p against log T at 15-50°K which amounted to 0.48 e.u. in the entropy, to 14.2 cal in $H° - H°_0$, and to 0.44 cal in $(H°_0 - F°)/T$ for Ag_2O at 25°C. If this "hump" were ignored, the free energy of formation of Ag_2O becomes —2654 cal, which agrees within 69 cal of that found herein.

It is also interesting, as was shown by Pitzer and Smith (7), that a value of —2649 cal is obtained by the sum of the equations:

$$2Ag + 2H^+ + 2Cl^- = 2AgCl + H_2 ; \quad \Delta F° = 10{,}259 \text{ cal (21)} \qquad \text{(III)}$$

$$2AgCl + 2\,OH^- = Ag_2O + H_2O ; \quad \Delta F° = 5{,}596 \text{ cal (22)} \qquad \text{(IV)}$$

$$2H_2O = 2H^+ + 2\,OH^- ; \quad \Delta F° = 38{,}186 \text{ cal (23)} \qquad \text{(V)}$$

$$H_2 + \tfrac{1}{2}\,O_2 = H_2O ; \quad \Delta F° = -56{,}690 \text{ cal (4)} \qquad \text{(VI)}$$

which agrees remarkably well, perhaps fortuitously, with that of Pitzer and Smith if their "hump" is ignored.

In spite of this agreement, the values of —2654 and —2649 may be low. Pitzer and Smith's evaluation of the heat content and entropy involves an extrapolation to absolute zero. They made this extrapolation with the aid of the Debye theoretical heat capacity equation. Inspection of their data at low temperatures suggests that their $H°_{15} - H°_0$ and $S°_{15} - S°_0$ values may be high by as much as 1.0 cal and 0.11 e.u., respectively.[2] Also, the low-temperature heat capacities of Ag_2O do not follow the simple or extended Debye equations. For the simple case, a straight line should be obtained if C_p/T were plotted against T^2 whereas a curve is obtained. For the extended case, constant values of θ, the characteristic temperature, should be found; actually values of θ decrease rapidly as the temperature becomes high.

Assuming that Pitzer and Smith's values are high by the above amount, —2683 cal is obtained for the free energy of formation of Ag_2O which agrees within 40 cal of that found herein. This agreement is considered good especially since the correction for the "hump" in the Pitzer and Smith data may have been arbitrarily chosen by the author of this paper as smaller than it actually is. Also, some uncertainty exists concerning the second of the 4 equations added above. Randall and Halford (22) used the equilibrium data of Noyes and Kohr (24) and Newton (25) in evaluating $\Delta F°$. They plotted the concentration equilibrium constants as obtained by these authors against the square root of the ionic strength and extrapolated to zero concentration whereby they obtained $-\log K = 2.050 \pm 0.003$ at 25°C from which $\Delta F° = 2798$. However, using the procedure of Lewis and Randall (26) and the same data 2779 is obtained for $\Delta F°$. Furthermore, Böttger (27) by conductivity measurements found the solubility product of Ag_2O in water at 25°C to be 1.96×10^{-8} which was confirmed by Johnston, Cuta, and Garrett (9). From the potentiometric data of Owen (28) and the conductometric data of Gledhill and Malan (29) a value of 1.778×10^{-10} is obtained for the solubility product of AgCl in water at 25°C. These two values lead to $\Delta F° = 2786$. Therefore, if this value is averaged with the Lewis and Randall value and used in the second of the 4 equations above, —2679 cal is obtained for the free energy of formation of Ag_2O which agrees

[2] These maximum uncertainties were arrived at as follows. A smooth curve was placed through the low-temperature heat capacities of Pitzer and Smith for their Series I and II, ignoring the "hump". The best curve was obtained by the method of least squares. The value at 15°K was then calculated from the least square equation and used in the Debye equation, $C_p = 464\,(T°/\theta°)^3 = aT°$ to obtain values of C_p down to absolute zero. By this procedure 9.7 cal is obtained for $H°_{15} - H°_0$ and 0.86 e.u. for $S°_{15} - S°_0$ whereas Pitzer and Smith gave 10.7 cal and 0.97 e.u., respectively.

quite well with the Pitzer and Smith maximum value given above, and is within 44 cal of that found herein.

Further insight into the thermodynamic consistency may be seen from a consideration of the entropy of Ag_2O. The entropy change for cell [*B*] is given by

$$\Delta S_{reaction} = 2S_{Ag} + S_{HgO} - S_{Hg} - S_{Ag_2O} \qquad \text{(VIII)}$$

or S_{Ag_2O} by

$$S_{Ag_2O} = 2S_{Ag} + S_{HgO} - S_{Hg} - \Delta S_{reaction} \qquad \text{(IX)}$$

The values for S_{Ag} and S_{Hg} are, respectively, 10.206 and 18.5 e.u. (4). The value for S_{HgO} is 17.29 e.u. (*see* Table III). The value for $\Delta S_{reaction}$ has been shown to be −9.12 cal. Therefore, the entropy of Ag_2O, as found herein, is 28.32 e.u. Pitzer and Smith (7) gave 29.09 ± 0.2 e.u. However, if the "hump" were ignored in their heat capacity curve, their value would be 28.61 ± 0.2 e.u. which agrees quite well with the value found in the present investigation. Also, their value could well be high due to uncertainty in their extrapolation to absolute zero. This agreement in entropy is comparable to that usually found between calorimetric and emf data (30).

From the present investigation a value of −0.342 v[a] is obtained for the standard potential of the Ag, Ag_2O electrode. This value is arrived at from the measurements of cell [*B*], the data of Table III, and the standard potential 0.8282 v (31) of the H electrode at unit activity of OH^- ion. This value is 0.002 v lower than that given by Latimer (32) who based his value on the data of Pitzer and Smith.

In conclusion, it has been shown how stable and reproducible Ag, Ag_2O electrodes may be prepared which give potentials reasonably consistent with thermodynamic data. The comparison of thermodynamic data involves low-temperature heat capacity measurements, high-temperature dissociation measurements, and free energy functions for Ag and O_2 on the one hand, as compared with combined emf measurements of Ag, Ag_2O and Hg, HgO electrodes and free energy functions of H_2O, Ag, Hg, and HgO on the other hand. A more direct comparison could be realized by comparing Ag, Ag_2O, and H_2 electrodes. Such measurements are contemplated, although they would be involved owing to the high solubility of Ag_2O in alkali.

Manuscript received July 2, 1956. This paper was prepared for delivery before the Cleveland Meeting, Sept. 30 to Oct. 4, 1956.

[a] According to the Stockholm IUPAC convention the sign here would be + with the half-cell reaction written as a reduction of Ag_2O.

Any discussion of this paper will appear in a Discussion Section to be published in the December 1957 JOURNAL.

REFERENCES

1. R. Luther and F. Pokorny, *Z. anorg. u. allgem. Chem.*, **57**, 290 (1908).
2. G. N. Lewis and M. Randall, "Thermodynamics and the Free Energy of Chemical Substances," p. 483, McGraw-Hill Book Co., New York (1923).
3. F. Fried, *Z. physik. Chem.*, **123**, 406 (1926).
4. "Selected Values of Chemical Thermodynamic Properties," National Bureau of Standards Circular 500 (1952).
5. H. N. K. Rördan, *Kgl. Danske Videnskab. Selskab, Mat-fys. Medd.*, **3**, No. 7 (1920).
6. K. K. Kelley and C. T. Anderson, *U. S. Bur. Mines Bull. 384* (1935).
7. K. S. Pitzer and W. V. Smith, *J. Am. Chem. Soc.*, **59**, 2633 (1937).
8. K. Kobayashi, *Science Repts. Tôkoku Univ.*, Ser. I, **35**, 173 (1951).
9. E. Cohen, *Z. physik. Chem.*, **34**, 69 (1900).
10. F. Ishikawa and G. Kimura, Sexagint, Y. Osaka, *Chem. Inst. Dept. Science Kyoto Imp. Univ.*, 255 1927.
11. H. S. Harned, *J. Am. Chem. Soc.*, **51**, 416 (1929).
12. A. F. Benton and L. C. Drake, *ibid.*, **54**, 2186 (1932).
13. J. N. Brönsted, *Z. physik. Chem.*, **65**, 84 (1908).
14. M. Chow, *J. Am. Chem. Soc.*, **42**, 488 (1920).
15. S. Mujamoto, *Sci. Papers, Inst. Phys. Chem. Res. Tokyo*, No. 4, **1**, 31 (1922).
16. F. L. E. Shibata and F. Murata, *J. Chem. Soc. (Japan)*, **52**, 399 (1931).
17. F. L. E. Shibata, Y. Kobayashi, and S. Furukawa, *ibid.*, **52**, 404 (1931).
18. Y. Kobayashi and S. Furukawa, *J. Sci. Hiroshima Univ.*, **5A**, 71 (1934).
19. G. N. Lewis, *J. Am. Chem. Soc.*, **28**, 139 (1906).
20. F. G. Keyes and H. Hara, *ibid.*, **44**, 479 (1922).
21. H. S. Harned and R. W. Ehlers, *ibid.*, **55**, 2179 (1933).
22. M. Randall and J. O. Halford, *ibid.*, **52**, 178 (1930).
23. H. S. Harned and G. E. Mannweiler, *ibid.*, **57**, 1873 (1935).
24. A. A. Noyes and D. A. Kohr, *Z. physik. Chem.*, **42**, 336 (1902).
25. R. F. Newton, *J. Am. Chem. Soc.*, **50**, 3258 (1928).
26. Ref. (2), p. 482.
27. W. Böttger, *Z. Physik. Chem.*, **46**, 521 (1903).
28. B. B. Owen, *J. Am. Chem. Soc.*, **60**, 2229 (1938).
29. J. A. Gledhill and G. McP. Malan, *Trans. Faraday Soc.*, **48**, 258 (1952).
30. D. A. MacInnes, "The Principles of Electrochemistry," p. 123, Reinhold Publishing Corp., New York (1939).
31. Ref. (32) p. 253.
32. W. M. Latimer, "The Oxidation States of the Elements and Their Potentials in Aqueous Solutions," 2nd ed., Prentice-Hall, Inc., New York (1952).

Effect of Ultraviolet Irradiation on the Growth of Anodic Ta_2O_5 Films

D. A. Vermilyea

Research Laboratory, General Electric Company, Schenectady, New York

ABSTRACT

Ultraviolet irradiation during the growth of amorphous Ta_2O_5 films in aqueous solutions results in the transformation of the outer portion of the film from Ta_2O_5 to a material which dissolves more rapidly than Ta_2O_5 in HF. If the formation field is high, the transformed region has a very high resistance and both Ta and oxygen are mobile in the region. When the formation field is low, the region has a lower resistance, contains water which can be removed partially by heating the film in air, and only oxygen is mobile. It is suggested that the transformation of the outer portion of the film occurs after an increased field, necessary to maintain the flow of electrons into the oxide from the solution by tunneling, is produced by a positive space charge in the outer portion of the film. Under the influence of this high field Ta ions migrate out of the outer part of the film, leaving defects. As the defect concentration increases, oxygen probably also starts to move in the film, and the film becomes either hydrated or porous depending on the applied field strength. Ultraviolet irradiation during growth also results in a similar transformation of the outer portion of crystalline anodic Ta_2O_5 films.

A recent note (1) reported that anodic Ta_2O_5 films grown while irradiated with u.v. light consisted of two layers, the one nearer the metal being a normal anodic Ta_2O_5 film and the outer one being less resistant to corrosion in HF and having a higher conductivity. This paper presents the results of a more extensive study of the nature and growth of the outer layer. It is suggested that this outer layer is formed by transformation of the original Ta_2O_5 film when a space charge produced by irradiation has caused a considerable increase in the electrical field strength at the oxide-solution interface.

Experimental

The Ta used in these experiments was 0.005 in. sheet,[1] and was stated to be 99.9% pure. The specimens had a surface area of about 6.4 cm^2. Only dilute aqueous electrolytic solutions (usually 1% Na_2SO_4) were used and identical results were obtained in all solutions (such as 0.1% KOH, 1% H_2SO_4) which did not adsorb the light and reduce the photo effect. The u.v. light source was a 4-w Hg vapor lamp.[2, 3] The source was placed outside a quartz beaker containing the specimen and the solution, and was about ½ in. from and parallel to the specimen. The maximum photocurrent obtained was about 1 ma/cm^2.

Two methods were used to obtain an estimate of the oxide film thickness. The first was a comparison with the interference color step gauge described previously (2). This method has the advantage that it gives a rough indication of the total thickness of the film, including both layers. The values obtained are accurate only for the dense amorphous Ta_2O_5 film, and the absolute value of the thickness measured when both layers are present might be considerably in error. The second method was a measurement of the electrical capacitance of a cell consisting of the specimen, a 2% HNO_3 solution, and a platinized Pt electrode of 100 cm^2 area. The series capacitance and series resistance of the cell were measured at 1000 cps. This second method has the advantage that a conducting layer in the oxide film behaves approximately like a resistance, and the capacitance is thus determined primarily by the dense inner Ta_2O_5 film. The actual equivalent electrical circuit of the oxide film is much more complex than a simple series resistance and capacitance and a determination of the true thicknesses of both films could only be made by making much more extensive measurements.

Results

Growth at High Current Density

Consider first the results of u.v. irradiation at an applied electric field of such a magnitude that the film would be growing at a fairly high rate, say about 0.1-10Å/sec, in the absence of light. It is found (Fig. 1) that as the film grows the optical thickness and capacitance are both smaller on the irradiated side. The capacitance of the irradiated side is found by calculating the capacitance of the dark side from the observed optical thickness and the dielectric constant, and subtracting the result from the total measured capacitance. At these high growth rates the series resistance of the condenser formed by the oxide film remains constant and equal to the resistance of the electrolyte. When the film is dissolved in HF the rates of decrease of the optical thickness and reciprocal capacitance (Fig. 2) indicate that the outer portion of the film on the illuminated side is not the ordinary Ta_2O_5 film found on the dark side. The fact that the series resistance is unchanged shows that this transformed material is highly insulating like the normal Ta_2O_5 film. It should be noted that the inner layer which comprises most of the film is apparently normal Ta_2O_5,

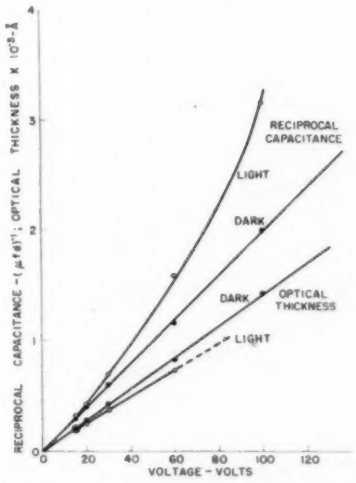

Fig. 1. Growth in thickness of a film formed at 3 ma/cm² in 1% Na_2SO_4 at room temperature with and without irradiation with u.v. light.

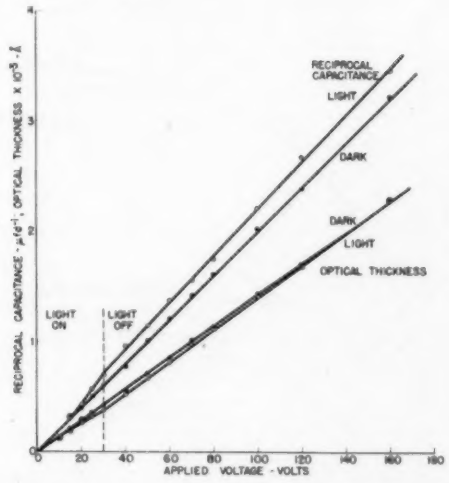

Fig. 3. Growth in thickness of a film formed at 1.5 ma/cm² in 1% Na_2SO_4 at room temperature, with one side irradiated for the first 30 v.

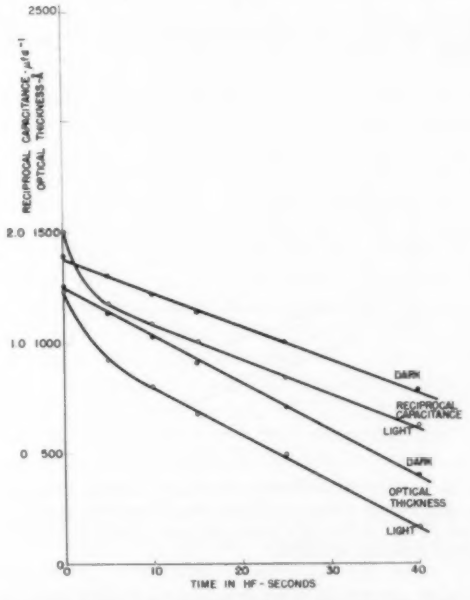

Fig. 2. Thickness decrease on solution in 48% HF of a film formed in a manner similar to that of Fig. 1.

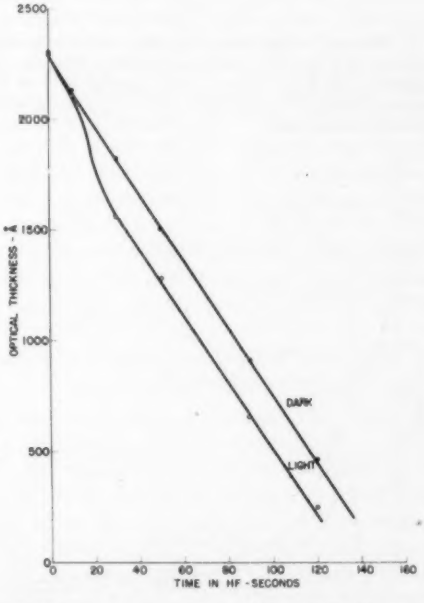

Fig. 4. Thickness decrease on solution in 48% HF of the film formed in Fig. 3.

since it has the same corrosion rate as the film on the dark side.

If the u.v. light is applied until the thickness has increased to about 400Å and then turned off while the formation is continued, the thickness and reciprocal capacitance increase as shown in Fig. 3. It may be seen that the change produced by the irradiation is permanent, the optical thickness and capacitance remaining smaller on the originally illuminated side. When the resulting film is dissolved in HF, it is found (Fig. 4) that the altered, rapidly dissolving film remains near the outer surface, but some normal Ta_2O_5 has been formed over the altered layer. It appears, therefore, that both oxygen and Ta are mobile in this altered layer [only Ta is mobile in normal Ta_2O_5 (3)]. Films formed under u.v. irradiation at these high growth rates behave in a manner which is very similar to that observed when anodic films are formed on Ta in solutions which are largely nonaqueous (3). Both types of formation produce films which have a layer of normal Ta_2O_5 next to the metal and a layer with different properties near the solution; both types of altered film become buried upon subsequent formation in simple dilute aqueous solutions.

Growth at Low Field Strength

Ultraviolet irradiation will cause the growth of Ta_2O_5 films held at such low field that no measurable growth would occur in the period of an experiment if the light was not present (4, 5). Fig. 5 shows plots of the values of series resistance, reci-

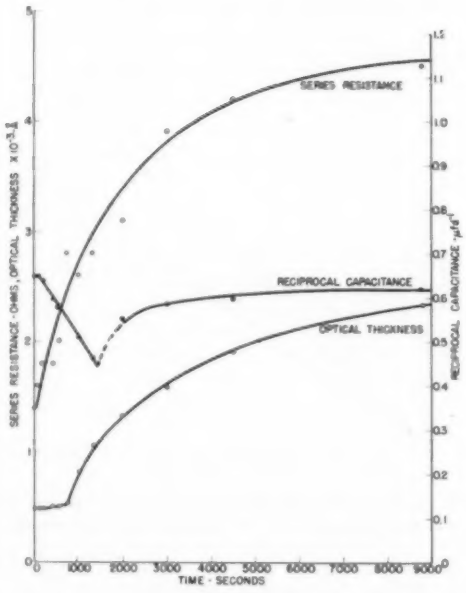

Fig. 5. Changes in thickness, reciprocal capacitance, and series resistance in the capacitance test on irradiation with u.v. light of a film initially 477Å thick with an initial applied field of 0.04 v/Å. The values plotted are for the light side; the thickness of the dark side remained unchanged.

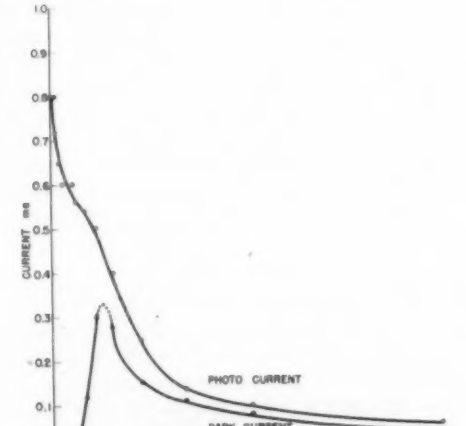

Fig. 6. Change of current with time for the experiment of Fig. 5. The current on the dark side was a negligible fraction of these currents.

procal capacitance, and optical thickness for a film formed in the dark to a thickness of 477Å and then held at a field of 0.04 v/Å with the u.v. light on. The series resistance and capacitance started to increase as soon as irradiation was started. The series resistance increased continuously at a decreasing rate during the entire run, while the capacitance first increased and then at about 1500 sec began to decrease again. The optical thickness began to increase very slowly at first, but at 750 sec the rate of increase suddenly became very great and the thickness increase then continued at a decreasing rate. Fig. 6 shows the values of photocurrent[4] and dark current during the experiment. The dark current was very low initially but became comparable with the photocurrent when the optical thickness began to increase very rapidly. The photocurrent decreased continuously during the experiment.

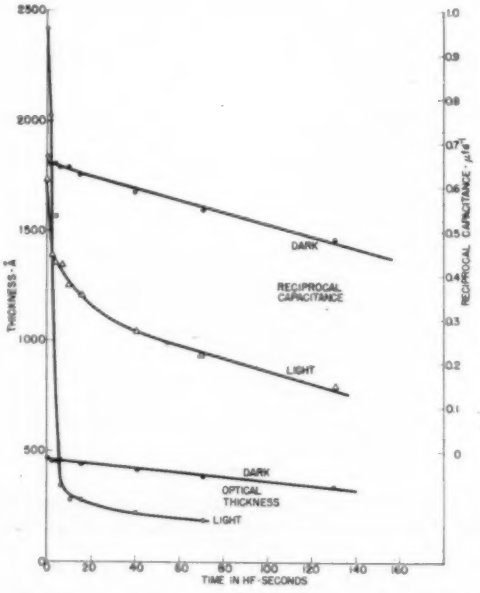

Fig. 7. Decrease in thickness on solution of the film of Fig. 5 in 24% HF.

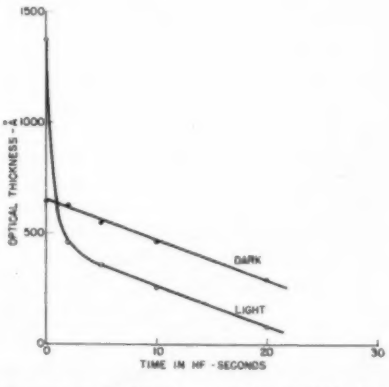

Fig. 8. Decrease in thickness on solution in 48% HF of a film grown in a manner similar to that of Fig. 5 until the optical thickness was 1050Å on the light side, and then formed at 1 ma/cm² to an optical thickness of 1380Å.

When a film formed with a low initial field was dissolved in HF the optical thickness and reciprocal capacitance decreased as shown in Fig. 7. There was a rapid initial decrease of both values for the film on the light side. After the rapidly dissolving part of the film was removed the rates of decrease of optical thickness and reciprocal capacitance became equal on both sides; hence it is likely that the remaining film on the light side was normal Ta_2O_5.

When a film was irradiated with u.v. light with a low initial applied field so that growth occurred as described above, and was then subsequently grown in the absence of u.v. light, it was found that the altered portion of the film remained at the oxide-solution interface. Fig. 8 shows the decrease of the values of reciprocal capacitance and optical thick-

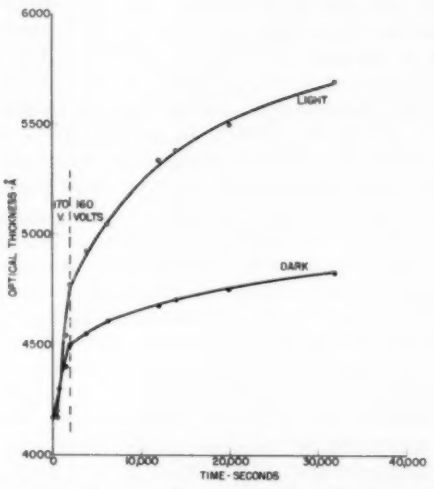

Fig. 9. Growth of a crystalline film illuminated with u.v. light on one side.

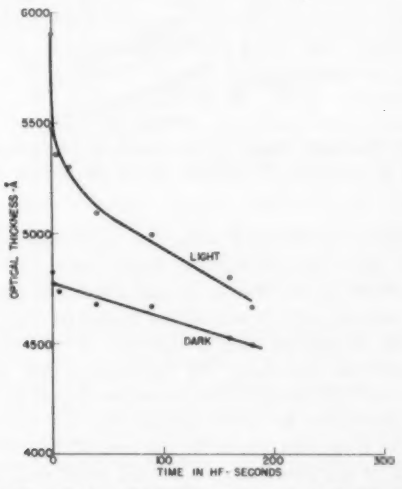

Fig. 10. Decrease in thickness on solution in 48% HF of the film of Fig. 9.

ness when such a film was dissolved in HF. The rapidly dissolving portion of the film was still on the outside of the film; thus, it appears that only oxygen is mobile in this portion of the film.

The transformed portion of the films formed with an initially low field strength is different from that of films formed at higher fields in several respects. In the first place, the conductivity of the altered layer of a low field film is much higher than that of a high field film, as shown by the fact that the altered low field film behaves approximately like a series resistance in the capacitance tests, while the high field film behaves like a pure capacitance. In the second place the dissolution rate in HF is much greater for the low field films (compare Fig. 2 and 7). Another difference is that the high field films are mostly Ta_2O_5 and have only a thin outer layer of transformed material. The low field films, on the other hand, are mainly transformed material with only a thin inner Ta_2O_5 film.

The final difference is that the low field film contains water which can be removed easily. For example, when a specimen formed at an initially low field to an optical thickness of 3580Å was heated to 500°C in air for 30 min, the optical thickness decreased to 3180Å. This change could be partly reversed; soaking the film in water resulted in an increase of the optical thickness to 3230Å after 15 min and to 3280Å after 16 hr. The optical thickness of another specimen heated to 200°C for 1 hr decreased from 3400Å to 3100Å, while on soaking in water for 1 hr the optical thickness increased to 3280Å. Holding at room temperature in a vacuum of 10^{-6} mm Hg changed the optical thickness of a third specimen from 3580Å to 3450Å, and this change could be reversed completely by soaking in water for 1 min. It appears, therefore, that there is some water present in the low field film which can be removed by evacuating or by heating. The high conductivity which short circuits the capacitance of the outer portion of the film is associated with the presence of this water, since after heating at 200°C for 1 hr the electrical capacitance of a specimen decreased from 2.52 mfd to 1.37 mfd, while after soaking in water for 3 hr the capacitance increased again to 2.33 mfd. The capacitance calculated from the optical thickness assuming a Ta_2O_5 film was 1.31 mfd, which is nearly identical with the 1.37 mfd observed after heating. For films formed at high fields, on the other hand, no change in optical thickness occurred on heating at temperatures up to 500°C, and the capacitance increased about 6% instead of decreasing. Such an increase is expected from other data obtained for normal Ta_2O_5 films (6). For high field films, therefore, any water present is bound so strongly that it is not removed by heating at 500°C.

Growth of a Crystalline Ta_2O_5 Film During U. V. Irradiation

U.V. irradiation also produces more rapid growth of a crystalline Ta_2O_5 film. Crystalline films can be formed by anodizing Ta specimens at 90 v in 2% HNO_3 at 100°C for about 15 hr (7). The response of these films to u.v. light was about the same in wave length dependence[8] and the magnitude of the photocurrent for a given light intensity as that of an amorphous Ta_2O_5 film. Upon irradiation of a crystalline film 4170Å thick with 170 v applied for the first 2000 sec and 160 v thereafter the optical thickness increased as shown in Fig. 9. There was a greater rate of growth on the irradiated side, and the outer portion of the film on the irradiated side subsequently dissolved at a more rapid rate in HF as shown in Fig. 10. There was an increase of about 2 ohms in the series resistance of the capacitor formed from the film, and the value of capacitance was about the same as would have been obtained for a film consisting entirely of crystalline Ta_2O_5 of the thickness of the dark side. The photocurrent decreased from 0.5 ma/cm² to 0.05 ma/cm² during the course of the experiment. The behavior is very similar to that observed with amorphous films.

Discussion

The two layer films produced by u.v. irradiation might be formed in the following manner. When a

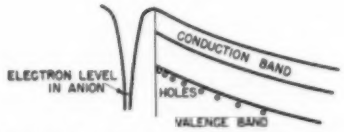

Fig. 11. Schematic drawing of the electronic levels in the oxide film and on anions in the solution during the passage of photocurrent.

Ta_2O_5 film is irradiated with u.v. light, electrons are excited into the conduction band, leaving holes in the valence band. Some of the electrons reach the metal, lowering its potential, as found by Young (4). If a field is applied across the film, a current flows, the electrons traveling via the conduction band to the Ta and the holes in the reverse direction. There would probably be little barrier for the passage of electrons from the oxide to the metal, but it would be difficult for electrons to tunnel from the solution to the full band of the oxide in order to fill the positive holes. A positive space charge would therefore develop near the oxide-solution interface, and the field at the interface would increase until the tunneling process was able to supply electrons from the solution rapidly enough to maintain the current. It is expected that a very large field would be required to bring the level of holes in the full band down to the level of electrons on ions in the solution (*see* Fig. 11). The Fermi energy of the anodic Ta_2O_5 film is not known, and hence an accurate estimate of the field required cannot be made. However, the electronic levels in the solution are many[6] volts below the vacuum and probably lie well below the top of the full band of the oxide. If the top of the full band is 1 v above the level of the electrons in the ions, a field in excess of 10^7 v/cm would be required to make the tunneling distance short enough so that a large current could be carried across the interface. The time required to develop a field of this magnitude at the observed photocurrent, assuming that all of the light is absorbed in the outer 400Å of the film, can be shown to be of the order of a few seconds.

If it is accepted that a positive space charge develops in the oxide film, then the observations made during the growth of the film at high fields can be explained as follows. While the film is very thin, most of the light would be absorbed in the metal rather than in the oxide, little space charge would develop, and the optical thickness and capacitance would be the same whether the film was illuminated or not. After the film had grown to a thickness of a few hundred Angstrom units, nearly all the light would be absorbed in the film (4, 9), an appreciable space charge would have developed and the field near the oxide-solution interface on the irradiated side would be very great. Now in addition to maintaining the photocurrent the increased field at the oxide-solution interface would increase the Ta ion current locally. Ta ions would move out of the outer layers of the oxide more rapidly than they came in from underneath, leaving behind a number of vacancies which could not be filled because of the smaller ionic current in the rest of the film. The resulting negative space charge would cancel part of the positive space charge, but the photo effect would again increase the field at the interface in order to maintain the flow of electronic current.

It is clear that this situation could not exist indefinitely because soon all the Ta ions in the outer portion of the film would be exhausted. Probably as soon as the defect concentration becomes sufficiently large, oxygen ions start to move inward. It would then be possible to reach a steady state with a large defect concentration of both ions in the outer layers and an increased field near the surface, both ions being mobile. Since the change produced in the film by the u.v. light is permanent during further formation in the absence of u.v. light, it is likely that some chemical change in the outer layer occurs in addition to the production of large numbers of ionic defects. By analogy with the films obtained upon formation in nonaqueous solutions which behave similarly and are solvated, it may be that the outer portion of the film becomes hydrated. There is a decrease in the photocurrent by about a factor of two when this altered film is present, perhaps because some of the charge carriers can recombine in the outer layers with its high concentration of ionic defects.

When a film is formed to a certain thickness and then irradiated with a low applied field, a similar transformation occurs as follows. Shortly after irradiation is started, the field at the outer interface is greatly increased in order to maintain the photocurrent. A defect structure is then produced as at a high field strength, and a transformed layer results. However, the experiments showed that the altered portion of the low field film has a different structure from that of the high field film, containing loosely bound water. It is suggested that this film is porous rather than simply hydrated. The explanation for the difference in the structure of the two types of transformed film can be attributed to the fact that some ionic motion occurs in the underlying Ta_2O_5 film when the initial field is high. The influx of ions into the transforming layer from underneath causes some repair of the defect structure, and hence a less drastic change from the original Ta_2O_5.

The curves shown in Fig. 6 and 7 for low field films can be explained in terms of the proposed mechanism in the following manner. Shortly after irradiation is started, the transformation of the outer layers begins. The series resistance and capacitance increase because the outer portion of the Ta_2O_5 is now a poor conductor instead of an insulator. The optical thickness increases slowly during this initial period as Ta leaves the outer portion of the film under the influence of the high field and forms new oxide at the oxide-solution interface. As the transformation proceeds the applied voltage is concentrated across the untransformed portion of the film, since the transformed layer has a low resistance, and the field in this portion therefore increases as transformation proceeds. Finally the field becomes great enough for ionic motion in the inner layer, and rapid growth begins. At this time the dark current, which is now ionic rather than electronic, increases very markedly and becomes comparable in magnitude with the photocurrent. As growth pro-

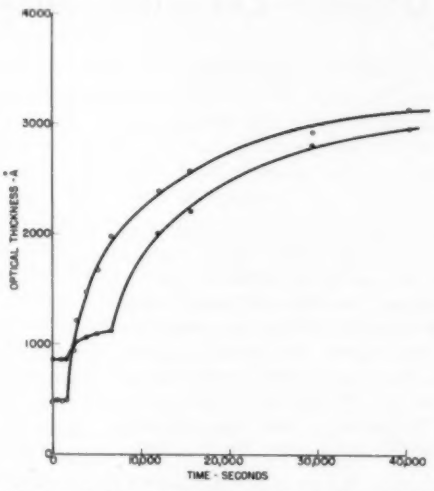

Fig. 12. Growth during illumination of two films initially 485Å and 860Å thick. Both films were held simultaneously at 20 v in 1% Na_2SO_4 solution at room temperature.

ceeds the new oxide formed underneath the transformed region is itself transformed, so that the inner Ta_2O_5 layer remains approximately constant in thickness and the field in it remains high. As the outer porous film becomes very thick, the capacitance decreases again since the porous film does contribute some capacitive reactance.

In order for this explanation to be possible it is necessary for the absorption of some u.v. light to occur in the inner Ta_2O_5 layer. The oxygen necessary for new growth under the porous layer comes from water in the pores. The decrease in photocurrent with time is caused presumably by absorption of some of the light in the porous layer of the film.

According to the proposed mechanism of formation of the highly conducting film, if the initial field was less but the applied constant voltage the same in a low field experiment, it should take longer for the rapid growth to start, since more of the original oxide would have to be transformed to conducting oxide in order to concentrate the voltage in the same small thickness of dense Ta_2O_5. In order to test this prediction, two films of different thickness (485Å and 860Å) were held simultaneously at 20 v in 1% Na_2SO_4 solution at room temperature while being irradiated. Fig. 12 shows that the thicker film required 7000 sec before rapid growth started as compared to 2000 sec for the thinner film.

Summary

1. When Ta_2O_5 films are irradiated with u.v. light while a strong electric field is present in the film, the outer layers of the film are transformed to a material of different composition which dissolves more rapidly in HF than does the Ta_2O_5 film. If the applied field is large enough to cause rapid film growth in the absence of irradiation, the transformed region is still a good insulator and is stable at temperatures up to at least 500°C. If the initially applied field is so low that no growth of the film would occur in the absence of irradiation, the transformed region becomes a poor conductor instead of an insulator, and contains water that can be removed partially by evacuation at room temperature. The low field film is probably porous, and may also be hydrated, while the high field film is probably simply hydrated.

2. When the initially applied field is very low, the production of the transformed layer of low resistance concentrates the applied voltage across the untransformed region of the film. As the transformation proceeds, the field in the untransformed layer rises until eventually ionic motion starts and rapid film growth occurs. The newly formed oxide is itself transformed so that the field in the inner layer remains high and growth continues.

3. Irradiation causes a similar transformation of a crystalline Ta_2O_5 anodic film.

4. It is suggested that the transformation occurs when an increased electric field is produced at the oxide-solution interface by the irradiation. A defect structure is produced as the Ta ion current is increased locally in this increased field, and eventually structural and chemical changes occur as well. The differences observed in the high and low field films are attributed to the partial repair of the defect structure at high applied field by the Ta ion current entering the transforming region from underneath.

Manuscript received May 16, 1956.

Any discussion of this paper will appear in a Discussion Section to be published in the December 1957 JOURNAL.

[1] From Fansteel Metallurgical Co.
[2] G. E. "Germicidal".
[3] Percentage of lamp watts in various spectral ranges as follows: below 2800Å 13%, 2800-3200Å 0.25%, 3200-3800Å 0.25%, 3800-5000Å 1%, 5000-7000Å 0.52%.
[4] The photocurrent is equal to the total current minus the dark current.
[5] Determined by the use of filters which cut off at approximately 2200Å, 2600Å, 2800Å, 3000Å, 3400Å (Corning numbers 2910, 9700, 7740, 0160, and 7380, respectively).
[6] The electronic levels of even the simple halogen anions are about 6-8 v below the vacuum, and other anions have still lower electronic levels (8).

REFERENCES

1. D. A. Vermilyea, *J. Appl. Phys.*, **26**, 489 (1955).
2. D. A. Vermilyea, *Acta Met.*, **1**, 282 (1953).
3. D. A. Vermilyea, *ibid.*, **2**, 482 (1954).
4. L. Young, *Trans. Faraday Soc.*, **50**, 153 (1954).
5. W. Bar, *Z. Physik*, **115**, 658 (1940).
6. D. A. Vermilyea, Submitted to *Acta Metallurgica*.
7. D. A. Vermilyea, *This Journal*, **102**, 207 (1955).
8. R. W. Gurney, "Ions in Solution," Cambridge (1936).
9. L. Apker and E. A. Taft, *Phys. Rev.*, **88**, 58 (1952).

Oxidation of 50 Weight Per Cent Uranium-Zirconium Alloy

Sidney Barnartt, Robert G. Charles, and Earl A. Gulbransen

Research Laboratories, Westinghouse Electric Corporation, Pittsburgh, Pennsylvania

ABSTRACT

The reaction of 50% uranium-zirconium with oxygen at 1 atm pressure was studied over the range 200°-500°C. Two forms of the alloy, the stable ϵ-phase and the quenched γ-phase, were reacted to an oxide-scale thickness of 0.1 mm at the higher temperatures. In general, the weight gain increased linearly with time, although in many cases the oxidation curve showed a bend and could be represented by two straight lines. At 400°C and above, the stable ϵ-phase reacted considerably faster than the γ-phase. The thick oxide scales were porous and showed uranium enrichment. During the formation of thin oxide films at 200° and 250°C the reaction followed the parabolic rate law approximately. The alloy oxidizes somewhat more rapidly than pure Zr, but very much more slowly than U.

Uranium tarnishes rapidly at room temperature. At elevated temperatures the reaction with pure oxygen is very rapid, and even bulk specimens become inflammable above 360°C (1,2). Plots of weight gain (w) vs. time (t) are approximately linear above 200°C, the linear oxidation curve being associated with a cracked, nonprotective oxide.

Zr, on the other hand, is moderately resistant to oxidation and forms a protective layer of ZrO_2 on the surface (3-5). The cubic rate law, $w^3 = k_c t$, is reported to be applicable to the reaction with oxygen over the temperature range 300°-950°C (5), although the parabolic rate law, $w^2 = k_p t$, shows better agreement in some cases (4, 6). It would be anticipated that the addition of U to Zr would decrease the oxidation resistance of the latter. If considerable U could be added, while maintaining high resistance to oxidation and corrosion at elevated temperatures, such alloys would be useful as reactor fuels.

This study concerns the reaction of oxygen with the 50% by weight U-Zr alloy (72 at. % Zr) at temperatures of 200°-500°C. The phase diagram of the uranium-zirconium system (7) indicates that this composition would be a two-phase alloy below 600°C. More detailed studies have shown that a stable ϵ-phase exists at and near the 50% composition (8-11).[1] Above about 650°C this material enters the γ-phase.

Two forms of the alloy were used in these studies. The first,[2] designated "as-rolled," was material that was heated to produce the γ-phase, then quenched rapidly in water and cold-rolled to sheet 0.63 mm (25 mils) thick. This should consist mainly of the γ-phase. The second form, designated "annealed," was prepared from the as-rolled sheet by heating for 24 hr at 800°C *in vacuo* (10^{-5} mm Hg) and then cooling slowly, in order to obtain the ϵ-phase. X-ray diffraction patterns confirmed these structures, although photomicrographs and x-ray data showed that each form of the alloy contained small amounts of a second phase, which was found to be α-Zr in the as-rolled alloy but was not identified in the annealed alloy.

[1] Note that ref. (8) uses an earlier system of naming the phases. The nomenclature used in this report is the one in general use now.
[2] Material supplied by Westinghouse Atomic Power Division.

Experimental

Oxidation Procedure

The rate of oxidation of the alloy in dry oxygen at 1 atm pressure was measured over the temperature range 200°-500°C. Test specimens were heated in a furnace in a slow stream of oxygen; periodically they were cooled and weighed on a microbalance. In this procedure, oxidized specimens were subjected to cyclic thermal stresses, so that the results may not be strictly applicable to conditions of uninterrupted heating.

The oxidizing furnace, shown schematically in Fig. 1, was simply a tube of Pyrex glass, 54 mm ID, with a heater wound over a 30-cm length at the constricted end. In an attempt to achieve a region of uniform temperature at the center of the furnace, the hot zone was surrounded by reflecting Al surfaces. A layer of Al foil covered the glass surface under the heater and around the constricted end of the tube. A perforated Al disk served as reflector at the other end of the furnace. The heating element was a Nichrome ribbon wound over a layer of asbestos and covered with asbestos tape. A stabilized voltage, which could be set at any desired value up to 130 v, provided a constant heat input to the heater. With this arrangement, a given setting of the applied voltage yielded constant furnace tempera-

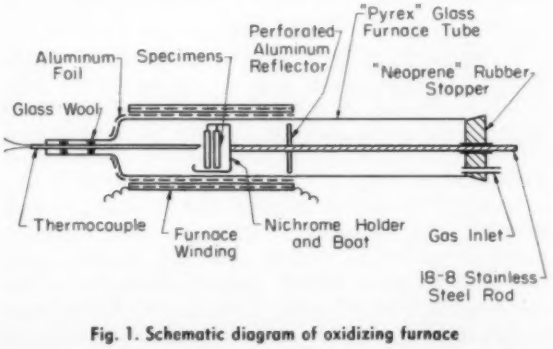

Fig. 1. Schematic diagram of oxidizing furnace

ture to ±3°C, and no change of setting was required for many hours. A Chromel-Alumel thermocouple, situated near the center of the furnace and attached to a recorder, provided continuous temperature-time records.

Test specimens of the alloy sheet were 3 cm x 2 cm in size. To each was attached a Pt hook for handling. Four such specimens, two of as-rolled material and two of annealed, were generally used for each run. They were hung from a Nichrome rod over a Nichrome boat designed to catch any oxide that spalled off during oxidation. (Actually no spalling was ever observed.) When this assembly was pushed into the hot zone, the four specimens were symmetrically situated around the center of the furnace. The temperature variation over the region occupied by the specimens was found to be approximately ±1°C.

The following procedure was used for each period of oxidation. The flow of oxygen through the furnace tube was maintained constant at 0.5 liter/min. Specimens were placed in the cold zone until the hot zone was at a predetermined temperature (10°-15° lower than the desired value). After the specimens were moved into the hot zone, the temperature as indicated by the thermocouple rose to within 3°C of the nominal value in 5 min and to the nominal value within another 10 min. The oxidation period was computed from the moment that the specimens were placed in the hot zone, although an unmeasured interval of time is required to bring the test specimens up to temperature. After the desired oxidation time, the reaction was quenched by moving the specimens to the cold zone and quickly switching the gas flow from oxygen to argon at 2 liters/min.

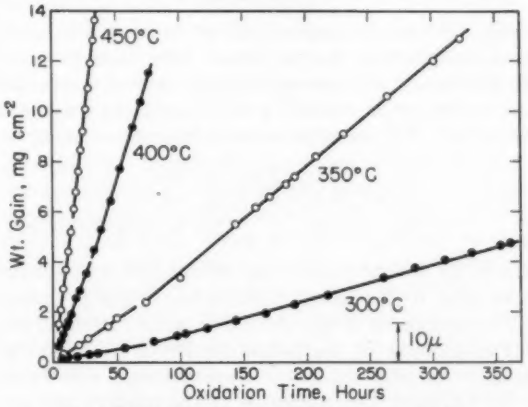

Fig. 2. Oxidation of as-rolled U-Zr alloy, 1 atm O_2

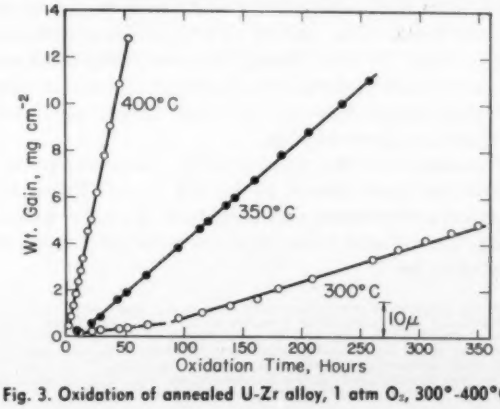

Fig. 3. Oxidation of annealed U-Zr alloy, 1 atm O_2, 300°-400°C

Materials

The alloy analyzed 49.7 ± 0.2% U and 50.1 ± 0.3% Zr. The oxygen content was 0.07%, as determined by the vacuum-fusion method using a Pt bath. The Hf content was estimated to be less than 0.005%, based on analyses of constituent metals. Spectrographic analysis indicated the presence of the following impurities (%):

$$Si < 0.07,\ Mn < 0.03,\ Fe < 0.01.$$

Forty-five other elements specifically sought were not detected spectrographically.

Test specimens were polished to a 4/0 finish using polishing paper wet with purified kerosene, then wiped with petroleum ether, and washed in redistilled acetone. The effects of variations in surface preparation were not studied, since oxidation rates after the formation of relatively thick oxide layers were the primary concern of this study.

The oxygen used was commercial 99.5+% grade, which was dried by passage through a column of $Mg(ClO_4)_2$.

Results and Discussion

Oxidation Rates

Fig. 2-5 show oxidation data obtained over the temperature range 300°-500°C. Each point on the

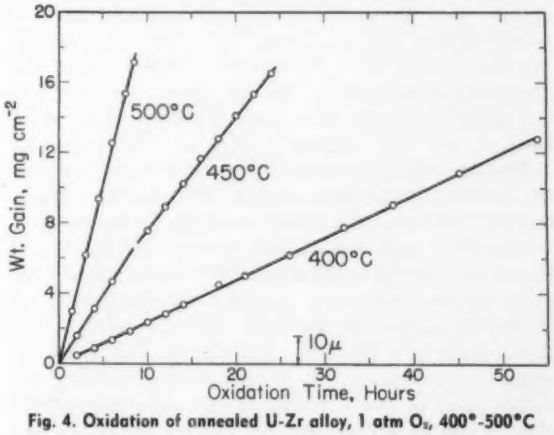

Fig. 4. Oxidation of annealed U-Zr alloy, 1 atm O_2, 400°-500°C

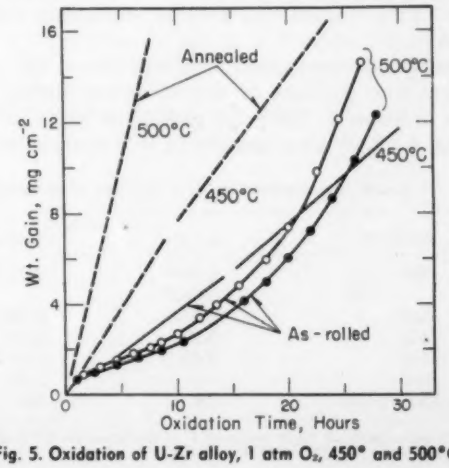

Fig. 5. Oxidation of U-Zr alloy, 1 atm O_2, 450° and 500°C

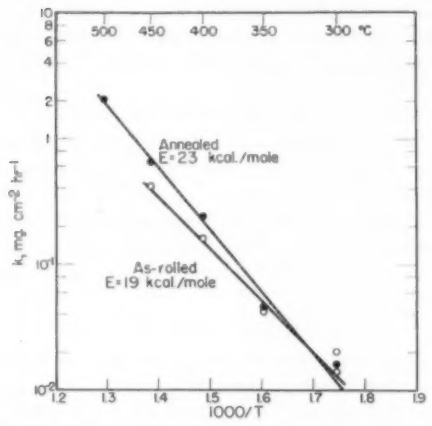

Fig. 6. Oxidation of U-Zr alloy; variation of linear rate constant k with temperature.

curves represents the average weight gain of duplicate specimens oxidized simultaneously. Duplicate specimens always yielded the same general shape of curve, but the individual weight gain varied from the average value by as much as 15%.

In general the 50% alloy, whether as-rolled or annealed, oxidized according to the linear rate law, $w = kt +$ constant. However, a change in the rate constant k, particularly with the as-rolled material (Fig. 2), sometimes occurred after the oxide had grown to an appreciable thickness. Where such a change was found, the linear portions of the curve were drawn with a break near the intersection, merely to accentuate the change in slope. Sharp discontinuities apparently did not occur. The bend in the oxidation curve was toward higher rates in all cases except one (annealed alloy at 450°C, Fig. 4).

The annealed material followed the linear law over the entire temperature range 300°-500°C (Fig. 3 and 4). The as-rolled material oxidized linearly between 300° and 450°C, but not at 500°C. Fig. 5 shows two curves obtained at 500°C in separate runs. Each curve represents average measurements on duplicate specimens oxidized simultaneously. The two curves are far from coincident, but have the same general shape. It is noteworthy that the as-rolled alloy at 500°C oxidized initially more slowly than it did at 450°C. At 400°C and above the annealed alloy reacted considerably faster than the as-rolled.

Linear rate constants, obtained from the final straight-line portions of the oxidation curves, are listed in Table I. They are plotted as log k vs. $1/T$ in Fig. 6. Each plot appears to be linear, although

TABLE I. Linear rate constant, k, as a function of temperature

Temp, °C		k, mg cm^{-2} hr^{-1} As-rolled	Annealed
300	(a)	0.014*	0.016
	(b)	0.020*	
350		0.042	0.046
400		0.16	0.24
450		0.42	0.64
500		—	2.05
E, kcal/mole		19.	23.

* Two separate runs. Each value of k is the average for duplicate specimens. Only run (a) is shown in Fig. 2.

the values of k at 300°C tend to be relatively high and less reproducible. The activation energy E for the oxidation reaction, calculated from the Arrhenius, equation is 23 kcal/mole for the stable ϵ-phase (annealed), and 4 kcal/mole lower for the supposedly unstable γ-phase (as-rolled). Transformation of the latter to epsilon would be expected to occur at an appreciable rate at 500°C, and this may have been a contributing factor in the nonlinear oxidation curve exhibited by the as-rolled material at 500°C.

Oxidation runs on the as-rolled alloy were made also at 200° and 250°C, for periods of 192 and 274 hr, respectively, but these were of a preliminary nature only. The procedure differed from that later standardized (described above) only in the use of an ordinary analytical balance for weighing; hence weight gains were less accurately determined. Nevertheless the oxidation curves obtained were roughly parabolic. Rate constants k_p are compared below with parabolic constants reported for Zr at these temperatures (3):

	k_p, (mg cm^{-2})^2 hr^{-1} 200°C	250°C
50% U-Zr, as-rolled	$3. \times 10^{-5}$	$18. \times 10^{-6}$
Zr	0.38×10^{-5}	3.0×10^{-5} (258°C)

Thus the alloy reacts with oxygen somewhat more rapidly than does Zr at these temperatures. In comparison with U, however, it reacts much more slowly (1, 2).

Oxide Layer

The chemical composition of the surface oxide[3] produced during the oxidation runs was found to be practically independent of the material oxidized (annealed or as-rolled) and of the temperature of oxidation. All analyses were within the range:

U — 40.8 ± 0.8% by wt
Zr — 37.6 ± 0.4 by wt
O — 21.6 by wt (by difference)

The U/Zr weight ratio in the oxide, 1.08, was greater than that in the alloy, 0.99, hence some preferential migration of U into the oxide layer had occurred.

The density of the oxide at 30°C, as measured pycnometrically by water displacement, was found to be 7.6 g/cc. The thickness of the oxide layer corresponding to a given oxygen uptake can be calculated from the density and composition of the oxide. The thickness scale shown in Fig. 2-4 was obtained in this way. It was found, however, that thickness values measured from metallographic cross sections averaged about 20% greater than those calculated, indicating a porous oxide.

The density of the original alloy, measured pycnometrically, was found to be 9.8 g/cc. From the chemical composition and density of the alloy and its oxide, the volume ratio (low temperature) was calculated to be:

[3] In the analytical procedure used, the oxide layer was separated mechanically and fused with potassium bisulfate. The fused material was dissolved in acid, and Zr precipitated as the phosphate. The latter was fused with sodium carbonate, dissolved in acid, precipitated with ammonia, ignited, and weighed as ZrO_2. U in the first filtrate was precipitated as the phosphate on neutralizing, then ignited and weighed as uranyl pyrophosphate, $(UO_2)_2P_2O_7$.

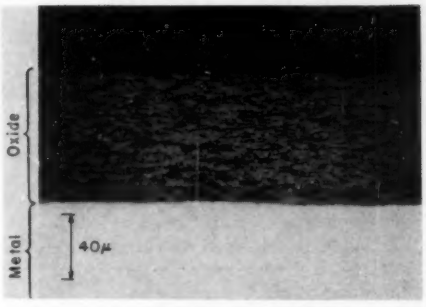

Fig. 7. Cross section of oxide layer produced on as-rolled 50% U-Zr alloy after 76.5 hr at 400°C in oxygen at 1 atm pressure.

$$\frac{\text{volume of oxide produced}}{\text{volume of metal reacted}} = 1.6$$

This ratio is much greater than unity; therefore, according to Pilling and Bedworth (12, 13), shrinkage of the oxide during its formation to yield a cracked layer would not be expected.

A polished cross section of the oxidized alloy is shown in Fig. 7. The oxide is seen to contain relatively large voids. The thick oxides produced over the temperature range 300°-500°C, whether on the as-rolled or the annealed alloy, all exhibited the same type of voids. The latter are elongated in a direction parallel to the oxide-metal interface, indicating periodic formation of blisters at the interface during the growth of the oxide (14). In no case was any transition layer observed at the oxide-metal interface.

As discussed in detail by Evans (14), blistering which forms voids large enough to admit oxygen leads to a linear oxidation curve. On this basis, the bending of a linear curve toward a higher rate of reaction, as was obtained in several cases above, can be explained qualitatively as resulting from an increase in the rate of blistering. Similarly, a decrease in rate constant, which was observed in one case, indicates a slowing down of the blistering process. Some variation in the average size and concentration of voids in the oxide was observed from specimen to specimen, but no correlation was apparent either with temperature or with the initial state of the alloy.

The annealed alloy oxidized to a uniform surface, whereas the as-rolled material exhibited small white spots on the oxidized surface. The white spots began to appear while the oxide layer was still relatively thin, and were grouped along rolling lines. They were similar in appearance to the white particles of ZrO_2 which have been observed in this laboratory on oxidized Zr.

Examination of the bulk oxide scale from the alloy specimens by x-ray diffraction, however, did not reveal the presence of ZrO_2. Diffraction patterns of all oxides produced over range 300°-500°C, with one exception, showed essentially the same lines, and hence indicated the same structure. The lines were too diffuse, however, to permit accurate indexing. Only the oxide produced on the as-rolled material at 500°C gave a different x-ray pattern, and the latter was also too diffuse to permit elucidation of the structure.

Acknowledgment

Data and advice from Dr. R. J. Ruka (x-ray diffraction), J. F. Reed (chemical analysis), and R. L. Anderson (metallography), aided materially in the interpretation of this work.

Manuscript received July 9, 1956. This paper was prepared for delivery before the Cleveland Meeting, Sept. 30 to Oct. 4, 1956.

Any discussion of this paper will appear in a Discussion Section to be published in the December 1957 JOURNAL.

REFERENCES

1. J. Loriers, *Compt. rend.*, **234**, 91 (1952).
2. D. Cubicciotti, *J. Am. Chem. Soc.*, **74**, 1079 (1952).
3. E. A. Gulbransen and K. F. Andrew, *J. Metals*, **185**, 515 (1949).
4. D. Cubicciotti, *J. Am. Chem. Soc.*, **72**, 4138 (1950).
5. J. Belle and M. W. Mallett, *This Journal*, **101**, 339 (1954).
6. E. A. Gulbransen and K. F. Andrew, "Oxidation of Zirconium between 400° and 800°C," paper submitted to *J. Metals*.
7. D. Summers-Smith, *J. Inst. Metals*, **83**, 277 (1955).
8. B. Lustman and F. Kerze, Jr., editors, "The Metallurgy of Zirconium," p. 477, McGraw-Hill Book Co., Inc., New York (1955).
9. A. G. Knapton, Discussion in *J. Inst. Metals*, **83**, 598 (1955).
10. A. N. Holden and W. E. Seymour, Preprint #101, A.I.M.M.E., Nuclear Engineering and Science Congress, Cleveland, Dec. 1955.
11. R. P. Larsen, *et al.*, Argonne Natl. Lab. Report ANL-5135, July 1954.
12. N. B. Pilling and R. E. Bedworth, *J. Inst. Metals*, **29**, 529 (1923).
13. O. Kubaschewski and B. E. Hopkins, "Oxidation of Metals and Alloys," p. 14, Academic Press Inc., New York (1953).
14. U. R. Evans, *Trans. Electrochem. Soc.*, **91**, 547 (1947).

Silicon Diffused Junction "Avalanche" Diodes

H. S. Veloric and K. D. Smith

Bell Telephone Laboratories, Inc., Murray Hill, New Jersey

ABSTRACT

Silicon N+, P, P+ diffused junction diodes have been made by diffusion of B and P into p-type Si. Units have been fabricated with breakdown voltages from 6 to greater than 200 v, with areas from 5×10^{-3} cm² to 5 cm². Design problems associated with high and low voltage diodes are discussed.

Reverse saturation currents at half the breakdown voltage are often in the order of 10^{-6} amp/cm². Impedance after breakdown is shown to be a function of the breakdown voltage and the magnitude of the avalanche current. The cut-off frequency is in the order of one megacycle, and is shown to increase with decreasing transition region capacitance. Some units with areas of 5×10^{-4} cm² have been operated at power levels of 10 w, with special provision for heat dissipation.

The diffusion technique for introducing impurities into semiconductors (1) has been shown to be a feasible method of producing large area p-n junctions or ohmic contacts in Si. This technology has been used to develop a family of diodes for various applications. A series of "avalanche" or voltage limiting diodes are considered in this paper. These diodes are characterized by rather high surge capability, low impedance in the breakdown region, and moderately low saturation currents.

Representative diffusion and fabrication techniques are described in the first sections of the paper; this material is followed by discussion of device characteristics. Of particular interest are the impedance before and after breakdown, temperature coefficient of voltage in the breakdown region, surge capability, and barrier capacitance. Reliability of these devices under various environmental conditions is being studied.

Diffusion of Phosphorus and Boron

If the diffusant is deposited, and serves as an infinite source, then the resulting added impurity distribution in the Si is given by

$$C = C_s \operatorname{erfc} \frac{x}{\sqrt{4Dt}} \qquad (I)$$

where C is the concentration at distance x below the surface, C_s is the surface concentration, D is the diffusion constant, and t is the time of diffusion. The indication is that, if elements in the third or fifth column of the periodic table are considered as diffusants for Si, then the surface concentration and diffusion constant decrease with increasing atomic weight (2). The high surface concentrations of B and P result in degenerate surfaces which facilitate low resistance ohmic contacts to the diode. High surface concentration is also necessary to convert low resistivity material.

For an error function impurity distribution, at some depth x_j the concentration of added donors equals the original acceptor concentration. Here the Si changes conductivity type, resulting in a p-n junction. The concentration gradient, a, at the junction is

$$a = \left.\frac{dc}{dx}\right|_{x=x_j} = \frac{-C_s}{\sqrt{\pi Dt}} \exp \frac{-x_j^2}{4Dt} \qquad (II)$$

The breakdown voltage (3), V_b, in a diffused junction may be increased by increasing the diffusion depth (4), thereby decreasing the impurity gradient. For a given diffusant

$$\frac{V_b}{V_{bo}} = \left(\frac{Dt}{D_o t_o}\right)^{1/4}_{\rho=k} = \left(\frac{x_j}{x_{jo}}\right)^{1/3}_{\rho=k} \qquad (III)$$

where ρ is the resistivity of the starting material, and the subscript o refers to a reference diffusion. For the devices reported here, P is used for the rectifying junction and B for the ohmic contact for diffusion into p-type silicon.

Fabrication

The preparation requires a number of sequential steps which are not inherently difficult. The most critical operations may be carried out on a number of Si slices at one time; each such slice may be used for the fabrication of a large number of device elements. The required Si raw material characteristics depend on the device performance objectives established. A particular breakdown voltage is feasible with a certain range of Si resistivity and diffusion program. Other fabrication details may remain essentially the same for a number of related device designs.

As an example, suppose it is desired to prepare single junction voltage reference diodes, having breakdown voltage near 20 v, using single-crystal p-type Si as the raw material. As noted in Fig. 1 the net acceptor concentration in the Si must be such as to make the resistivity lie in the general range 0.02-0.15 ohm-cm if a reasonable diffusion program is to be used. Thus, the first step in the preparation is to secure sufficient usable material, slice and lap it into 10 mil slices, and to measure the resistivity of these slices in order that the diffusion program may be determined.

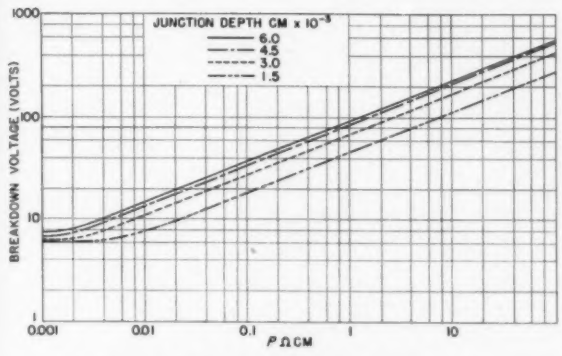

Fig. 1. Breakdown voltage for P diffused *p*-type Si as a function of resistivity and junction depth.

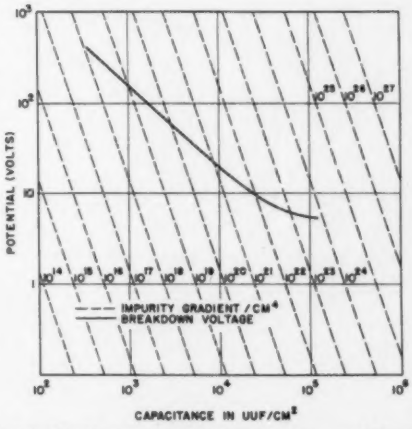

Fig. 2. Relationship for a Si *P-N* junction between impurity gradient, capacitance, and potential.

Diffusion operations are carried out in a quartz tube, in the temperature range 1100°-1350°C. Si slices are exposed to a gaseous environment by standing them on edge in small slots in a quartz boat which is placed in the hot zone of the globar furnace. The diffusant source, in the first case P_2O_5, is located in the quartz furnace tube on the inlet side, at a temperature of about 200°C. Dry N gas is flowed over the P_2O_5 and the Si during the run; this carries sufficient P_2O_5 vapor into the diffusion zone to provide P atoms in high concentration at the Si surface. A high surface concentration of the diffusant is necessary for diode devices, to permit very low resistance electrical contacts to be made. The above procedure results in P surface concentrations in the range 10^{21}-10^{22} at./cm³, thus the surface is degenerate.

After the P diffusion the p-type Si slices have a thin *n*-layer all over their exposed surfaces. To prepare single junction reference diodes, the *n*-layer is lapped off one side of each slice, which is then treated at the diffusion temperature in an atmosphere containing a small concentration of BCl_3 gas. BCl_3 reacts with the exposed Si, depositing B. This second diffusion step may be carried out at a lower temperature or for a shorter time than the initial diffusion, since only a thin p-layer is required to obtain low contact resistance to the Si body. Contact resistances of 10^{-3} ohm are achieved for areas of 1 cm², by application of an electroless nickel plating (5). The plating is subsequently fired for a few minutes in a N atmosphere at a temperature in the 800°-900°C range. After this firing or sintering operation, a second electroless Ni plating is given to facilitate later soldering operations.

Up to this stage in the fabrication, operations are carried out on a group of whole Si slices, of any convenient size or shape. These slices must now be cut into smaller elements before assembly into devices. The sub-assembly is then mounted in a suitable package, which is flushed with an inert gas, and hermetically sealed.

Where appreciable power is to be dissipated, care must be exercised in the design to keep the thermal impedance between the *p-n* junction and external heat sink low. With an element area of 5×10^{-2} cm², mounted directly to a Cu stud, it is not difficult to keep the internal temperature rise below 2°C/w dissipated. The means for external cooling depend on the particular installation.

Design Considerations

Fig. 1 indicates that it is possible to predict the breakdown voltage of a diffused junction in the range from 5 to 1000 v. Fig. 2 shows[1] that for one junction impurity gradient there is one breakdown voltage. The error in predicting the breakdown voltage is the error in predicting the impurity gradient from the measured impurity concentration in the Si and the selected diffusion parameters. Previous work (4) shows that in the range of 10-100 v the mean value of the breakdown voltage of a large group of units can be predicted to within 2%.

Certain design problems are encountered with units intended for voltage limiting applications below 9 v. In this range the ionization rate of electron-hole pairs (3) increases slowly as the field in the barrier region increases. Fig. 2 shows that in this low voltage range the field at breakdown increases rapidly with decreasing breakdown voltage. The maximum field in a diode which breaks down at 4 v has been calculated to be greater than 10^6 v/cm. At these high fields mechanisms other than avalanche also play a role in the breakdown process (6). In Fig. 1 the breakdown voltage levels off in the range near 5 v. The picture is further complicated by the "soft" breakdown characteristics obtained in these low voltage diodes.

In Fig. 3 a plot of the I-V characteristics is given for several typical diffused junction diodes with cross-sectional area in the order of 10^{-2} cm². Two low voltage diodes are shown which have impurity gradients[2] in the order of 10^{24} and 5×10^{26}, respectively. Diffused junction diodes which pass 100 ma at less than 8 v reverse bias are characterized by the "S" shaped curve observed in Fig. 3. It may be noted from Fig. 2 that the breakdown voltage in this range is not very sensitive to variation in the impurity gradient.

The units with breakdown voltages above 10 v have saturation currents less than 10^{-4}Å at low volt-

[1] The relation between "avalanche" breakdown, impurity gradient, and breakdown voltage was calculated from unpublished data supplied by K. G. McKay.

[2] These values were calculated with C. S. Fuller's data (2).

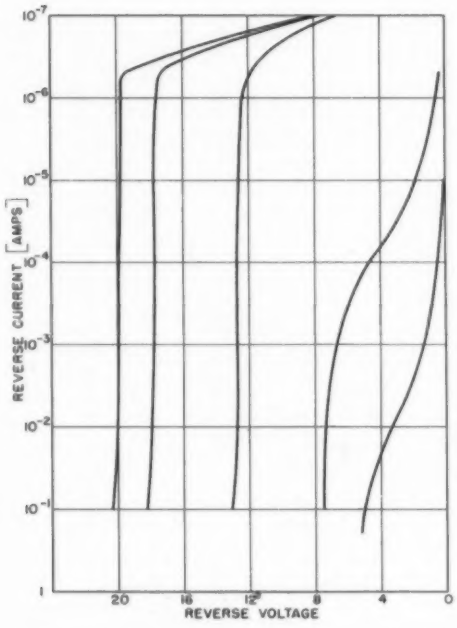

Fig. 3. Current-voltage characteristics of some typical diodes

age and at avalanche breakdown the voltage changes less than 0.5 v for a current change of several decades. In the current range of 10^{-1} to 10^{-5}A series resistance and thermal effects cause a somewhat larger voltage change.

The prediction of breakdown voltage above 100 v is a more difficult problem. In the derivation of Eq. (III) the diffused impurity gradient at the junction was assumed to be linear over the width of the space charge (4) region. In a p-n junction where the depletion layer extends beyond the graded region, the electrical characteristics will approach those of a "step" junction rather than a linear graded one.

Some information on conditions in the space charge region can be obtained by measurements of barrier capacitance at different barrier bias potentials. In plotting log $(V_A + V_i)$ vs. log C, a relation $VC^{m=k}$ would be obtained, where V_A is the applied voltage, V_i is the internal or "built in" barrier voltage, C is the capacitance, and n is a constant. For a linear graded junction, $n = 3$; a step junction, $n = 2$. In Fig. 4, log-log plots of V vs. C are given for several diodes with junction depths in the order of 2.5×10^{-5} cm. It is noted that n is in the range from 2.8 to 3.0 for diodes with V_b less than 60 v. For the 150-v units $n \doteq 2.7$ at low bias, but decreases as the applied voltage is increased. For higher breakdown voltage, barrier conditions approximate those for a step junction at high reverse bias, and the observed value (7) of n is as low as 2.2. The extrapolation to 500 v in Fig. 1 is therefore not strictly justified.

Attempts to use Fig. 1 to predict breakdown voltage for diodes in the range 150-200 v, or higher, gave erratic results. Departures in the order 15% from the predicted values were observed. Further experimentation showed that if Si containing the order of 10^{15} acceptors/cm^3 was heated in the range 1200°-1300°C, relatively large changes in resistivity

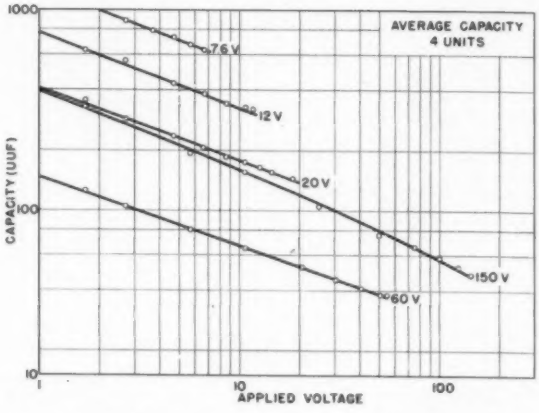

Fig. 4. Depletion layer capacitance of diffused junction diodes

resulted. These changes were unpredictable, and the amount of change varied from crystal to crystal.

In Table I some of the observed resistivity changes are listed. It is interesting to note that use of resistivity values after heat treatment for prediction of breakdown voltage gives better correlation than if the initial resistivities are used. The largest resistivity changes are observed for resistivities above 15 ohm-cm.

Electrical Characteristics

The diffused junction Si avalanche diodes show promise of extensive application as voltage control and surge protection devices. Of particular interest are the low effective impedance in the breakdown condition, and the power handling capabilities. Some other characteristics which have been evaluated are the temperature coefficient of the breakdown voltage, frequency limitations, and some preliminary aging data.

The current-voltage characteristics of a diffused junction diode depend on the internal atomic structure, surface conditions, and the junction area. P-N junction theory (8) predicts reverse saturation current at room temperature in the order of 10^{11} amp/cm^2. This value should be independent of applied reverse bias until the field becomes sufficient to result in avalanche multiplication. In a typical diode

TABLE I. Some thermally induced resistivity variations

	Crystal #	Starting ρ (Ω cm)	(1) After heat treatment ρ (Ω cm)	V_b (Observed) v	(2) V_b (Calculated)
# 1	A–380	11.5	11.5	190	200
	A–320	10.6	8.8	185	185
	314	10.	15.	215	230
	314	7.8	8.1	195	175
	Si IV–378	8.7	8.4	180	180
	Si IV–378	8.7	13.1	185–195	210
# 6	Si A–102	6.2	8.8	135–140	160
	Si A–102	6.2	9.1	145	160
	Si A–102	6.1	7.3		
	Si V–1392	6.6	46.2	180–190	300
	Si V–1392	6.4	35.1	180	290
	Si V–1392	6.9	21.7		

(1) Si was heated in N_2 at 1200° for 16 hr.
(2) The breakdown voltage was calculated from the heat treated resistivity using Fig. 1. P_2O_5 was diffused at 1225° for 16 hr in lot 1 and at 1200° for 16 hr in lot 6.

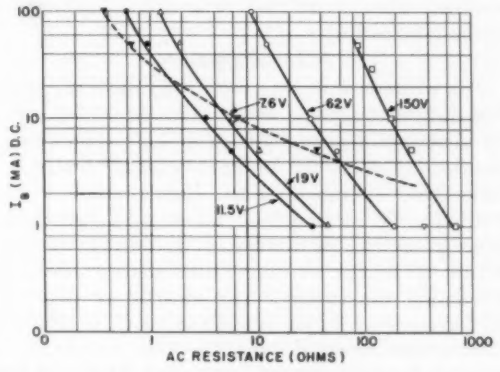

Fig. 5. Impedance in the breakdown region as a function of current

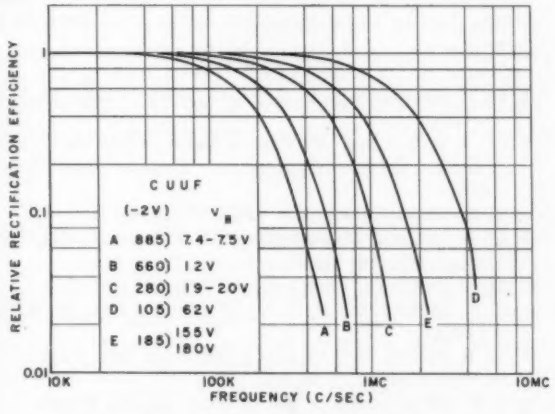

Fig. 6. Frequency response of diffused diodes as low voltage rectifiers.

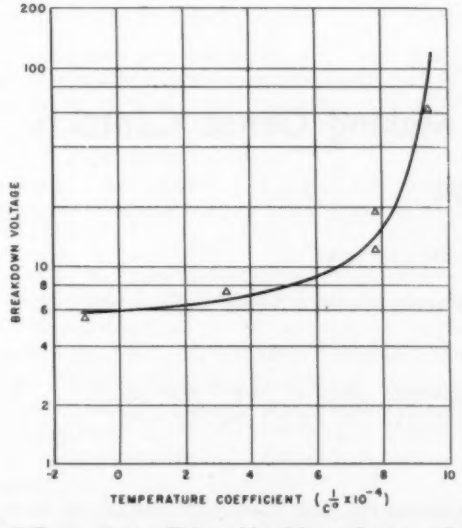

Fig. 7. Temperature coefficient of breakdown voltage vs. voltage

the observed reverse current is many orders of magnitude greater than the predicted saturation current and increases slightly with increasing bias. Diodes with breakdown voltages less than about 7 v exhibit large reverse currents which increase rapidly as the breakdown voltage is approached. This characteristic varies considerably from diode to diode. For all breakdown voltages the transition from high impedance before breakdown to low impedance in the breakdown region is more gradual than predicted by multiplication theory (9) from the low voltage saturation current. Typical current-voltage curves for several diodes are shown in Fig. 3. The forward characteristics of the diodes are as would be expected for a Si p-n junction device, if the body resistance is included in the calculation. The body resistance term becomes small for the lower voltage diodes made of very low resistivity material; forward currents in the order of 1 amp at 1 v forward bias are commonly observed for diodes with breakdown in the 10-20 v range.

The impedance in the breakdown region is a function of the diode structure and the avalanche breakdown current. Impedance at the onset of breakdown is very large; at very high current densities this reduces to a value approaching the body resistance. McKay's breakdown mechanism (10) describes the current as being transmitted by 50-80 μa pulse increments carried in a small spot in the junction. This mechanism would predict a high impedance for a small number of pulses; the impedance should decrease as additional pulses are turned on. For extremely high current densities, such as a pulse of 10^4 amp/cm^2, essentially the entire diode is turned on and only the body resistance is observed. Fig. 5 is a plot of the low frequency a-c resistance in the breakdown region for various breakdown voltages as a function of reverse current. The resistance values were obtained by superimposing a small a-c signal on an adjustable d-c bias current, and measuring the a-c potential across the diode.

The high barrier capacitance associated with large area low voltage breakdown diodes restricts their application to some extent. In Fig. 6 a plot of the rectified a-c current as a function of frequency for several diffused junction diodes, the frequency cutoffs (output D.C. down 3 DB) are observed to be proportional to the transition region capacitance. Curves A, B, C, and D in Fig. 6 are for a series of diodes of approximately 10^{-3} cm^2 area; curve E is for a power diode of about 5×10^{-2} cm^2 area. The location of the response curves along the frequency axis in a plot such as Fig. 6 depends on the load resistance, each curve shifts to a higher frequency if the load resistance is reduced.

Pearson and Sawyer (11) have shown that for certain Si step junctions the breakdown voltage varies linearly with temperature between −196° and 25°C, or

$$V_{B(T)} = V_{B(T_0)}\,[1 + \beta\,(T - T_0)] \qquad \text{(IV)}$$

where $V_{B(T_0)}$ is the breakdown voltage at a reference temperature, and $V_{B(T)}$ is the breakdown voltage at any temperature T. The equation for the temperature dependence of breakdown voltage in a diffused junction has been observed (6) to have the same linear variation. An analysis for diodes of various breakdown voltages in the range −90°-150°C is in qualitative agreement with this picture. Fig. 7 is a plot of the temperature coefficient vs. breakdown voltage. Diodes having substantially zero temperature coefficient of breakdown may be fabricated in the 6 v region.

At this stage in the development it is not possible to make accurate estimates of reliability or life expectancy for the diffused junction avalanche diodes. On the basis of information obtained so far, the following summary statements appear reasonable: *(a)* with present technology, reliable high performance Si junction devices must be hermetically sealed; *(b)* a long life is to be expected if a sufficient heat sink is provided to keep the junction temperature at a reasonable value. Several of the units of element size 5×10^{-2} cm^2 have been operating continuously for more than a year without significant deterioration, at a power dissipation of 10 w. These units were provided with a heat dissipation fin to hold the junction temperature below 100°C.

Conclusion

The gaseous diffusion technique has been used to fabricate a family of avalanche Si diodes with a wide range of breakdown voltage and of junction areas. These diodes have application as voltage regulation or control devices, as voltage reference elements, or in signal circuits as surge protective elements. The impedance of these devices is lower, and the power capability higher, than have been available previously.

Several design and fabrication problems are simplified by use of the diffusion technology: the junction depth may be controlled within 3×10^{-4} cm; the breakdown voltage for a particular Si resistivity can be controlled over a moderate range, by adjustment of the diffusion program; the same fabrication techniques may be used for a wide range of junction areas and device properties; the more critical operations may be carried out on large slices of Si, which are later cut as desired into small elements for device fabrication.

Acknowledgments

It is evident that this work has been made possible only through the cooperative efforts of a number of individuals. In addition to the specific footnote acknowledgments the authors wish to thank T. J. Vasko who obtained all the data on device characteristics, D. W. Bodle for his unpublished data on surge properties of diodes, S. L. Miller, A. Uhlir, and M. B. Prince for many stimulating discussions concerning the theory. The method of presenting the data in Fig. 2 was suggested by C. H. Knowles.

Manuscript received June 13, 1956. This paper was prepared for delivery before the San Francisco Meeting, April 29 to May 3, 1956.

Any discussion of this paper will appear in a Discussion Section to be published in the December 1957 JOURNAL.

REFERENCES

1. G. L. Pearson and C. S. Fuller, *Proc. I.R.E.*, **42**, 760 (1954).
2. C. S. Fuller and M. Tannenbaum, I.R.E. Semiconductor Device Conference, Philadelphia, June 1955.
3. K. G. McKay, *Phys. Rev.*, **94**, 877 (1954).
4. H. S. Veloric, M. B. Prince, M. J. Eder, *J. Applied Phys.*, **27**, 895 (1956).
5. M. V. Sullivan, *This Journal*, **104**, 226 (1957).
6. K. G. McKay and K. B. McAfee, *Phys. Rev.*, **91**, 1079 (1953).
7. M. B. Prince, *Bell System Tech. J.*, **35**, 661 (1956).
8. W. Shockley, *ibid.*, **28**, 435 (1949).
9. S. L. Miller and J. J. Ebers, *ibid.*, **34**, 883 (1955).
10. K. G. McKay, *Phys. Rev.*, **94**, 877 (1954).
11. G. L. Pearson and B. Sawyer, *Proc. I.R.E.*, **40**, 1348 (1952).

Electroless Nickel Plating for Making Ohmic Contacts to Silicon

Miles V. Sullivan and John H. Eigler

Bell Telephone Laboratories, Inc., Murray Hill, New Jersey

ABSTRACT

A technique is described whereby an adherent plate of nickel may be deposited on silicon for use as an electrical contact. The contact may be used on either *n*- or *p*-type silicon.

The use of Si in semiconductor devices is growing very rapidly and each device requires at least two electrical connections to the Si. It has not been possible to make simple reliable soft-solder connections directly to Si as was done in the case of Ge. As a result quite a number of different types of contacts have been devised for use on Si each having certain advantages and certain disadvantages. No one contact, however, has been entirely satisfactory, and the final choice by the device engineer has been a compromise.

Some of the most successful contacts to Si depend on alloying the contact metal with the Si. Some of the metals used for this alloying are Ag, Ni, Al, and Au. All of these are sufficiently soluble in Si to alloy quite deeply. This solubility is a disadvantage when one desires to control closely the depth of penetration of the surface contact metal. Also the resulting alloys are rather brittle and the over-all mechanical properties of the contacts may not be as good as desired. The use of Pb at alloying temperatures under 1000°C avoids both of these difficulties.

Because of its limited solubility in Si the depth of alloying is quite shallow (1), and because of the soft nature of unalloyed Pb there is a minimum of mechanical difficulties.

Although alloy-type contacts are extremely useful, they usually involve high fabricating temperatures which in turn generally result in a loss of the minority charge carrier lifetime of the Si. For some applications this degradation of lifetime is undesirable. Of the various methods studied for making contact at low temperature, an electroless nickel plating appears to be outstanding from both a mechanical and an electrical standpoint.

The method of applying electroless Ni is based on a technique developed by Brenner (2, 3). It involves the catalytic reduction of Ni in a system which is also liberating H. A number of companies have made limited commercial applications of this plating process. The scope of some of these applications and an evaluation of the electroless process has also been reported (4-6). It is believed that the present application to Si is new.

Plating

The reaction is catalytically controlled, and since one product of the reaction, namely, the Ni, catalyzes the reaction, the plate continues to build up indefinitely as long as the temperature, and the supply of appropriate ions are maintained. This is in contrast to a displacement type plating which stops as soon as the base metal is covered by the plate.

Detailed discussion of the various plating bath compositions and general operating features may be obtained from Brenner's articles (2-4). The composition of the plating bath which was used in the present work was as follows:

Nickel chloride ($NiCl_2 \cdot 6H_2O$)	30 g/l
Sodium hypophosphite ($NaH_2PO_2 \cdot H_2O$)	10 g/l
Ammonium citrate [$(NH_4)_2HC_6H_5O_7$]	65 g/l
Ammonium chloride (NH_4Cl)	50 g/l

Solution was filtered

Ammonium hydroxide (NH_4OH) was added until the solution turned from green to blue (pH 8-10).

This solution keeps indefinitely at room or elevated temperatures. When used for plating, the solution becomes depleted in Ni, hypophosphite, and hydroxyl ions. The only addition recommended for laboratory work, however, is that of ammonium hydroxide in sufficient quantity to maintain the blue color. This addition is more necessary in systems like an open beaker where ammonia is lost to the atmosphere.

The hot (90°-100°C) alkaline plating bath with a rapid evolution of H exhibits an excellent cleaning power, and in many cases no special cleaning of the Si is necessary to obtain an adherent Ni plate. In order to make all of the data consistent and reproducible, however, Si was cleaned in the following manner. Surfaces reported as "polished" were mechanically polished with various grades of abrasives ending with 0.1 μ Al_2O_3, and were given a chemical etch (HNO_3, 44%; HF, 18%; H_2O, 38%). Specimens were stored in this condition. Immediately prior to plating the specimens were given a 10-sec dip in HF (48%) and a thorough rinsing in water. Specimens reported as "lapped" were lapped with 600 mesh Carborundum and scrubbed clean with detergent (sodium hexametaphosphate) and water. Immediately prior to plating these specimens were dipped for 3-5 min in boiling NaOH (5%) and rinsed thoroughly with water. A few experiments were performed in which room temperature HF (48%) was substituted for the hot NaOH with no apparent difference in results.

At a temperature of 95°±2°C the Ni plate thickness as a function of plating time was determined and is shown in Fig. 1. (Plating rate increases at higher temperatures and decreases at lower temperatures.) A fresh plating bath containing about 35 cc of plating solution for each square centimeter of Si surface was used for each sample. The initial rate appears to be about 0.02 mm Ni/hr but after about one-half hour the rate drops to about 0.005 mm/hr. This is in reasonably good agreement with the value of 0.008 mm/hr reported by Brenner. Data were taken on lapped Si surfaces; the rate appears to be almost identical, however, on polished surfaces.

The high initial deposition rate has not been explained. Although Ni would be expected to displacement plate on the Si, the high initial deposition rate cannot be attributed entirely to displacement, since other base metals, including Ni itself, cause a high initial deposition rate. Since the high initial rate is observed when plating on any one of several base metals, one immediately considers the bath and its composition as a function of plating time. It is known that a certain ratio of Ni to hypophosphite ion is most efficient (7) and it is possible that in use the bath is departing from this optimum ratio.

Results

A semi-quantitative evaluation of the adhesion of the electroless Ni to Si was made by measuring the

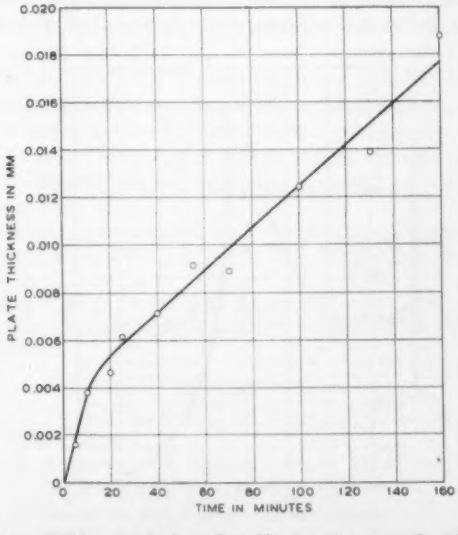

Fig. 1. Thickness of electroless Ni deposits as a function of plating time. The plating rate is about 0.005 mm/hr after the first ½ hr. Each point is one sample. Bath temperature is 95°±2°C.

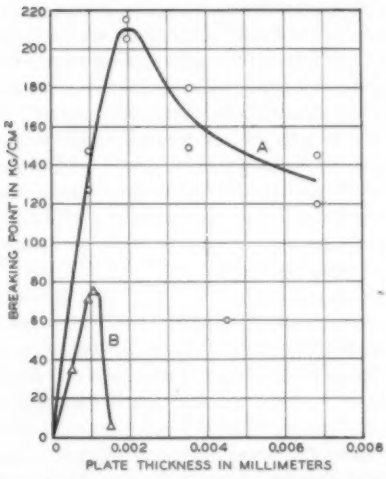

Fig. 2. Adhesion of electroless Ni as a function of plate thickness. Curve A is for a surface which had been lapped with 600 mesh Carborundum and Curve B for a chemically polished surface. Each point is one sample.

force required to pull from the surface a Cu wire that had been soldered to the Ni in the following manner. Tinned copper wire A.W.G. No. 20 was stretched to provide straight sections and was ground flat on one end perpendicular to the axis of the wire. This flat end was butt soldered to the large face of a slice of Ni-plated Si about 0.75 mm thick. A small amount (0.5 mg) of tin-lead solder (50-50) was used so that little or no fillet would be formed and the cross-sectional areas of the bonds would be uniform. Rosin-in-alcohol flux was used.

No heat treatment was given these samples except for the heat involved in the soldering. The force required to pull the wire from the surface was measured with a simple spring-type gauge; the breaking point was then calculated. Fig. 2 shows how this breaking point varied with the thickness of Ni plate. The corresponding deposition times varied from 1 to 30 min. The upper curve is for a surface lapped with 600 mesh Carborundum and the lower curve for a surface which was first mechanically polished (ending with 0.1 μ Al_2O_3) and then chemically polished (HNO_3, 44%; HF, 18%; H_2O, 38%). On lapped surfaces the break was always in the Si. On polished surfaces the separation was predominantly at the Si-Ni interface although small sections of Si were often pulled out. The average area of the break was 1.05 mm² with an average deviation of 15%.

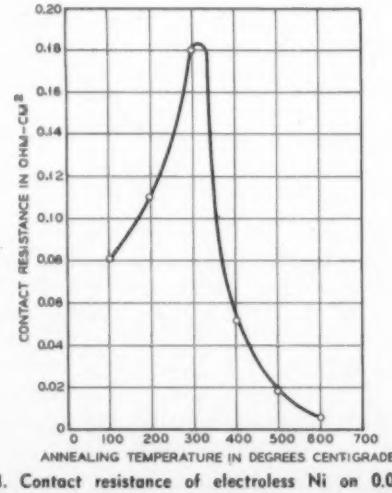

Fig. 3. Contact resistance of electroless Ni on 0.05 ohm-cm *n*-type Si as a function of annealing temperature. Total of 18 samples, 3 for each point.

For these surfaces the optimum adherence was observed for a plate thickness of about 0.002 mm on the lapped surface and 0.001 mm on the polished surface. The increased height of the curve for the lapped surface compared to the height for the polished surface is probably due mainly to the keying action of the surface with the Ni, but it may be due in part to the larger actual surface area involved. The loss of adhesion for thick films is probably due to the increase of internal stress in the Ni with increasing thickness.

The electrical measurements were made by soldering leads to opposite faces of Ni-plated slices of Si about 0.5 mm thick and about 1 cm². The Ni plate was removed from all edges by grinding. The resistance, that is, the d-c voltage divided by the d-c current, was then measured on this specimen. The resistance attributable to the Si itself was calculated from the Si resistivity and subtracted from the measured resistance. The remainder is what is called here the contact resistance and is reported as the number of ohms for a 1 cm² contact.

In view of the fact that the deposited Ni contains phosphorus, one might anticipate doping under some conditions. This means that one might expect to obtain a good ohmic contact to *n*-type Si but a poor, or possibly a rectifying contact, to *p*-type Si if the conditions are such that the phosphorus can diffuse or alloy into the Si.

Contact resistance on 0.05-ohm-cm *n*-type Si is plotted in Fig. 3 as a function of annealing temperature. The samples were annealed for a period of about 1 hr. A second Ni plate was then applied in order to facilitate making the measurements and the contact resistance was measured at room temperature. No significant changes occurred in the Si resistivity. As expected, the contact resistance goes down as a result of high temperature annealing, but the rise in resistance after treatment at intermediate temperatures was not anticipated. The cause of this rise is not known, but it is interesting to note that the peak in the contact-resistance curve occurs in the same range of temperatures that is effective in modifying the hardness of the Ni. As deposited the Ni is quite hard compared to electroplated Ni. On heating at temperatures near 400°C the hardness at first increases, but on heating for longer times or higher temperatures the hardness decreases and the Ni may even become somewhat ductile (4).

With 1-ohm-cm *n*-type Si a similar result is obtained as shown in Curve A of Fig. 4, except that the contact resistance is higher in this case than it was for 0.05-ohm-cm material. In diode fabrication a common technique which is used for improving such a contact is the introduction of a thin layer of highly doped Si between the Ni and the main body of Si. The resistance between a metal and heavily

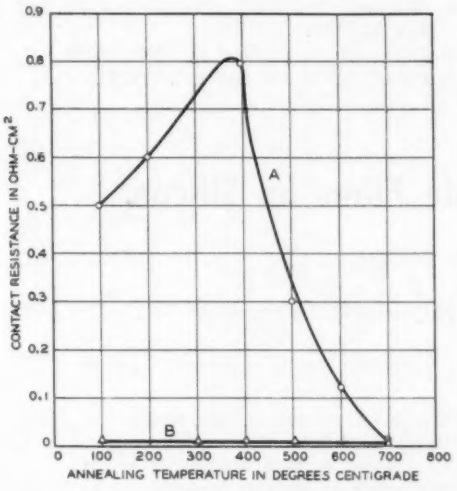

Fig. 4. Curve A, contact resistance of electroless Ni on 1.0 ohm-cm *n*-type Si as a function of annealing temperature. Curve B, similar to Curve A but on material with a diffused *n* layer about 1 mil deep on the 1.0 ohm-cm Si. Total of 22 samples, 2 for each point.

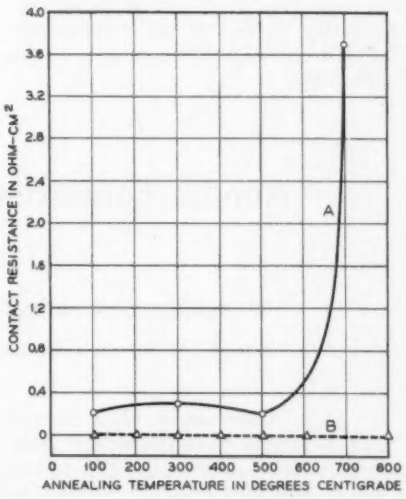

Fig. 6. Curve A, contact resistance of electroless Ni on 1.5 ohm-cm *p*-type Si as a function of annealing temperature. Curve B, similar to Curve A but on material with a diffused *p*-layer about 1 mil on the 1.5 ohm-cm Si. Each point is one sample.

doped (degenerate) *p*- or *n*-type Si is known to be quite low. Such a layer may be formed by diffusing phosphorus from the gaseous phase into the 1-ohm-cm Si to a depth of about 0.01 mm[8]. Curve B shows the resistivity of an electroless Ni contact on such a surface. No peak occurs in the curve.

On *p*-type Si, on the other hand, high temperature annealing causes the contact resistance to become very great and rectification may be observed. Contact resistance on 0.04 ohm-cm *p*-type Si is shown in Fig. 5. It should be noted that for normal temperatures encountered in use, that is 100°-300°C, low contact resistance is obtained. Some simple diodes have been kept on test at 150°C for almost a year with no apparent degradation of the contact.

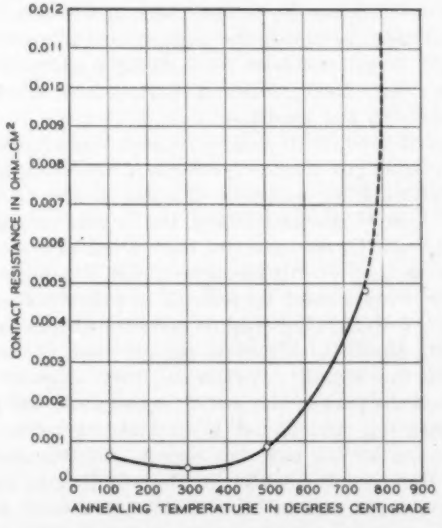

Fig. 5. Contact resistance of electroless Ni on 0.04 ohm-cm *p*-type Si as a function of annealing temperature. Total of 16 samples, 4 for each point.

On the 1.5 ohm-cm *p*-type Si the resistance was appreciably higher as shown in Curve A of Fig. 6. However, just as in the case of the *n*-type Si in Fig. 4, the contact resistance can be reduced considerably by introducing a thin highly doped layer on the surface of the Si. Curve B shows the resistivity of an electroless Ni contact on such a surface. In this case the doping was obtained by diffusing B into the Si (8).

Some of the properties of electroless Ni have already been mentioned, namely, the hardness of the Ni as deposited, the changes which occur on heat treating, the solderability, and the presence of phosphorus in the Ni. Several other properties are also of interest in connection with the present application. The deposit is fine-grained laminar, bright in appearance and relatively nonporous. Deposition occurs quite uniformly over the exposed semiconductor surfaces, thus eliminating excessive build-up on points and thin deposits on recesses. The magnetic permeability is lower than for pure Ni. This is presumably due to the presence of the phosphorus. It is reported that if the deposit contains as much as 11% phosphorus it is no longer ferromagnetic (7). Electroless Ni may also be used in a similar manner on Ge.

Manuscript received May 9, 1956. This paper was prepared for delivery before the Pittsburgh Meeting, Oct. 9-13, 1955.

Any discussion of this paper will appear in a Discussion Section to be published in the December 1957 JOURNAL.

REFERENCES

1. M. V. Sullivan and J. H. Eigler, *This Journal*, **103**, 218 (1956).
2. A. Brenner and Riddell, Grace, E. J., *Proc. Am. Electroplaters' Soc.*, **33**, 16 (1946).
3. A. Brenner, and Riddell, Grace, E. J., *ibid.*, **34**, 156 (1947).
4. A. Brenner, *Metal Finishing*, **52**, No. 11, 68 (1954).
5. A. Brenner, *ibid.*, **52**, No. 12, 61 (1954).

6. Joseph Haas, *Am. Machinist*, **99**, No. 6, 158 (1955).
7. W. A. Wesley, *Plating*, **37**, No. 7, 732 (1950).
8. C. S. Fuller and J. A. Ditzenberger, *J. Appl. Phys.*, **27**, 544 (1956).
9. P. Baeyens, *Nat. Bur. Standards Circ.* 529, p. 25, May 22, 1953.
10. P. H. Eisenberg, *Plating*, **42**, 1268 (1955).
11. L. Pessel, (RCA) U. S. Pat. 2,430,581.

Anodic Formation of Oxide Films on Silicon

P. F. Schmidt and W. Michel

Research Division, Philco Corporation, Philadelphia, Pennsylvania

ABSTRACT

Dense oxide films have been formed anodically on *p*- and *n*-type single-crystal Si in connection with the electrical properties of Si surfaces. Concentrated HNO_3 or H_3PO_4 permit forming, but the highest voltage obtainable is less than 200 v. A solution of KNO_3 in *N*-methylacetamide permits forming to 560 v, and is also preferable in other respects.

The field during forming is of the order 2.6×10^7 v/cm corresponding to a thickness increment of about 3.8Å/v. The ratio has been found as well from interference colors and direct weighing, as by capacitance measurements. Above an oxide thickness of 400Å the rate-limiting step for film growth is inside the oxide.

The ionic current efficiency of film growth is very low. In methylacetamide it can be increased by addition, for example, of chloride ions or more so by fluoride ions. The oxide is an electrolytic rectifier and behaves similar to an oxide on Al or Ta. The direction of easy flow for electrons is from the Si to the electrolyte.

Anodic formation of dense oxide films and the manufacture of electrolytic rectifiers is well known. The classical work on Al was done by Guenterschulze and Betz (1); in recent years, Van Geel (2-5) and Decker (6), Charlesby (7-11), Young (12), Vermilyea (13-16), Adams, Maraghini, and Van Rysselberghe (17), and Misch and Fisher (18) have published on the anodization of Al, Zr, Ta, and U. An extension of the theory of Mott and Cabrera (19) to include the case of thick oxide films was offered by Dewald (20), who also reported work on indium antimonide (21).

There seems to be only one reference to the formation of dense oxide films on Si, given by Guenterschulze and Betz (1), who mention that incomplete forming[1] can be accomplished in concentrated H_2SO_4.

Experimental

Production of dense oxide films on Si was first tried using concentrated acids and some of the electrolytes commonly used for Al (i.e., borate solutions). Formation in concentrated acids (HNO_3) or (H_3PO_4) proved possible but, as already found (1), forming cannot be continued to high voltages in strong acids because of the large concentration of the acid anion. In ammonium borate a dense oxide of comparatively low resistance was formed; porous oxides were formed in oxalic acid or chromate solutions.

Most of the work reported here has been carried out in *N*-methylacetamide,[2] the *N*-methylacetamide being used without further purification. This solvent was used because of its high dielectric constant, 179. The forming was done in an 0.04*N* solution of potassium nitrate in methylacetamide, the bath being kept at room temperature. *N*-methylformamide also permits forming of Si but not nearly so well as methylacetamide. No particular efforts were made to thermostat the system for reasons made obvious below. Addition of a salt like KNO_3 is necessary in order to increase the conductivity of the electrolyte and in order to supply the oxygen for the anodic reaction. Si will not form in *N*-methylacetamide containing only NaCl; forming starts when nitrate or sulfate ions are added.

The Si used, both *n*- and *p*-type, was of resistivity 2-5 ohm cm, single crystalline, 111 oriented,[3] and had lifetime for minority carriers in the order of 10-20 μ sec. Prior to forming, the Si was etched in a 2:1 HF—HNO_3 mixture and then dried in air.

The method of introduction of the Si sample into the electrolyte must be such as to prevent creep of the electrolyte. One way to accomplish this is first to form the Si to a higher voltage than is reached during the actual experiment, then dissolve the oxide at the part of the wafer farther removed from the base tab, and to use the remaining oxide as a protection for the base tab region. Another method is to immerse the wafer in the electrolyte to the desired depth and to blow a slow stream of air at

[1] *Incomplete forming* means that formation in a given electrolyte cannot be carried to the same voltage, which the concentration of the anion in the solution would permit (e.g., if Ta were to be formed in the same solution), but which the solubility of the oxide does not permit to reach. The true maximum forming voltage depends only on the concentration of the anion, provided that the anion does not contain a heavy metal ion like, e.g. $KMnO_4$, compare (1).

[2] Supplied by Distillation Products, Rochester, N. Y.

[3] No effect of crystal orientation was noticed using a 511 plane instead. We are indebted to Dr. Charles Sutcliffe of our metallurgy group for preparation of the samples.

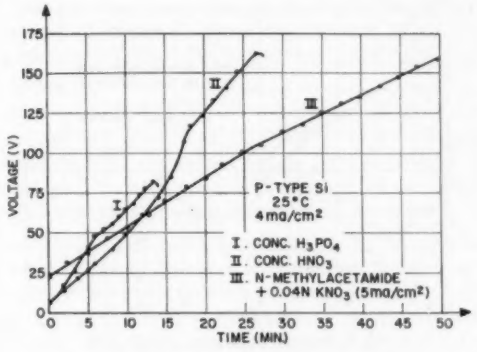

Fig. 1. Forming of *p*-type Si in different electrolytes

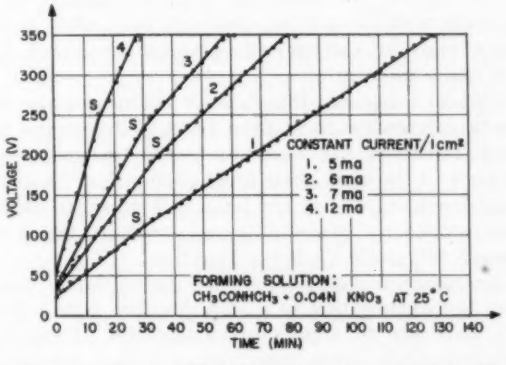

Fig. 2. Forming of *p*-type Si at different constant current densities

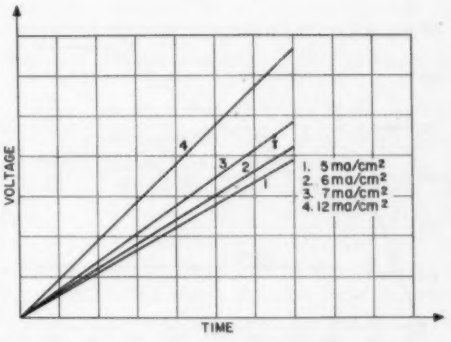

Fig. 3. Replotting curves of Fig. 2 employing a normalized voltage scale.

the rest of the wafer. This method is quite effective against creep of the electrolyte and gives a rather sharply defined area of oxidation. Stop-offs cannot be used at higher voltages because of the very high electrostatic field, which forces the electrolyte underneath the insulation.

Results

Anodic Formation of Oxide Films on p-Silicon

Fig. 1 shows voltage-time curves at constant current density on *p*-type silicon, formed in concentrated HNO_3, concentrated H_3PO_4, and in *N*-methylacetamide.[4] It is evident that the true maximum forming voltage is not reached in the concentrated acids and that also the voltage-time curve is not nearly so linear as in M.A.

Fig. 2 shows oxidation runs on *p*-silicon at different current densities. Several points deserve mentioning.

1. The current density is very high compared to the current density usually employed in the investigation of oxide formation on other metals. The reason is that under the given conditions of forming the ionic current efficiency is only about 0.8%, i.e., of a nominal current density of 7 ma/cm², only 54μa are used for oxide growth, the rest is electronic current due to discharge of ions in the electrolyte. Proof of this assertion is offered in the section on oxide thickness determination.

2. Each curve shows a point, marked "S", at which the slope decreases abruptly. This change in slope is well known in the oxidation of other metals, where it is associated with the onset of the so-called "metal sparks". On Si, no sparks were seen at point "S" or in the branch of the curve above it. This may be due to the very low ionic current efficiency or possibly that the light emission occurs only in the ultraviolet. The curves have been idealized in that small oscillations which always occur, particularly above point "S", are not shown. They are caused by the "metal sparks" and become appreciable when the true maximum forming voltage is approached.

3. If anodization at constant current density is continued after the voltage has risen to 350 v, the oxide breaks down; the voltage starts to oscillate without rising any further, while severe damage to the oxide results. This breakdown phenomenon is not shown in the graph.

4. The higher the current density, the steeper the slope of the curve. In Fig. 3 the same curves up to point "S" are plotted again. The value of V_0 (voltage at time = 0) has been subtracted so that all curves start from the origin, and all current densities have been normalized to unity by dividing the ordinate for each curve by the original value of the current density for the given curve. The curve corresponding to the highest current density has the steepest slope. This must mean that the resistance of the oxide deposited at the higher current densities is larger. This larger resistance could be due either to a thicker oxide layer, i.e., a higher current efficiency, or to a higher resistivity of the oxide.

Even after normalizing the voltage ordinate, the curves are, strictly speaking, not yet comparable because it takes a slightly larger voltage to drive a larger current through the same oxide thickness (log I ≈ field).

On curve No. 3 of this figure is shown the reduction in voltage necessary to drop the current from (its actual value of) 7 ma/cm² to 5 ma/cm². This point was obtained experimentally. This factor is not sufficient to make the 7 ma/cm² curve coincide with the 5 ma/cm² curve.

Samples were always prepared in the same manner, i.e., after a cleanup etch in the HNO_3-HF mixture they were carefully washed under running distilled water, dried in warm air, and inserted in the M.A. bath. However, in view of the large effect of

[4] This solvent is hereafter symbolized by M.A.

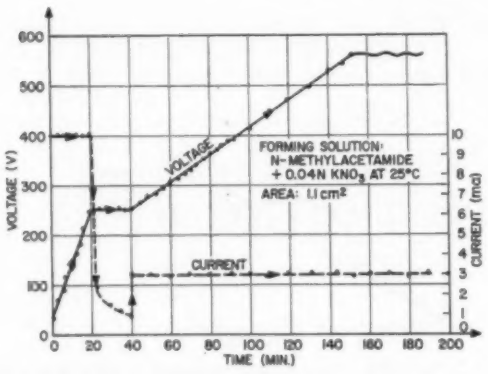

Fig. 4. Forming of p-type Si to a maximum voltage of 560 v

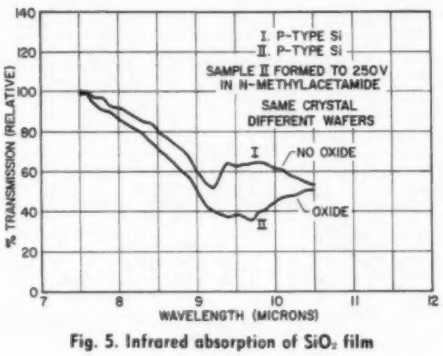

Fig. 5. Infrared absorption of SiO_2 film

fluoride ions on ionic current efficiency, (*see* section on factors influencing the ionic current efficiency) there is a possibility that the rates could be influenced by traces of fluoride having remained on the Si surface. The trend of the curves should not be affected by this.

Measurement of the increases in weight or the changes in interference colors would in principle permit to differentiate between an increase in current efficiency or a change in the nature of the film. On Si, neither of these methods is very sensitive (compare section on oxide thickness determination). However, it is likely that a combination of both effects is involved: on metals like Ta and Al an increase of current efficiency with increasing current density has been reported [*see* e.g. (1) and (8)] and on Zr and Hf formation of low resistance films at very low current densities has also been reported (18).

If a Si sample is held at a constant voltage of 300 v for some time, forming thereafter can be continued up to 560 v. At 560 v bright sparks appear in the solution, the true maximum forming voltage having been reached (*see* Fig. 4).

The slope of the curve after forming at constant voltage is considerably steeper than before, i.e., the ionic current efficiency is higher. For a given increase in forming voltage the increase in thickness is considerably greater than it was before forming at constant voltage as shown by the interference colors. It is likely that forming at constant voltage induces a structural change of the oxide. Vermilyea (16) has reported similar phenomena on Ta.

Determinations of the Oxide Thickness

Thicknesses of oxide films *in situ* can be measured by direct weighing of the sample, by optical methods, and by capacitance measurements.

Weighing.—Direct weighing of p-silicon sample before and after anodization gave an average value of about 9 μg of weight increase/cm² for each 100 v increase in forming voltage (forming done at a current density of 6.2 ma/cm² and the sample then kept at constant voltage for 10 min). This indicates a thickness increment of about 4Å of SiO_2 for 1 v rise in forming voltage. The determination presumes that no SiO_2 is lost by solution in the electrolyte. In view of the fact that only electrolytes with an extremely low dissolving power for the oxide permit obtaining the true maximum forming voltage (as is possible with Si in M.A., although only after forming at constant voltage) this assumption is probably not much in error.

Optical methods—Interference colors and also infrared absorption have been tried to determine the oxide thickness. Fig. 5 gives infrared measurements. In view of the high noise level encountered in these measurements, it has not been attempted to utilize this method for oxide thickness determinations, although this could probably be done.

Interference colors on Si are rather faint; however, by evaporation of a thin Au film (20Å) they can be made to appear quite brilliant. Thickness determinations from interference colors require a knowledge of the refractive index of the film. In order to obtain the refractive index of the film *in situ*, the method indicated by Charlesby (8) has been applied. On Si, the first order blue extends up to 300 v. Above 350 v the thickness voltage relationship valid up to 350 v is lost; consequently, only different shades of blue and a silver-green film (350 v) are available for the determination. Determination of the refractive index in white light gave a value of about 1.5 which is a reasonable value for silica.

For the blue wave lengths a value of $n = 1.55$ was adopted with some degree of arbitrariness for the calculation of the oxide thickness. Using $n = 1.55$ the voltage-thickness relationship as given in Fig. 6 was calculated. The straight line relationship is very gratifying in view of the many inaccuracies involved. A small negative phase shift can be noted in Fig. 6. Such a negative phase shift of a similar

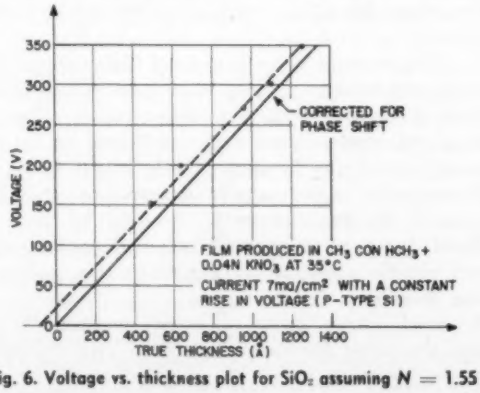

Fig. 6. Voltage vs. thickness plot for SiO_2 assuming $N = 1.55$

magnitude is also observed on Al (1). The thickness-voltage increment from Fig. 6 is 3.8Å/v and checks with the increment found by direct weighing of the sample.

If the charge required for deposition of an oxide film of a given thickness is compared to the total charge passed during anodization (compare Fig. 2) it can be seen that at a current density of 7 ma/cm² the ionic current efficiency is only about 0.8%.

Capacitance measurements.—Assuming a surface roughness factor of about 1.5, capacitance measurements of the Si-oxide system yielded the same voltage-thickness increment as obtained from interference colors. Capacitance measurements, however, are not a convenient way of measuring the oxide thickness on a semiconductor like Si, since the capacitance includes also the space charge inside the Si. Capacitance measurements are being made at present with the purpose of investigating the behavior of the barrier inside the Si as a function of oxide thickness, and of investigating space charges inside the oxide according to the methods developed by Van Geel (4, 5).

An exact measurement of oxide thickness would permit establishing the dependence of the ionic current on the electric field strength; present data are not good enough for this purpose. From the ratio of 3.8Å/v it can only be said that fields of the order of 2.6×10^7 v/cm are involved, which is not surprising in view of the great stability of the SiO_2 lattice. It is obvious that a more accurate determination of the thickness-voltage increment could be made either gravimetrically, or by interferometry using monochromatic light, or by use of the polarimetric method developed by Vasicek (22); such was not attempted, however, because other measurements appeared more urgent.

Factors Influencing Ionic Current Efficiency

Addition of small amounts of water to the M.A.-KNO_3 solution increases the forming rate by a factor of about two without apparently effecting the thickness-voltage relationship. The best forming is at 2.5 vol % H_2O. However, the deviation in rate, i.e., the divergence of the voltage-time curves, becomes apparent only after a certain anodization time, e.g., after 2 min at a current density of 10 ma/cm². On the other hand, drying of the M.A. with calcined K_2CO_3 does not change the slope of the voltage-time curve.

Fig. 7 shows anodization runs in M.A. + KNO_3 in the presence of chloride ions. A very great increase in ionic current efficiency can be seen, but again it becomes apparent only after a certain time has elapsed. The curves show a slope increasing with time, which can probably be ascribed to a continuous increase in temperature of the oxide layer.

Recent experiments using fluoride ions instead of chloride ions (e.g., a solution of 40 mg KNO_3 and 5 mg NH_4F in 10 cc of M.A.) showed the same effect even more pronounced. The ionic current efficiency increases to above 50%; at the same time the film thickness (for a given forming voltage reached at constant current operation) is reduced to about half of its value in the absence of fluoride ions. It was observed, furthermore, that at constant voltage the film thickness increases quite rapidly.

Tentatively the authors attribute the phenomenon to the incorporation of fluoride ions into the oxide film.

Anodic Oxidation of N-Type Si

The anodic current is in the reverse direction for a barrier on *n*-type Si, consequently, the rate of the anodic oxide growth is limited by the supply of minority carriers, holes, to the Si-oxide interface. Therefore, it is to be expected that the rate of forming is sensitive to minority carrier generation, and that the voltage-time curves on *n*-Si have different shapes in the dark than under illumination. Fig. 8 shows that this is indeed the case. Several peculiarities deserve discussion.

In the dark, the voltage necessary to drive a current of 7 ma/cm² is initially about 200 v but drops rapidly to about 100 v, becoming more or less stable at this value until the voltage after about 6 min of anodization again begins to rise linearly with time.

The initial drop from 200 to 100 v cannot be attributed only to excessive power dissipation across

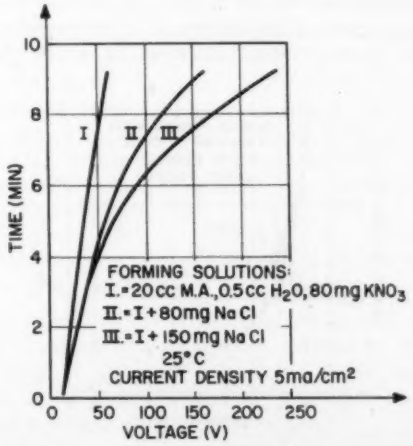

Fig. 7. Forming of *p*-type Si in the presence of chloride ions

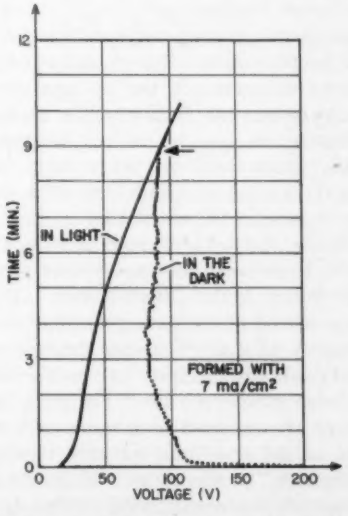

Fig. 8. Forming of *n*-type Si at a constant current density in darkness or under illumination.

the reversely biased n-Si barrier, as can be seen from the following simple experiment. After the voltage has dropped to 100 v forming is discontinued for several minutes; if forming is then resumed at the same current density, the voltage shows no tendency to go much beyond the value at which forming was discontinued.

It would appear that the first layers of oxide deposited decrease the height of the barrier inside the n-type Si.

The curve taken under illumination of the wafer is similar to that on p-Si but is slightly convex to the ordinate. The illumination was rather weak; in strong light the curve would probably straighten out completely.

The following method was used to measure the heat generated by power dissipation across the barrier in the Si. An Al alloyed diode was formed on the reverse side of a wafer to be anodized. The alloyed region was at a distance of 3 mils from the front surface of the wafer. The reverse saturation current of the diode as a function of temperature was measured in a separate run. Monitoring the magnitude of the reverse saturation current of the diode was then used as a measure of the temperature inside the Si during anodization. Only the front surface of the wafer was accessible to the electrolyte, the rest was embedded in plastic.

This measurement indicated that the temperature at a distance of 3 mils from the front surface rose to approximately 65°C within 30 sec of anodization at a current density of 6 ma/cm^2, the bath temperature being 25°C.

Fig. 8 shows that the curves in light and in the dark merge at about 100 v, corresponding on p-Si to an oxide thickness of about 380Å. Above this point anodic oxide growth on n-Si is no longer sensitive to hole injection by light or other means. The oxide thickness on n-Si, when formed under illumination is also about 380Å, as shown by the interference colors. The oxide thickness on a sample anodized in the dark is somewhat larger, because this oxide grew at a higher temperature because of the large power dissipation.

If light is shone onto an n-type Si wafer, anodized in the dark, or, conversely, if illumination of an n-type Si wafer is cut off, the voltage necessary to drive a given current will change sharply. This photosensitivity is lost at an oxide thickness of about 400Å. From there on, the voltage-time curve is a straight line. A thickness of 400Å is reached somewhat sooner in the dark than under illumination, due to the above mentioned heating effect. The dark curve, therefore, becomes linear earlier than the curve taken under illumination. If an n-Si sample is anodized at a constant voltage of less than 100 v (actually 45 v were chosen for this particular experiment), photosensitivity of the anodic current disappears also after some time. Forming under constant voltage should lead to a more ordered structure of the oxide, and thus increase the mean free path of electrons in the oxide. It seems plausible that the loss of photosensitivity is due to collision ionization in the Si by electrons coming out of the oxide at high speeds.

Loss of photosensitivity has a twofold meaning in that it indicates that above about 400Å the rate-determining step for oxide growth occurs inside the oxide, and that the field at the oxide-Si interface (or perhaps the energy dissipation there) is large enough to satisfy the supply of minority carriers for the growth of the oxide.

This assertion can be proved better if anodization is done at constant voltage instead of at constant current. At constant voltage, the current decays to a small value. In the dark, part of the voltage is dropped across the oxide, part across the reversely biased n-Si barrier. If light is now allowed to shine onto the wafer, more of the voltage will be dropped across the oxide; simultaneously, positive ions become available at the oxide-Si interface. A larger current can now flow, which results in an increase in the oxide thickness. When the oxide has reached the thickness corresponding to the given voltage drop the current again decays to a small value. This process is repeatable with successively higher voltages, provided the sample is not kept under constant voltage for any greater length of time, (compare above), but only up to a limiting oxide thickness of about 400Å. Above this thickness the magnitude of the forming current at constant voltage does not depend on illumination or hole injection by other means.

These measurements could mean that above an oxide thickness of about 380Å the barrier inside the n-Si disappears. Fig. 9 shows that this is not the case. The sample was formed to 150 v under illumination, then, without forming at constant voltage, the bias over a period of 80 sec was reduced to zero. During the same time chopped light fell onto the wafer (duration of the light and dark pulse 1.66 sec each). There is a voltage range in which the resistance of the system is photosensitive. The capacitance behaves in the same manner. The higher the voltage, to which the sample had been formed, the narrower the region of photosensitivity (Fig. 10).

Electrolytic Rectification by the Oxide Film

Fig. 11 shows the voltage necessary to drive the same current either anodically or cathodically as a function of time of anodization or oxide thickness. The cathodic curve for p-Si is shown both in the dark and under illumination, as is the anodic curve for n-Si. Since the current densities on Si, Al, and

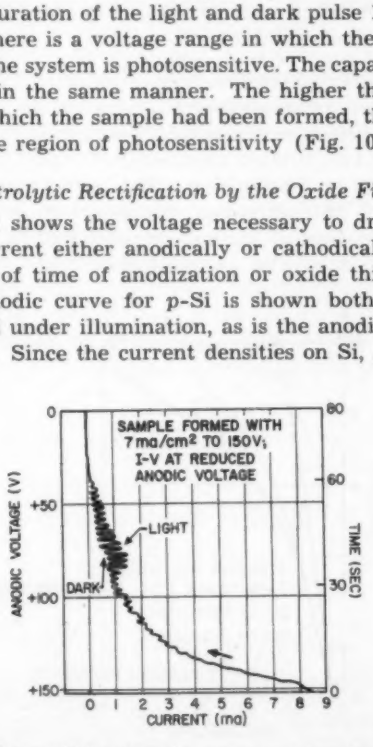

Fig. 9. Photosensitivity of anodic current on n-type Si at reduced voltage. Sample formed to 150 v.

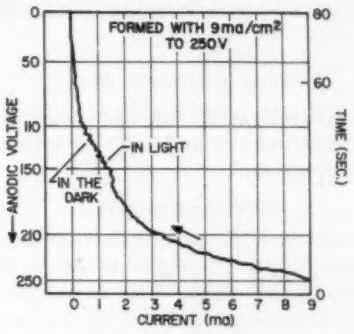

Fig. 10. Photosensitivity of anodic current on *n*-type Si at reduced voltage. Sample formed to 250 v.

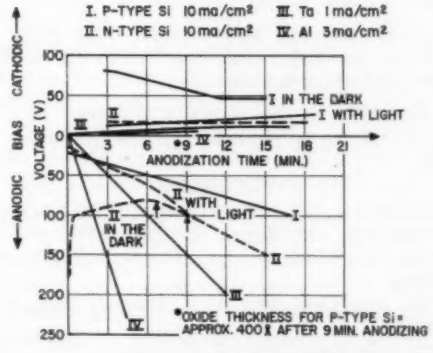

Fig. 11. Rectification by anodically formed oxide films on Si, Ta, and Al.

Ta are different, the anodic curves for the three metals have greatly different slopes.

As can be seen *n*-Si behaves cathodically like Al or Ta. The cathodic curve has hardly any slope at all.

P-type Si under illumination behaves cathodically in the same manner as *n*-Si. In the dark, the cathodic curve shows a peculiar behavior which, as yet, has not been investigated closely. At greater oxide thicknesses the cathodic voltage on *p*-Si is definitely much smaller than the anodic voltage for the same current density.

If a formed *n*-Si wafer is cathodized above a certain critical voltage, about 12-15 v, the current suddenly increases in magnitude. If cathodizing is continued, the oxide is "deformed"; and on switching the current in the anodic direction, the voltage necessary to drive a given current is much smaller than before cathodizing, however, returning to its old value within about 30 sec. Exactly the same phenomenon was reported by Van Geel and Bouma (3) for Al.

Electronic Current Through the Oxide in the Direction of Difficult Flow

Fig. 12 shows the current in the anodic direction on the same *p*-type Si sample, formed to 300 v and then kept at 300 v for 1 hr, 5 hr, 23 hr, and 35 hr. There is, of course, a strong decrease in current during forming at constant voltage.

Vermilyea (14) has reanalyzed Charlesby's (9) data concerning the electronic current through thin

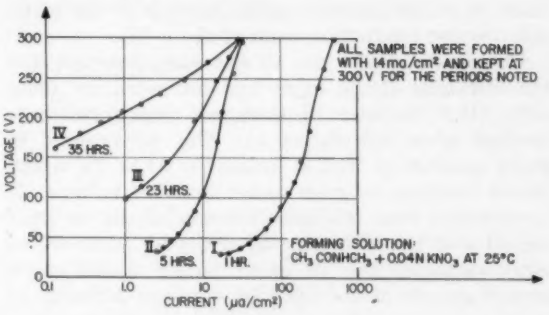
ALL SAMPLES WERE FORMED WITH 14 ma/cm² AND KEPT AT 300 V FOR THE PERIODS NOTED
35 HRS.
23 HRS.
5 HRS.
1 HR.
FORMING SOLUTION: CH₃CONHCH₃ + 0.04N KNO₃ AT 25°C
VOLTAGE (V)
CURRENT (μa/cm²)

Fig. 12. Electronic current through SiO_2 film on *p*-type Si in the anodic direction after differing forming times.

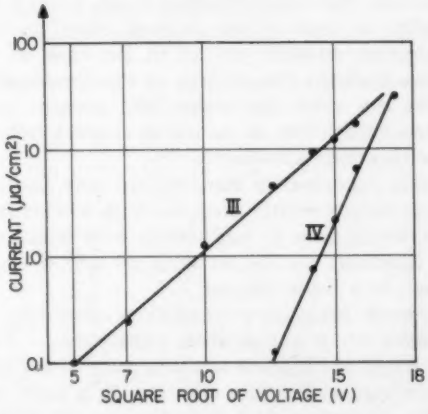

Fig. 13. Replotting of curves III and IV from Fig. 12 according to Vermilyea.

layers of ZrO_2. He suggests a mechanism which yields a linear relationship on plotting log I vs. square root of the voltage. If the same method of plotting current vs. voltage is used for a well-formed *p*-type Si sample, e.g., the ones formed for 23 and 35 hr, a linear relationship results in the voltage range 250-25 v, as shown in Fig. 13.

The longer the time the sample is kept under constant voltage, the larger the range in which the linear relationship holds, and the steeper the slope of the straight line. According to Vermilyea it should be possible to calculate the dielectric constant of the oxide from this slope. There is a strong tendency for the slope to go toward the expected value with increasing time of forming at constant voltage; however, the value for ϵ for the sample formed for 35 hr at 300 v is still too large by a factor of 2.20, assuming $\epsilon = 3.78$ for fused quartz. After forming for 35 hr, part of the oxide became opaque indicating a structural change in the oxide and probably also a change in dielectric constant. Therefore, the experiment was discontinued at this point. Vermilyea's theory does not explain the existence of rectification by the oxide. On the other hand, Schottky (23) has recently considered the possibility of electron tunneling occurring through the whole oxide layer under the influence of the very high electric field in the oxide. This assumption, in conjunction with Vermilyea's derivation, could perhaps explain the I-V characteristic, as well as the existence of rectification. No high barrier would

exist for electrons entering the oxide from the metal side (or the conduction band of the *n*-Si).

During the 35-hr run it was also observed that the thickness of the oxide had increased by about 30% (this increase in thickness was taken into account when calculating ϵ). This behavior is in sharp contrast to that of oxides on Al or Ta which do not continue to grow under constant voltage. It is surmised that this phenomenon might be connected with the wide spacing of the SiO_2 lattice and with vacancies in the anion lattice which could permit growth of the oxide by outward diffusion of oxygen vacancies.

Rectification of Metal Contacts on Si

The fact that the SiO_2 film is an *n*-type semiconductor, at least at the oxide-Si interface, raises the question whether or not in the case of metal contacts made to the surface of the semiconductor (24, 25) the very thin oxide film present around and underneath the Si to metal contact influences the rectification behavior.

As was reported by Bornemann (26), low work function metals rectify on *p*-Si, high work function metals rectify on *n*-Si, and metals with intermediate work functions rectify on both *p*- and *n*-type Si, although to a lesser degree.

The work function picture alone, however, does not suffice for a quantitative explanation. Among other things, the highest barriers on *p*-Si are higher than the highest barriers on *n*-Si. It is quite likely that the oxide film has something to do with this behavior.

Gold electrodes have been evaporated onto formed *n*- and *p*-type Si, and *n*-type rectification was found on *n*-Si, and *p*-type rectification on *p*-Si. Normally, as already stated, gold is ohmic on *p*-Si.

Comparison of Forming in Aqueous Solution and in M.A.

Vermilyea (15) reported that forming of Ta in ethylene glycol solution resulted in the deposition of two different oxide layers, one on top of the other. Except for a greater brilliance of the interference colors obtained in aqueous solution, there appeared to be no difference between Si samples formed to the same voltage in M.A. and in concentrated HNO_3. However, in view of the extreme thinness of the SiO_2 film, small differences in interference colors might be difficult to detect.

In order to check the influence of the M.A. on the oxide film with a more sensitive indicator, Ta was formed both in aqueous KNO_3 solution and in M.A. Except for a greater brilliance of the colors obtained in aqueous solution, no difference in thickness was observable. The thickness of the tantalum oxide film as determined from interference colors agreed with the thickness determination from capacitance measurements.

Forming of Ge *in M.A.*

Both *p*- and *n*-type Ge can be formed in M.A. in much the same manner as Si. These measurements are now in progress.

Acknowledgments

The authors wish to acknowledge the helpful discussions and criticisms extended by Dr. E. H. Borneman and Mr. J. F. Walsh. The work described in this paper was supported in part by the Department of Navy, Bureau of Ships, under Contract No. NObsr-64760, Index No. NE-110458-Subtask 3. The authors are grateful to Bureau of Ships for permission to publish.

Manuscript received May 1, 1956. This paper was prepared for delivery before the San Francisco Meeting, April 29 to May 3, 1956.

Any discussion of this paper will appear in a Discussion Section to be published in the December 1957 JOURNAL.

REFERENCES

1. A. Guentherschulze and H. Betz, "Elektrolytkondensatoren," M. Krayn, Berlin (1937).
2. W. Ch. van Geel, *Philips Research Repts.*, **6**, 54 (1951).
3. W. Ch. van Geel and B. C. Bouma, *ibid.*, **6**, 401 (1951).
4. W. Ch. van Geel, *ibid.*, **8**, 47 (1953).
5. W. Ch. van Geel, *Halbleiterprobleme*, **1**, 299 (1954).
6. A. J. Decker, *J. Applied Phys.*, **21**, 708 (1950).
7. A. Charlesby, *Proc. Phys. Soc. (London)*, **66B**, 317 (1953).
8. A. Charlesby, *Acta Metallurgica*, **1**, 340 (1953).
9. A. Charlesby, *ibid.*, **1**, 348 (1953).
10. A. Charlesby, *ibid.*, **2**, 314 (1954).
11. A. Charlesby, *ibid.*, **2**, 668 (1954); **2**, 698 (1954).
12. L. Young, *Trans. Faraday Soc.*, **50**, 153 (1954); **51**, 1250 (1955).
13. D. A. Vermilyea, *Acta Metallurgica*, **1**, 282 (1953).
14. D. A. Vermilyea, *ibid.*, **2**, 346 (1954).
15. D. A. Vermilyea, *ibid.*, **2**, 482 (1954).
16. D. A. Vermilyea, *This Journal*, **102**, 207 (1955).
17. B. Adams, Jr., M. Maraghini, and P. Van Ryssel-berghe, *ibid.*, **102**, 502 (1955).
18. R. D. Misch and E. S. Fisher, *ibid.*, **103**, 153 (1956).
19. N. Cabrera and N. F. Mott, *Repts. Prog. Phys.*, **12**, 163 (1948-9).
20. J. F. Dewald, *This Journal*, **102**, 1 (1955).
21. J. F. Dewald, *ibid.*, **104**, 244 (1957).
22. A. Vasicek, *Czechoslovak J. Physics*, **4**, 204 (1954).
23. W. Schottky, *Halbleiterprobleme*, **2**, 233 (1955).
24. W. E. Bradley, J. Tiley, R. E. Williams, R. Kansas, R. F. Schwarz, J. Walsh, and J. Angell, *Proc. IRE*, **41**, 1702 (1953).
25. E. Bornemann, R. Schwarz, and J. Stickler, *J. Applied Phys.*, **26**, 1021 (1955).
26. E. Bornemann, to be published.

Semiconducting Properties of Some Vanadate Glasses

P. L. Baynton, H. Rawson, and J. E. Stanworth

Research Laboratory, British Thomson-Houston Co. Ltd., Rugby, England

ABSTRACT

Glasses have been made in the systems $BaO-V_2O_5-P_2O_5$ and $Na_2O-BaO-V_2O_5-P_2O_5$ with V_2O_5 contents ranging between 50 and 87 mole %. The glasses were found to be semiconductors, those with the highest V_2O_5 contents having a specific conductivity of the order of 10^{-5} ohm^{-1} cm^{-1} at room temperature. The relationship between the specific conductivity, σ, and the temperature was determined, and it was found that the slope of the $\log \sigma - 1/T$ plots was equivalent to an activation energy in the range 0.35-0.40 ev for all the glasses. The value of $\log \sigma$ at 25°C plotted against the mole per cent V_2O_5 gave a straight line relationship for each series of glasses. Conductivity values obtained could be easily reproduced and were not sensitive to variations in melting conditions.

The preparation and properties of a number of glasses based on vanadium pentoxide were described in a previous publication (1). It was shown that glasses could be made from certain binary oxide mixtures of V_2O_5 with the oxides P_2O_5, As_2O_3, GeO_2, TeO_2, BaO, and PbO. The V_2O_5 contents of these glasses were quite high; thus, in the $V_2O_5-P_2O_5$ system, glasses containing as much as 90% of V_2O_5 could be made easily. Measurements of the electrical properties of some of the glasses showed that they were semiconductors; the sign of the thermo-emf was observed for a few of the glasses and it was found that the hot junction was positive for each glass tested, indicating that the glasses are *n*-type semiconductors.

This paper deals with the electrical properties of some of the glasses in more detail.

Preparation of the Glasses

A number of glasses was melted in the system $BaO-V_2O_5-P_2O_5$ and the compositions, calculated from the compositions of the raw material mixtures and expressed in mole per cent, are shown in Table I. A similar series of glasses in the system $Na_2O-BaO-V_2O_5-P_2O_5$ was also melted and their compositions are shown in Table II. The glasses of Table I were melted from mixtures of $BaCO_3$, V_2O_5, and P_2O_5; those in Table II were melted from $BaCO_3$, V_2O_5, and commercial meta phosphoric acid which was shown by chemical analysis to contain 17.0% Na_2O.

The glasses were melted in silica crucibles in a nichrome wound furnace at 950°C on a scale sufficient to yield about 20 g of glass. In general, the melts were quite fluid at this temperature and the crucible was agitated frequently during the melting period, so that after about 15 min the melt appeared to be quite homogeneous and free from bubbles. It was then poured into carbon molds to produce cylindrical rods of glass about 1 cm long and 1 cm in diameter.

TABLE I. Composition of the glasses melted in the system $BaO-V_2O_5-P_2O_5$

Glass No.	Mole percentage composition		
	V_2O_5	P_2O_5	BaO
1	87.5	12.5	—
2	80.0	20.0	—
3	75.0	20.0	5.0
4	70.0	20.0	10.0
5	69.5	22.5	8.0
6	65.0	20.0	15.0
7	62.5	25.0	12.5
8	60.0	20.0	20.0
9	55.0	30.0	15.0

TABLE II. Composition of the glasses melted in the system $Na_2O-BaO-V_2O_5-P_2O_5$

Glass No.	Mole percentage composition			
	V_2O_5	P_2O_5	BaO	Na_2O
10	83.0	10.0	—	6.5
11	75.2	16.5	—	8.2
12	72.6	17.4	2.3	7.7
13	70.6	16.5	4.7	8.2
14	65.8	16.5	9.4	8.2
15	61.2	16.5	14.1	8.2
16	58.0	20.3	11.6	10.2
17	50.8	24.4	13.9	10.8

As soon as possible after pouring, the molds containing the glass were placed in a muffle furnace and the glass annealed at a temperature in the range 250°-300°, depending on the composition. (Measurements of the thermal expansion of the glasses indicated that their annealing temperatures were within this range of temperature.)

Little volatilization of P_2O_5 occurred during melting, less than 1% in each case tested by analysis. No attack on the silica crucibles could be detected after melting the glasses.

All the glasses were very intensely colored, and appeared black in any thickness other than that of very thin films, the color of these films being dark green.

Several of the glasses were examined by x-ray diffraction methods to test for the presence of crystalline material but none was found.

Techniques Used for Determining the Specific Conductivity of the Glasses

The ends of the cast glass cylinders were ground plane and parallel, and gold contacts were evaporated on to the ground surfaces. The resistance be-

tween the contacts was then measured, using a commercial d-c bridge resistance measuring set.[1] This instrument measures resistances up to 5×10^6 ohm, and the applied voltage varies up to a maximum of 25 v depending on which resistance range is being used. The use of different test voltages raised the question of whether or not the resistance varies with the test voltage. This point was checked by a-c measurements on a very thin sheet (0.020 in. thick) of one of the glasses, the test voltage being applied parallel to the plane of the sheet. An oscilloscope was used to observe the form of the voltage-current curve and no departure from ohmic behavior was observed with fields up to 1500 v/cm.

To reduce surface leakage caused by adsorbed moisture films on the glass surface, samples were maintained at 140°C for 3 hr, after which they were allowed to cool in a desiccator before resistance measurements were made. As the resistances of the glasses were always less than 10^7 ohms, it was considered that the effect of surface leakage on the resistance values obtained would be negligible.

The resistance of the glasses did not appear to be very sensitive to differences in heat treatment and the resistivities of different samples cast from the same melt did not differ by more than 10%, provided that no devitrification had occurred. In cases where devitrification had occurred, the resistance decreased by a factor of ~100.

When measuring the resistances of a few of the specimens, a very slight change of resistance with time was observed. The resistance soon settled down to a steady value, however, which rarely differed by more than 10% from the original value.

Measurements were made at room temperature and various temperatures up to 150°C. The specimen was mounted in a simple holder which provided pressure contacts on to the gold contact films; this was immersed in clean liquid paraffin in a liter beaker. This was slowly heated and the resistance of the samples measured at intervals of approximately 15° during the heating period. A further set of measurements was made on cooling. Values obtained on heating usually were a little higher than those obtained on cooling, but the difference was never more than 10%; in plotting results, average values were used.

Results and Discussion

Crystalline vanadium pentoxide is a semiconducting oxide of the excess metal type. Arsenev and Kurchatov (2) showed that for the particular sample of vanadium pentoxide which they investigated there was a deficiency of oxygen of about 0.1 at. %.

Boros (3) investigated the electrical properties of single crystals of the material and showed that the conductivity was n-type. The conductivity varied according to the direction in the crystal in which it was measured, the average value at 20°C being approximately 10^{-4} ohm^{-1} cm^{-1}.

It is clear from the experimental work described in this paper that the vanadate glasses are also semiconductors. This is not a surprising result since Yurkov (4) has already shown that molten V_2O_5 is semiconducting and semiconductivity has also been observed in molten materials by other workers (5-7). Furthermore, both liquid and amorphous selenium are well known for their semiconductor behavior. Thus, it is not necessary for a material to have a regular crystalline structure for it to show semiconductivity.

Fig. 1 shows the relationship between the logarithm of the conductivity (σ) and the reciprocal of the absolute temperature T for a number of glasses in the BaO-V_2O_5-P_2O_5 system. On the same figure is plotted the relationship obtained from measurements on a rod sample of crystalline V_2O_5 produced by pouring the molten material into a carbon mold. It is seen that the slope of the lines is greater for the glasses than it is for the crystalline material. Fig. 2 shows the curves for the Na_2O-BaO-V_2O_5-P_2O_5 glasses.

The equation for plots of this type is usually expressed in the form

$$\sigma = \sigma_0 e^{-E/kT}$$

where σ_0 is a constant for the material, k is Boltzmann's constant, and E is a term having the dimen-

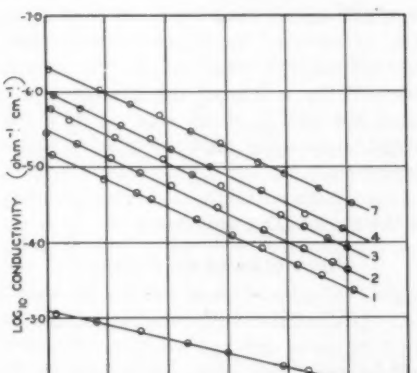

Fig. 1. Relationship between conductivity and temperature for polycrystalline V_2O_5 and glasses in the system BaO-V_2O_5-P_2O_5. (See Table I for compositions).

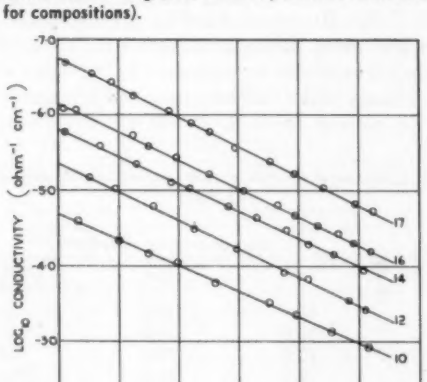

Fig. 2. Relationship between conductivity and temperature for glasses in the system Na_2O-BaO-V_2O_5-P_2O_5. (See Table II for compositions).

[1] A Baldwin "Logohm" meter. Tests had previously been made to assess the magnitude of the contact resistances. They were made on a rod sample onto which gold current and voltage contacts were evaporated. These tests indicated that the contact resistance could be neglected.

TABLE III. Values of E in expression $\sigma = \sigma_0 e^{-E/KT}$ derived from Fig. 1 for BaO-V_2O_5-P_2O_5 glasses

Glass No.	Mole % V_2O_5	E (e.v.)
1	87.5	0.36
2	80.0	0.37
3	75.0	0.37
4	70.0	0.36
7	62.5	0.36

TABLE IV. Values of E in expression $\sigma = \sigma_0 e^{-E/KT}$ derived from Fig. 2 for Na_2O-BaO-V_2O_5-P_2O_5 glasses

Glass No.	Mole % V_2O_5	E (e.v.)
10	83.0	0.34
12	72.6	0.37
13	70.6	0.35
14	65.8	0.35
15	61.2	0.37
16	58.0	0.37
17	50.8	0.39

sions of energy which in semiconductor theory is related to the energy e, necessary to raise an electron from the donor levels to the conduction band. In fact E is equal to e or $e/2$ depending on the proportion of electrons which have been activated to the conduction band (8).

It seems unlikely that in a random structure such as that which exists in a glass there would be a single value of e since each donor center has slightly different surroundings from the rest. The fact that a straight line is obtained when $\log_{10} \sigma$ is plotted against $1/T$ does not necessarily imply that there is a single value of e or that the range of values of e is small. The straight line relationship may still hold over a limited temperature range even when the range of values of e is appreciable, because of the peculiar properties of the e^{-x} function. It appears, however, that the average value of the energy necessary to raise the electrons into the conduction band in the glasses is greater than in crystalline vanadium pentoxide.

Tables III and IV show that the value of E, derived from the slope of the lines in Fig. 1 and 2, remains constant at about 0.36 e.v. over the range of composition studied in both series of glasses. There is evidence that similar barium phosphate glasses containing smaller percentages of V_2O_5 (5-20%) show much smaller conductivities but have greater values of E. Any interpretation of these results can only be conjectural in the absence of knowledge of the structure of vanadate glasses.

Fig. 3 shows that, when the logarithm of the conductivity σ_{25} at 25°C is plotted against the molecular percentage of V_2O_5 in either series of glasses, a straight line is obtained with very little scatter of the experimental points. The general trend of increasing conductivity with increasing V_2O_5 content is of course easy to understand, but the low scatter of the points about the lines is quite remarkable, particularly when one remembers that the BaO/P_2O_5 ratio is not constant throughout the series. This indicates that the conductivity of these glasses is not strongly influenced by factors other than the V_2O_5 content. Conductivity values for a glass of given composition are also easily reproducible, showing that small variations in melting conditions do not greatly influence the conductivity. Even melting under strongly reducing conditions has very little effect. Thus a glass of the composition V_2O_5 87.5%, P_2O_5 12.5% was melted in air at 900°C from a mixture of vanadium pentoxide and red phosphorus. When the melt had become homogeneous it was cast to form rods. The conductivity of these rods was $10^{-4.2}$ ohm^{-1} cm^{-1}. On melting the glass for longer periods of time, the value slowly decreased to $10^{-4.5}$ ohm^{-1} cm^{-1}, only slightly higher than that normally obtained for a glass melted from V_2O_5 and P_2O_5.

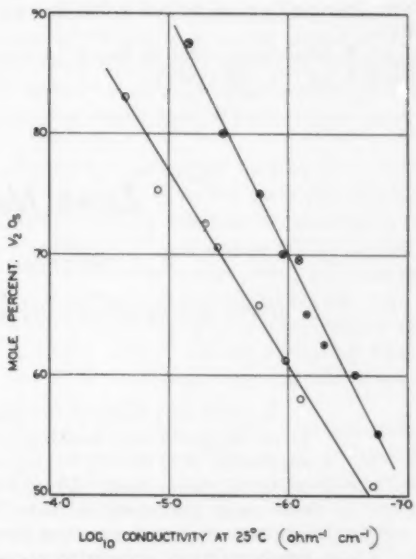

Fig. 3. Relationship between the conductivity and composition of glasses. Cross in open circle—refers to glasses in the system BaO-V_2O_5-P_2O_5; open circle—refers to glasses in the system Na_2O-BaO-V_2O_5-P_2O_5.

Fig. 3 shows that the conductivity of glasses in the system Na_2O-BaO-V_2O_5-P_2O_5 is greater than the conductivity of those in the system BaO-V_2O_5-P_2O_5. This effect of soda of increasing the conductivity is not easy to understand. It is considered most improbable that the effect is due to the transport of Na^+ ions. If this were so, then polarization effects would certainly be apparent during the resistance measurements, but no polarization was observed. Also the magnitude of the difference in conductivity between the two series of glasses is not proportional to the percentage of Na_2O which they contain. It would seem more probable that the introduction of soda into the glass disturbs the balance of the $V^{5+} \rightleftharpoons V^{4+}$ equilibrium to an extent which is dependent on the percentage of V_2O_5 present.

Manuscript received June 20, 1955.

Any discussion of this paper will appear in a Discussion Section to be published in the December 1957 JOURNAL.

REFERENCES

1. E. P. Denton, H. Rawson, and J. E. Stanworth, *Nature*, **173**, 1030 (1954).
2. A. Arsenev and B. Kurchatov, *Zhur. Eksptl. Teoret. Fiz.*, Ser. A, **4**, 576 (1934).
3. J. Boros, *Z. Physik*, **126**, 721 (1949).
4. V. Yurkov, *Zhur. Eksptl. Teoret. Fiz.*, **22/2**, 223 (1952).

5. A. Joffe, Jubilee Collection, No. 1, 305, Izv.A.N. M-L (1947).
6. A. Blum, N. Mokrovsky, and A. Regel, *Izvest. Akad. Serja Fiz.*, **16** (2), 139 (1952).
7. N. Mokrovsky and A. Regel, *Zhur. Tekh. Fiz.*, **22**, 1281 (1952).
8. N. F. Mott and R. W. Gurney, "Electronic Processes in Ionic Crystals," p. 156-160, Oxford (1940).

Zone Melting of Uranium

C. I. Whitman, V. Compton, and R. B. Holden

Atomic Energy Division, Sylvania Electric Products Inc., Bayside, New York

ABSTRACT

A study was made of the possible application of the zone melting technique to the separation of uranium from fission products and other impurities. Bar specimens of U having various alloying elements were zone purified in thoria-coated alumina boats. Uranium bars previously irradiated in the Brookhaven pile were also zone melted. Zone melting has potential application in the removal of such impurities as B, Fe, Si, Ni, and Co from ordinary U. In the reprocessing of irradiated U, zone melting offers a method for removing such fission products as Zr, Nb, Ru. However, as employed here, it shows little promise as a method for complete decontamination of irradiated U from fission products, primarily because of concurrent slagging effects.

Zone melting is a purification technique which has been used to prepare very pure Ge metal in which the quantity of impurities present is of the order of parts per billion. The success of this technique with Ge suggested an investigation of its possible application to the purification of U from fission products and other impurities. This report presents the results of such an investigation.

In the zone melting process a narrow molten zone, produced by induction or resistance heating, is made to traverse the solid metal by movement either of the heater or of the metal, as shown in Fig. 1. Since the solubility of an impurity is generally different for solid and liquid, segregation occurs as the solid refreezes at the rear solid-liquid interface. Impurities which are more soluble in the liquid phase tend to concentrate in the molten zone and are carried to one end of the bar. Impurities which are more soluble in the solid phase tend to move to the opposite end, and thus the center portion of the bar is purified. Additional passes in the same direction produce further purification, although eventually an "ultimate distribution" is reached after which additional passes have no effect.

Fig. 1. Single-coil arrangement for zone melting

A measure of the tendency of the impurity to migrate is given by the distribution coefficient k, which is defined as the ratio of the solute concentration in the solid to that in the liquid at equilibrium. The greater the factor by which k differs from unity, the more readily impurities migrate.

A simple theory of zone melting has been developed by Pfann (1), in which it is assumed tnat solute diffusion in the liquid is sufficiently rapid that the impurity concentration is uniform in the molten zone while diffusion in the solid phase is negligible. From this theory it is possible to calculate the effect of repeated zone passes if the distribution coefficient is known. In practice, one expects less migration than that calculated, because the assumptions of complete equilibrium on which the calculation is based are not strictly true. In any case, the purification attained depends on the number of passes, the ratio of molten zone length to bar length, the equilibrium distribution coefficient k, and the rate of zone travel.

In Table I are given k values for some metals in U, estimated from the particular uranium-metal phase diagrams (2). It should be noted that these k values are at best approximate since generally the phase diagrams have not been accurately determined in the region of low impurity concentration. The theoretical ratio of impurity concentration at the low concentration end of the bar before and after

TABLE I. Distribution coefficients for some metals in uranium

Element	k*	Theoretical concentration ratio† for seven zone passes: [Impurity concentration in purified end after zone melting / Initial impurity concentration]
Fe	0.1	$\sim 10^{-5}$
Mo	1.0	1
Ni	0.03	$<10^{-6}$
Nb	5.0	$<10^{-6}$
Si	0.2	$\sim 10^{-4}$
Sn	1.0	1
Zr	2.0	$\sim 10^{-3}$

* Estimated from available phase diagrams.
† Taken from calculations by I. G. Dillon, kindly furnished by L. Burris and I. G. Dillon of Argonne National Laboratory.

seven zone passes (zone-length to bar-length ratio of 1:10) is also given.

Experimentation

Apparatus

Two types of apparatus were employed in the study; one, used for the most part, in which the coil moved relative to the bar, and one in which the bar was moved.

In the single-coil arrangement shown in Fig. 1, the induction coil was mounted on the travelling carriage of a small lathe bed. The coil was advanced by means of a gear reduced motor connected to a "Zero-Max" adjustable ratio torque converter, which in turn was used to drive the lead screw of the lathe. In this way, rates of molten zone travel of 0-12 in./hr could be obtained. The U was contained in a boat placed within a Vycor tube, approximately 2 in. in diameter, closed at one end. The other end of the tube was connected by means of a 75/50 semi-ball connection to a high vacuum system consisting of a three-stage oil diffusion pump and a mechanical pump. If desired, the zone melting could also be carried out in an inert atmosphere.

The multi-coil apparatus shown in Fig. 2 utilized stationary coils surrounding a Vycor tube. The boat containing the sample was pulled through the coils by means of a Zr wire attached to the rod of a National Research Corp. rotary, push-pull vacuum seal at one end of the Vycor tube. The wire was wound on the rod at an adjustable rate controlled by a variable ratio "Zero-Max" torque converter in a manner similar to the simple coil arrangement discussed previously. The vacuum seal was connected to the glass vacuum system through a metal male ground joint. The other end of the tube was attached by means of a 75/50 semi-ball connection to a high vacuum system similar to the one described previously. This arrangement operated satisfactorily but was developed late in the program and used for only a few runs.

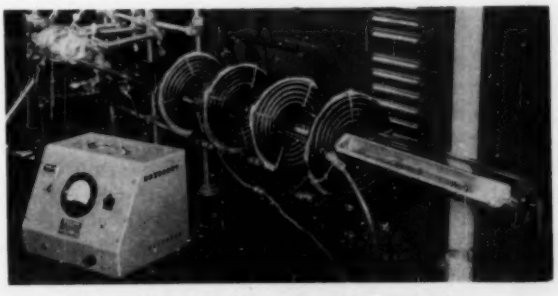

Fig. 2. Multiple-coil arrangement for zone melting

A double pancake-type coil (2¼ in. ID) with a total of ten turns (five for each pancake) of ⅜ in. diameter Cu tubing was used in these studies. Power for the single-coil apparatus was supplied from a Sylvania induction heater with an operating frequency of 400 kc and an output rating of 10 kw. The multi-coil apparatus used a Ther-Monic Generator with a 10 kw output and an operating frequency of 400 kc. Both induction heating units were of the vacuum tube type.

Container Materials for U.—The development of a suitable container material for U proved to be the principal experimental problem encountered. Graphite boats, which were used early in the program, reacted excessively with the U. Stabilized zirconia boats were used next. Although these were sufficiently inert with respect to U attack, they had extremely poor thermal shock resistance under the conditions of zone melting, and as a result cracked frequently in use. Alumina (Norton Co. mixture RA 98) was found to be more resistant to thermal shock and was used subsequently in preference to zirconia.

Alumina boats used to contain the uranium were obtained by cutting furnace tubes (12 in. long, ¾ in. bore) in half length-wise and plugging the ends with alumina disks. A thoria wash, consisting of ThO_2 powder suspended in a nitrocellulose, lacquer (Raffi and Swanson No. 2695) diluted 5-to-1 with *n*-butyl acetate, was applied to the inner surface of the boat and to the end plugs. This served to reduce any attack of alumina by U. Three such coats were usually applied, with drying under an infrared lamp between coats. The boats were then fired at 900°-1000°C to form a loosely adhering protective coating of thoria. The use of higher firing temperatures resulted in a decrease in the thermal shock resistance of the alumina. Boats made in this manner have been used for as many as 20 zone passes without breakage. If this treatment were omitted, the principal effect would be Al pickup by the U.

Prior to use, the alumina boats were outgassed to a vacuum of <0.02 μ by heating a bar of Zr within the boat to approximately 1300°C. The boat containing the U was placed in an outer boat which would prevent U from flowing onto the Vycor tube in case of failure of the inner boat.

Atmosphere.—The uranium alloys used in the study were prepared by powder metallurgy hot-pressing techniques (3). This material contained far more residual gas than the usual vacuum-cast U.

Upon melting of the alloys under vacuum, considerable outgassing occurred, which was sometimes violent enough to spatter U over the interior surface of the Vycor tube. This was avoided by melting under a static atmosphere of 200-300 mm of A.

Zone melting of vacuum-cast U was conducted under a continuous vacuum of $\leqq 0.01$ μ. The resulting bar had a smooth, steel-gray surface (presum-

TABLE II. Representative results

Alloy	Nominal comp. Wt %	No Passes	Speed in./hr	Analysis		Concentration ratio*	
				First to freeze	Last to freeze	Theo.	Obs'd
Nb	0.5	7	1	0.59	0.30	10^{-2}	0.6
Zr	0.5	3	2	0.44	0.16†	10^{-2}	0.3
Ru	0.5	8	1	0.5	0.9		
Ni	0.1	4	1	0.065	0.19	10^{-4}	0.65
Fe	0.2	1	2	0.13	0.26	10^{-1}	0.65
Si	0.2	2	4, 2	0.17	0.24	10^{-1}	0.85
Sn	0.5	6	1	0.5	0.6	1.0	1.0

* As defined in Table I.
† Anomalous concentration peak observed.

ably UO) which remained virtually unchanged for weeks.

Zone length.—The boats used varied in length from 6 to 12 in. and in width from ¾ to 1½ in. The boundaries of the molten zone were distinguished by a slight jarring of the apparatus. Experiments in which boats cracked demonstrated that the zone was molten all the way through. Generally, the desired zone length was 1/10 the bar length, but experimentally this was difficult to maintain. Most of the runs were conducted at a constant power input in which the zone length for 10 in. bars varied from ¾ in. in the center portion to 2 in. at the ends of the bar.

In spite of this increased zone length at the ends, it is believed that this procedure is preferable because the frequent manual power adjustment required in attempts to maintain a constant zone length cause a back and forth motion of the liquid-solid interface. This rapid melting and solidifying is not conducive to establishment of the equilibrium impurity distribution between the liquid and the solid.

The increase in zone length at the ends is attributed to heat transfer from the molten zone through the uranium bar in only one direction; whereas in the center portion heat transfer occurs in two directions. In some experiments variation in zone length was corrected by appropriate adjustment of the power input, resulting in a uniform zone length of ¾-1 in.

Results

Zone melting was applied to: binary uranium alloys; vacuum-cast uranium; irradiated uranium, in that order. Suitable experimental procedures were developed simultaneously as the investigation progressed. A rate of zone travel of 1-2 in./hr was eventually adopted as the best for these reasons: *(a)* at faster zone travel rates, separation was poorer; *(b)* while slower rates may have increased separation because of a closer approach to equilibrium conditions, any practical application of zone melting would require a reasonable rate of zone travel for economic reasons; and *(c)* with this rate it was not necessary to allow experiments to run unattended overnight.

Uranium Alloys

The early experimental work was performed with binary uranium alloys using graphite and stabilized zirconia boats. Little migration was observed until the zone travel rate was reduced to 2 in./hr. Representative results are summarized in Table II. Samples about 0.1 in. thick were cut from each end of the bar.

Where comparison is possible with Table I, it is seen that the actually observed differences are, at best, only factors of two or three whereas factors of 10 to 100 and more would be expected from theory. There experiments were the earliest and suffered from experimental difficulties with container materials and outgassing as noted previously. In addition, the zirconia boats available were 6 in. in length and zone lengths at the beginning and end of the runs were as much as 2 in. Problems also arose in the manufacture and analyses of the alloys and were incompletely resolved prior to proceeding to work on vacuum cast uranium. This is especially noticeable in the discrepancies in Table II between the nominal composition and analysis on Zr, Ru, and Sn alloys. For this reason, absolute significance should not be attached to the observed concentration ratios although it is believed they are sufficiently accurate to justify the comparison that has been made with theory. If these experiments were to be repeated, improved results would be expected because of subsequent improvements in container materials, boat length, etc., although it is unlikely that anything resembling the theoretical migration would be attained except with impractically slow rates of zone travel.

Vacuum Cast Uranium

The results of two representative experiments on migration of impurity elements in vacuum cast U are summarized in Table III. In Run 27, seven samples, approximately 0.1 in. in length, were cut from each end of the bar and at approximately 2 in. equally spaced interval along the bar, sample 1 being the first portion to freeze and sample 7 the last. The same applies to Run 34, except that a total of only six samples were taken. The zone travel rate was 2 in./hr in Run 27 and 1 in./hr in Run 34. In this latter run additional metallic impurities[1] were deliberately added to the uranium. The influence of zone travel rate on the extent of migration shows clearly in the comparison of the two runs since greatly enhanced migration is evident for B, Co, Fe, Ni, and Si at the slower zone travel rate of Run 34. Of the remaining elements that were detectable spectrographically, V showed some segregation. Al,

[1] Ag, Al, Co, Cu, Mn, Mo, Ni, Pb, Si, Sn, V, were added.

TABLE III. Effect of zone travel rate on impurity migration.
Run 27 (9 zone passes) @ 2 in./hr

	First to freeze	Direction of zone travel →					Last to freeze
Sample Impurity	1	2	3	4	5	6	7
B	<0.2	<0.2	<0.2	<0.2	0.20	0.22	0.22
Co	—	—	2	5	5	5	7
Cu*	<1	<1	<1	<1	<1	<1	<1
Fe	28	21	29	48	50	63	68
Ni	20	15	20	30	40	40	60
Si	20	20	20	30	20	30	30

All concentrations given in ppm.
* The concentration of Cu prior to zone melting was 10 ppm. The anomalous zone melting behavior may be due to volatility of the Cu during zone melting.

Run 34 (9 zone passes) @ 1 in./hr

	First to freeze	Direction of zone travel →				Last to freeze
Sample Impurity	1	2	3	4	5	6
Al	200	200	200	200	200	200
B	—	—	—	<0.2	0.20	0.41
Co	10	10	30	50	70	150
Cu	1	2	5	5	5	5
Fe	15	15	30	45	70	200
Mg	<5	<5	<5	<5	<5	<5
Mn	5	5	5	5	5	5
Mo	100	100	100	100	100	100
Ni	20	20	30	50	100	200
Si	20	20	50	50	70	200
Sn	50	50	50	50	50	50
V	30	30	30	50	50	50

All concentrations given in ppm.

Mo, and Sn did not segregate and Mg and Mn evidently volatilized in the course of zone melting. While still far less than that expected on the basis of the equilibrium k derived from the phase diagram, migration is sufficiently extensive to suggest the possibility of using zone melting as a method of producing high purity U.

Irradiated Uranium

A bar of U metal, irradiated in the Brookhaven pile at a flux of 10^{13}nv for 55 min followed by approximately 60 days cooling, was subjected to 10 zone passes (ZM-36); the single-coil arrangement was used in these experiments. Autoradiographs were taken and the total radiation level along the length of the bar was measured.

The individual behavior of fission products was not observed but the autoradiographs and counting experiments indicated a definite migration of activity to each end of the bar. Considerable radioactivity concentrated in the surface layer of the U where it could be removed by pickling and a substantial amount also diffused into the alumina boat.

A possible explanation for these qualitative observations is as follows: The activity concentration noted at one end was probably due to Zr and Nb, and that at the other due to Ru since these migrate in opposite directions. The conditions under which the zone melting was carried out are exactly those for a combined oxide slagging and volatilization. As has been determined experimentally (4), the major portion of the fission products, comprising the rare earth, alkali and alkaline earth metals either enter a slag layer, volatilize, or diffuse into the oxide container. The remaining important fission products Zr, Nb, Ru, and Mo are incompletely removed by this oxide slagging and volatilization. Of this group only Mo does not migrate. This suggests that zone melting has potential application for removal of Zr, Nb, and Ru in conjunction with oxide slagging pyroprocessing methods currently being considered for application to certain types of reactor fuels (4) where a high degree of decontamination of the fuel is not required. It should be noted that slagging was not a factor in the experiments reported earlier since only metals more active with regard to oxide formation will enter a slag layer and none of the impurities observed in these experiments were in that classification.

It would be extremely difficult to eliminate slagging completely in zone melting of irradiated U since oxide slag can be formed through interaction with oxygen in the container material, with oxygen traces in the atmosphere and from oxygen originally present in the metal itself.

A high-vacuum floating zone technique (5) using oxygen-free U is a possible approach which might prevent the formation of an oxide skin. It would be interesting to compare the results of floating zone experiments with those in which a ceramic container is used for the U. However, it appears rather unlikely that the floating zone technique is adaptable to processing commercial quantities of U.

When slagging occurs concurrently with zone melting important limitations on the use of zone melting as a reprocessing technique are imposed. A fission product present in a slag skin is in equilibrium with the fission product concentration in the melt and hence acts as a source, resupplying fission product to the melt as rapidly as zone melting might move it away. This fact plus the relatively slow rate of travel of impurities makes it doubtful that zone melting by the techniques developed here could ever effect the degree of decontamination required for direct handling of recovered material.

A report (6) on the zone melting of U appeared when this paper was in review. It is noted that the results obtained in these two entirely independent investigations are quite consistent and in at least qualitative agreement, although a direct comparison is difficult because of substantial differences in the experimental arrangement, concentration ranges studied, and methods of analysis.

Summary and Conclusions

1. Satisfactory apparatus for the zone melting of U has been developed. An alumina boat, coated with a loosely adhering layer of thoria, was the most satisfactory container found for U from the standpoint of inertness and resistance to thermal shock.

2. Migration of B, Fe, Ni, Co, Si, Cu, Zr, Nb, and Ru was observed. No migration was detected for Al, Mg, Mn, Mo, and Sn. It was found that a slow zone

travel rate (~1 in./hr) improved the extent of migration appreciably, presumably because of a closer approach to equilibrium conditions.

3. An autoradiograph of irradiated U subjected to zone melting showed that migration had occurred to each end of the bar. This was attributed to Zr, Nb, and Ru. A considerable amount of activity was found to concentrate in the surface of the bar.

4. Zone melting shows promise as a means of purification of U from traces of such elements as B, Fe, Ni, Co, Si, and Cu, although under the conditions employed the extent of migration was not as extensive as would be expected on the basis of simple zone melting theory.

5. The removal of such elements as Zr, Nb, and Ru is a potential application for zone melting in conjunction with oxide slagging pyroprocessing methods currently under consideration for use with certain types of reactor fuels. However, zone melting, as employed here, shows little promise as a method for complete decontamination of irradiated U from fission products, primarily because of concurrent slagging effects.

Acknowledgment

The assistance of H. R. Mullin of the Atomic Energy Commission, New Brunswick Laboratory, in providing spectrographic analyses is gratefully acknowledged.

Manuscript received June 29, 1956. The work on this paper was supported by A.E.C.

Any discussion of this paper will appear in a Discussion Section to be published in the December 1957 JOURNAL.

REFERENCES

1. W. G. Pfann, *Trans. Am. Inst. Mining Met. Engrs.* **194**, 747 (1952).
2. H. A. Saller and F. A. Rough, BMI 1000, June 1, 1955 "Compilation of U.S. and U.K. Uranium and Thorium Constitutional Diagrams."
3. H. H. Hausner and J. L. Zambrow, *Nuclear Science and Engineering*, **1**, 92 (1956).
4. H. M. Feder, "Pyrometallurgical Processing of Nuclear Materials" Geneva Conference, paper 544 (1955).
5. P. H. Keck, W. Van Horn, J. Soled, and A. MacDonald, *Rev. Sci. Insts.*, **25**, 331 (1954).
6. J. E. Antill, *Nuclear Power*, **1**, 155 (1956).

The Kinetics and Mechanism of Formation of Anode Films on Single-Crystal InSb

J. F. Dewald

Bell Telephone Laboratories, Inc., Murray Hill, New Jersey

ABSTRACT

Studies of the kinetics-of-formation and composition of anode films on several crystal faces of indium antimonide are reported. A marked dependence of oxidation rate on crystal face is observed at low fields, the (111) and (332) faces oxidizing at more than ten times the rate of the (110) and ($\bar{1}$11) and ($\bar{3}$32) faces. At high fields all faces oxidize at the same rate. Data are interpreted in terms of the detailed structure of InSb and the theories of Cabrera and Mott and of Dewald. With one major exception, the composition effects, the data may be qualitatively understood in terms of these theories.

In the past few years a sizable effort has been made by many workers to achieve a detailed understanding of the mechanism of formation of anode films generally. Experimental work has been concerned largely with simple metal systems, in particular the Ta, Al, and Zr systems (1-5).

The present study was undertaken to illuminate some of the ambiguities which have arisen in the theoretical interpretation of experimental data on simple metal systems. The intermetallic compound, InSb, was chosen as the electrode for study because its crystal structure and its binary nature uniquely highlighted the effects being studied.

The theory of the high-field formation process was first put in quantitative form by Cabrera and Mott (6). It has recently been extended by Dewald (7). Two major uncertainties are implicit in both of these developments, *(a)* the nature of the mobile species, and *(b)* the location of the rate-determining step. Cabrera and Mott assumed that cations move through the film interstitially and that the rate-determining step is located at the metal/oxide interface. Dewald also assumed ionic transport by interstitial cations, but allowed for the existence of space charge effects in the event that passage through the film was the rate-determining step.

Charlesby and co-workers (3) attempted to resolve the second of these uncertainties by studying the rate of formation on different crystal faces of Al. If entrance into the film were the difficult step, one might expect differences in kinetics depending on the crystallographic orientation of the surface being oxidized. Charlesby's apparently negative result implies either that the potential energy parameters of the faces studied [(100) and (110)] do not differ greatly or that the rate-determining step is located elsewhere than at the metal/oxide interface. It is difficult to choose between these alternatives since

the structure of Al (f.c.c.) is not one likely to exhibit large differences in bonding energy between the (100) and the (110) face. A surface atom makes 8 bonds to the crystal on the (100) face and 7 bonds to the crystal on the (110) face. Since each bond is rather weak, and breaking the surface bonds is only a part of the total activation process, it would not be at all surprising if the difference in activation energy between the (110) and (100) faces were as small as 5%, the experimental uncertainty in Charlesby's experiments. Differences in activation energy on different faces of InSb were expected to be many times as great as on Al (*see* below).

The data of Young (5) and Vermilyea (2) on Ta_2O_5 films also offer an uncertainty as to the location of the rate-determining step in the formation process. The formation rate appears to be a simple exponential function of electric field over the entire range of fields studied, suggesting that a single activation process is operative over this range of fields. An anomalous temperature independence of Tafel slope $\left[\left(\frac{\partial \bar{E}}{\partial \log i}\right)_T\right]$ was observed, however, which has been taken by Dewald (7) to indicate the existence of two rate-determining processes, one operative at high fields, the other at low fields. He identified the two steps as passage into and passage through the film, but could not identify uniquely which was the high- and which the low-field process.

The validity of some sort of a duplex process in the Ta_2O_5 system has now been confirmed by new data of Vermilyea (8). Using a technique of measurement especially designed to minimize the effects of heating at high current density, Vermilyea now finds that the formation rate is not a simple exponential function of the field but rather that there are two exponential regions, at high and at low fields, with different slopes and a smooth transition in between.

To the extent that one believes the hypothesis of Cabrera and Mott and of Dewald, that interstitial ions move through a perfect lattice and are the only mobile species, one is strongly led to the conclusion that the two processes correspond to entrance into and passage through the oxide film. However, if this is the case, a significant space charge should arise in the film. Such a space charge would be expected to give rise to a small dependence of formation rate on film thickness, the field being kept constant. Vermilyea has looked for such a thickness dependence with negative result (9). This suggests that a reconsideration of the nature of the mobile species may be necessary or that lattice imperfections may play a significant role. The experiments described below on the composition of the films formed on InSb give additional insight into this problem.

Experimental Methods

Crystal and Surface Preparation

The indium antimonide single crystals employed in this study were grown from zone-refined material and were pulled in the (100) direction. The impurity content, as estimated from Hall effect and conductivity measurements at liquid nitrogen temperature, was approximately 5×10^{16} at./cc, (corresponding to 1 part in 10^7). This value would include any departures from stoichiometry. The crystals were oriented with an x-ray goniometer and then cut abrasively to any desired orientation.

Perhaps the most subtle and at the same time most troubling problem encountered in the course of this work was in the preparation and identification of the precise nature of the surface condition of the crystals.

First, there is the problem of locating the positive direction of the crystal. InSb has the ZnS structure. In this structure the (100) axis is not a fourfold axis but rather a fourfold inversion axis and thus, although standard x-ray diffraction techniques cannot distinguish the dissymetry involved, the face (h k l) does not in general have the same properties as the face ($\bar{h}$ k l). The simplest set of faces on which one may see the differences is the [111, $\bar{1}$11] set. On one of these faces (what label it is given is completely arbitrary) any surface antimony atom makes three bonds to the crystal, any surface indium atom makes just one bond to the crystal. On the other face just the reverse is the case, every surface indium is three-bonded, every surface antimony is one-bonded. The similar orientation problem has been solved for ZnS using the absorption edge technique (10); however, since the atomic numbers of In and Sb differ by only two, this is not possible in the present case. Index (111) has been assigned arbitrarily to the face which forms the thicker oxide films under the same formation conditions.[1]

An even greater ambiguity arises from the distinction that must be made between the macroscopic, the microscopic, and the atomic nature of the surface. Depending on the method of surface preparation and the particular face in question, these three ways of defining the orientation may or may not be the same. Four general methods of surface preparation have been used; cleavage, crystallographic etches, and chemical and electropolishes. Three crystal faces have been studied in some detail, the (110), the (332), and the ($\bar{3}$32). These faces were chosen primarily because they are the cleavage planes of the crystal, and cleavage should yield surfaces in a much less ambiguous condition than can be achieved by any other technique. The (110) face is the primary cleavage plane while the (332) and ($\bar{3}$32) planes appear to be the secondary cleavage planes.[2]

Much of the data for the (110) face have been obtained on freshly cleaved surfaces. Using a simple razor-blade guillotine, mirror bright (110) surfaces as large as 1 cm^2 have been obtained. These generally show several steps, but apart from these, the

[1] It is shown below that the kinetic data can be understood only if the (111) face (as defined above) is the face with 3-bonded antimony atoms and 1-bonded indium.

[2] G. Wolff (11) has reported secondary cleavage on the (111) plane. In a few cases fragmentary cleavage has been observed on faces which are approximately in the (111) direction. However, goniometric measurements on two such cleavages showed the optical surface to be much closer to the (332) than to the (111) plane. Since the (111) plane is not electrically neutral, i.e., contains either all indium or all antimony atoms, cleavage was not expected to occur on the (111) plane.

macroscopic, microscopic, and atomic planes should be identical. The crystals were immersed in the electrolyte within a few seconds after cleavage. The fragmentary cleavages which have been obtained on the (332) and ($\bar{3}32$) faces have been used for the colorimetric determination of the effect of crystal orientation; however, the inability to produce these surfaces at will and in large area has required dependence primarily on other techniques of surface preparation for the study of the effects of temperature and electric field, on the (332) and ($\bar{3}32$) faces. The efficacy of these other methods of surface preparation was checked by colorimetric comparison with the films formed on the fragmentary ($\bar{3}32$) and ($\bar{3}32$) cleaved surfaces.

Data on the ($\bar{3}32$) face have been obtained largely on faces prepared using a crystallographic etch of the composition: 48% HF, 4 pts; Conc. HNO_3, 5 pts; H_2O, ~12 pts. This etch develops microscopic faces which, regardless of the macroscopic orientation, are most closely identified as ($\bar{3}32$). As in the case of the cleaved faces, goniometric data show deviations as large as one or two degrees from the theoretical angles. The indexing as ($\bar{3}32$) is made as a relatively simple indexing of what is probably a considerably "stepped" atomic configuration.

A crystallographic etch to develop (332) surfaces could not be found and therefore it was necessary to use nonselective methods of surface preparation on this face. Crystals were oriented by the combination of x-ray and kinetic techniques discussed above and then were mechanically lapped and polished to the (332) face. Just prior to the formation of the anode films, they were either chemically or electrochemically polished to remove the mechanically disturbed surface layer. The chemical polish had the composition; HNO_3, 40 pts., 48% HF, 24 pts., acetic acid, 24 pts. Polishing times ranged from 5-30 sec. The electropolish had the composition: $HClO_4$, 10 pts; acetic anhydride, 40 pts; H_2O, 2 pts. It was employed at ~5°C at a current density of ~50 ma/cm^2 and yielded a solid black film of oxidation product which was readily stripped off under a stream of water leaving a mirror bright surface.

Various techniques were employed for masking the faces of the crystal other than the face under study. A coat of polystyrene, applied in a toluene solution to a lapped-but-not-polished surface, seemed to give completely adequate protection. The coating was generally applied over the edges of the face under study in an attempt to minimize edge effects; however, since there were almost certainly edges or steps present in the initial surface proper, this was probably a futile effort.

The electrolyte employed in all the experiments reported here has been 0.1*N* KOH. This electrolyte dissolves the pure antimony oxides, as antimonites and antimonates, but does not dissolve In_2O_3.

Chemical Analysis of Films

Chemical analyses of the oxide films for their In and Sb content were made by microtechniques closely similar to those devised by Moeller (12) for In and by Luke and Campbell (13) for Sb.

Films were formed on large area crystals which showed (110) faces primarily. Crystals were chemically polished just prior to anodic treatment. The films, ranging in thickness from 200 to 1000Å, were dissolved in tartaric acid. They dissolve slowly and, judged by the perfectly uniform interference colors, at a uniform rate, thus allowing a layer-by-layer analysis of their composition. The sensitivities of the analytical methods (0.1 μg for Sb and 1 μg for In) were sufficient to allow determination of the In/Sb ratio with a precision of about 5% on layers as thin as 20Å.

Kinetic Measurements

The determination of the kinetics of anode film formation resolves itself into the measurement, for any given crystal face and temperature, of the instantaneous electric field and the rate of film growth. Different workers have used many different methods of determining these quantities.[3] The evaluation of the precise absolute value of the electric field, involving as it does the measurement of film thicknesses in the range from 100Å to perhaps 5000Å, is difficult. Fortunately, one does not need to know the precise absolute value of the electric field in order to understand the main features of the kinetic mechanism. Any uncertainty in the absolute field will reflect itself only in an uncertainty about the "jump" distance parameter [cf. (6, 7)]. Since the jump distance is at present only an incompletely defined quantity, only cursory coulombic measurements of the absolute fields have been made in this investigation.

Two techniques were employed to obtain the relative fields; a colorimetric method and a new method described below. These methods are both based on the fact that the ratio of the fields acting across two films of the same thickness is simply the ratio of the voltage drops across the films. The methods differ only in the manner of obtaining films of the same thickness: *(a)* films were formed, under identical conditions of surface preparation, temperature and formation rate, to the same voltage; *(b)* films were formed to the same interference color. Method *(a)* was used to obtain the dependence of formation rate on temperature and electric field on each of the crystal faces studied. Method *(b)* was used to determine the dependence of formation rate on crystal face.

Colorimetric methods such as *(b)* have been used by a number of workers in the past. Vermilyea (8) for example has made particularly effective use of the technique in the study of the Ta_2O_5 system. As in the previous work, an optical step-gauge proved to be quite a simple method of comparison of film thickness. The gauge was constructed using a series of cleaved (110) surfaces, these being formed at 25°C and at a rate of 0.1 v/sec, to various voltages in the range from 10 to 30 v. Comparison of a film of unknown thickness with the step gauge allowed the determination of the relative thickness within perhaps one half of a volt in the most sensitive

[3] See, for example, references (1), (2), (5), and (8). See also, A. Vasicek, Czech. Jl. Phys. 4, 204-19, (1954).

region of the spectrum. The first order colors are very intense.[4]

Method *(a)* is a novel and particularly sensitive one for studying the kinetics of these processes and should be of general applicability. The procedure is illustrated in Fig. 1, and described in some detail below.

A particular crystal face, a convenient temperature (T_0), and a convenient formation rate (S_0) are selected. Under these conditions a number of films are formed to the same voltage, V_0; these films are then all of the same thickness. The formation rate, or the temperature, or both, are then changed to a different value on each film and the change of voltage with time is measured under the second conditions. The voltage rises, rapidly at first, passes through a maximum, then a minimum, and finally rises again, now linearly with time, at a rate closely proportional to the external current density. The final linear rise in voltage with time corresponds to the steady-state behavior for which the various theories have been derived.

The transient effects shown in Fig. 1 have been separated from the steady-state effects by extrapolation of the linear voltage rise portion of the formation curve back to the time when the current was reapplied. This is shown by the dotted line in Fig. 1. The ratio of the extrapolated voltage (V_1) to the initial voltage (V_0) gives the relative field (referred to the initial field) under the final conditions of formation rate and temperature. The validity of the extrapolation procedure has been checked by experiments in which the final formation rate and temperature were made the same as the initial values. The extrapolated voltages (V_1) under these conditions were found to be identical (within ~0.1%) to the voltages (V_0) to which the films had been formed.[5]

Voltages were measured against a Hg-HgO reference electrode which was separated from the solution by a 0.1*N* KOH salt bridge. The tip of the bridge was placed approximately 1 mm away from the InSb electrode. The voltages in the data reported below have been referred to the InSb electrode, which in 0.1*N* KOH is ~0.7 v[6] more active than the Hg-HgO electrode, by adding 0.7 v to the measured voltage; thus the voltages below represent the voltage drops across the oxide film itself.

Formation rates have been determined from the rate of voltage rise with time. Since, at a given formation rate, the electric field is, to a very good approximation, independent of the film thickness, the formation rate is taken to be given by the rate of change of voltage with time divided by the electric field at that formation rate. The data below were obtained on films formed initially at T_0 = 25°C, S_0 ≈0.1 v/sec to V_0 = 5, 10, and 15 v. Owing to variations in surface area and formation efficiency, the initial formation rate could not be controlled precisely to 0.1 v/sec and therefore the rate of change of voltage with time under the initial conditions was determined experimentally and corrections applied for the departure from 0.1 v/sec.

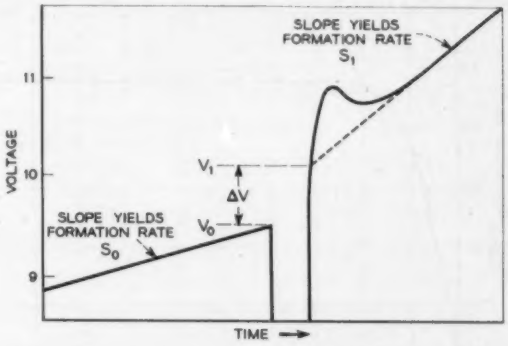

Fig. 1. Typical voltage vs. time curves for the formation of anode films on InSb. Note the initial transient and the extrapolation used to eliminate its effects.

Most of the experiments were performed allowing just enough time between the initial formation process and the final formation process to get the film to the new temperature. However, identical results were observed when the films were allowed to stand in contact with the electrolyte for as long as 70 hr between the initial and final formations. The films apparently do not dissolve on prolonged contact with KOH.

Voltage-time curves similar to Fig. 1 were obtained using a Sanborn Model 127 recorder in conjunction with a Sanborn Model 126 amplifier (10 meg input impedance) and a calibrated voltage-zero-suppressor. The recorder has a response time of about 0.01 sec for full scale deflection. Data presented here on the InSb system show a precision of the order of one half a percent in relative field, on films as thin as 100Å; similar data on somewhat thicker Ta_2O_5 films have been obtained with a precision approaching 0.1%.

For want of a better name, this technique might be called an isopachic (for equal thickness) method.[7]

Results and Discussion

Composition of the Films

The composition of the anode films formed in 0.1*N* KOH has been determined as a function of both the position in the film and the rate of formation of the film. Fig. 2 shows a typical result of the layer by layer chemical analyses. The Sb to In ratio is very low close to the electrolyte interface; however, it rises sharply as one goes into the bulk of the film, approaching the value 1 at a distance about 100Å into the film and remaining essentially constant all the way from there to the metal/oxide interface. This behavior is difficult to rationalize with the interstitial transport of positive ions. One would

[4] Unfortunately the second order colors in the InSb system are quite faint, and, toward the "blue" end of the second order, the films appear gun-metal to black in color. The restriction to the first order makes the colorimetric method less attractive in the InSb system than it has been in other systems.

[5] The transients observed in these measurements constitute an interesting problem in themselves. Almost identical effects have been observed on Ta_2O_5, SiO_2, and Nb_2O_5 films [*see* ref. (15)].

[6] J. F. Dewald, unpublished data.

[7] Adams and co-workers (14) have used a technique somewhat similar to this.

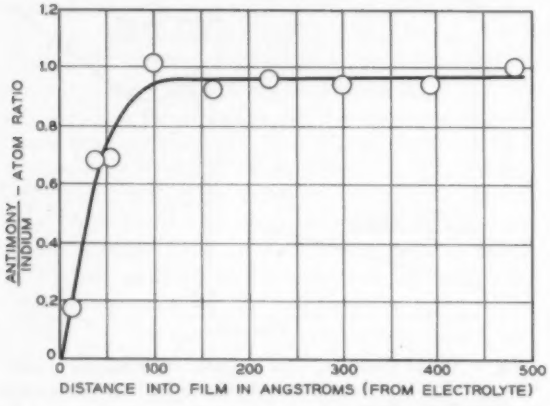

Fig. 2. Typical dependence of anode film composition on position in the film. Close to the electrolyte (KOH) the Sb content is very nearly zero while at depths greater than about 100Å, the composition is practically that of the base material.

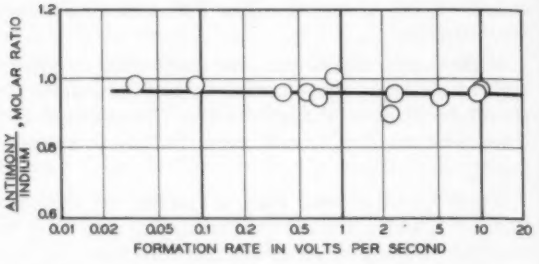

Fig. 3. The Sb/In ratio deep in the film plotted as a function of the rate of formation on the film.

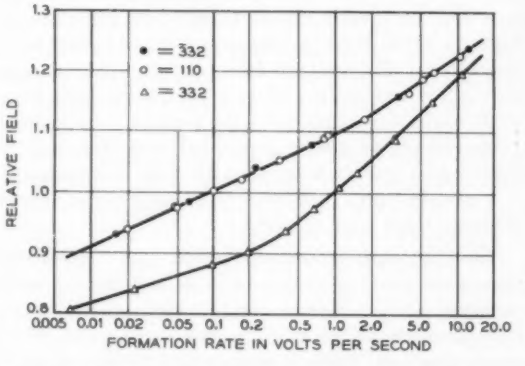

Fig. 4. Tafel plots, showing the dependence of electric field on formation rate, for the (110), (332), and ($\bar{3}32$) faces of InSb at 25°C.

expect, in view of the large and fairly rapid solubility of antimony oxides in KOH, that any Sb ion arriving at the electrolyte interface would dissolve. A part of the Sb does dissolve, but the largest fraction of it remains in the film.

Such behavior might be accounted for if the dissolution rate of antimony oxide were slow and the antimony ions arriving at the electrolyte interface were covered up by subsequent In ions before they could dissolve. This explanation is contradicted by the experimental data shown in Fig. 3. Within experimental error, the composition of the films is independent of the formation rate. Coupling this fact with the observation that, even at current densities appreciably higher than those of Fig. 3, an Sb electrode dissolves anodically in KOH without film formation, it is concluded that most of the Sb ions never come in contact with the electrolyte and that thus the use of the interstitial mechanism of film formation is probably an oversimplification.

Kinetic Data on the (110), (332), and ($\bar{3}32$) Faces

The kinetic data which have been obtained are illustrated in Fig. 4 and 5, and are summarized in Table I. Fig. 4 shows typical Tafel plots of field vs. the logarithm of formation rate for the (110), (332) and ($\bar{3}32$) faces. These data were obtained at 25°C, on films formed initially to 10 v. Fields are expressed relative to the field on the (110) face at a formation rate of 0.1 v/sec, and formation rates are expressed in volts/sec at this field.

A number of features of the data in Fig. 4 should be noted. First, the electric field is not a simple logarithmic function of formation rate on any of the faces studied. In the extremes of both high and low formation rate, the field on each of the faces may be adequately represented as a simple logarithmic function of the formation rate. This behavior seems to imply a duplex process, similar to that observed in the study of Ta_2O_5 films, with the rate-determining step shifting from one site at low fields to a different site at high fields.

The respective locations of the two rate-determining sites may be inferred from the data in Fig. 4. At low and intermediate fields a large effect of crystal orientation is observed, the (332) face oxidizing more than 10 times as rapidly, at the same field, as do the other two faces. At high fields, on the other hand, the three faces oxidize at nearly the same rate. Thus the low field process must be associated with the metal/film interface, and it seems reasonable to suppose that the rate-determining step in the high field process is located elsewhere.

Another rather interesting feature of the data in Fig. 4 is that the ($\bar{3}32$) and (110) faces show almost identical formation rates over the entire range of fields studied at this temperature. This should not be taken to mean that the various kinetic parameters are identical on the two faces, for at temperatures other than 25°C the formation rates on the two faces are not identical.

Data given in Fig. 4 show a small inconsistency between the two methods which have been used to determine the relative field. As mentioned in the experimental section above, the colorimetric method was employed to determine the relative field [referred to the (110) face] on the (332) and ($\bar{3}32$) faces, this comparison being made (arbitrarily) at a formation rate of 0.1 v/sec. The curves in Fig. 4 were then drawn from the isopachic data which covered the entire range of formation rates. Now films formed at high formation rates (greater than about 5.0 v/sec) show no crystallographic effect on colorimetric comparison. Thus, if the two methods of determining the electric field were completely consistent, the curves of Fig. 4 should all superimpose at formation rates above about 5.0 v/sec. As can be seen the two curves seem to be approaching

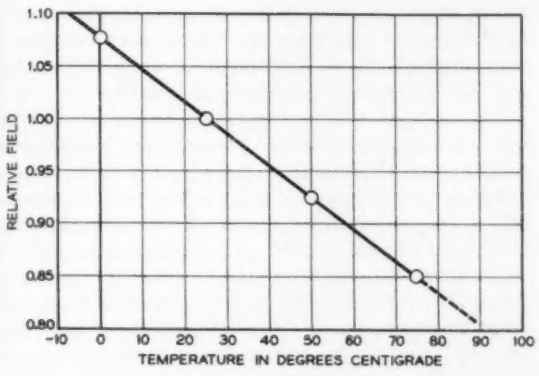

Fig. 5. Temperature dependence of field at constant formation rate on the (110) face.

one another but, even at the highest formation rates, they differ by about 4% in field. This difference is roughly twice the estimated uncertainty in the colorimetric method in the first order range of colors and seems to be a real effect. It may be that the index of refraction of the film depends on the face on which it is formed, or that the optical properties of the base "metal" vary from face to face [such a variation would be unlikely to occur between the (332) and ($\bar{3}32$) faces]. In any case, the discrepancy is a relatively small one and should not affect the qualitative conclusions presented.

The data in Fig. 5 show the temperature dependence of the electric field for 10-v films formed on the (110) face at 0.1 v/sec. Both the Mott-Cabrera and the Dewald models of the system predict an essentially linear dependence of field on the temperature at any given formation rate. The dependence shown in Fig. 5 is in accord with these predictions, over the range from 0° to 75°C. Similar linear dependences of field on temperature have been observed on the (332) and ($\bar{3}32$) faces both at low and at high fields.

Since the functional dependences of field on formation rate and on temperature are fairly simple in the extremes of high and low field, and the transition from the low to the high field behavior is moderately sharp, the experimental data may be summarized in the form of three coefficients (one of each for the high- and one for the low-field region), $\bar{E}$, $(\partial\bar{E})/(\partial \log i)_T$, and $(\partial\bar{E})/(\partial T)_i$. The values of these coefficients vary from face to face in the low field region but show only small, if any, orientation

TABLE I. Summary of experimental data

Formation rate	Crystal face	$\bar{E}/E_0$	$\frac{1}{E_0}\frac{\partial\bar{E}}{\partial \log i}$	$\frac{1}{E_0}\frac{\partial\bar{E}}{\partial T}$
Low (0.1 v/sec)	110	1.00*	0.092	—0.00306
	$\bar{3}32$	1.00	0.092	—0.00380
	332	0.85	0.060	—0.0020
High (10 v/sec)	110 & $\bar{3}32$	1.22	0.17	—0.0036
	332	1.17	0.18	—0.0035

* By definition of E_0.
E_0 = the field on the 110 face at 25°C and a formation rate of 0.1 v/sec

TABLE II. Parameters derived from data in Table I using equation of Cabrera and Mott

	Face	bq* (Å)	q (assumed)	b (Å)	ϕ (e.v.)	i_0 (Å/sec)
Low field						
	110	12.8	3	4.3	1.22	$10^{10.1}$
	$\bar{3}32$	12.8	3	4.3	1.37	$10^{12.7}$
	332	20.0	5	4.0	1.4	$10^{10.3}$
High field						
	Any	7.0	3	2.3	0.8	10^{8}

* bq values calculated using $E_0 = 5\times10^6$ v/cm.

effects at high fields. They are summarized in Table I.

Table II shows the data from Table I re-expressed in the form of the kinetic parameters of the interstitial transport model. At either low or high fields the theory of this model predicts dependences essentially of the form

$$i = i_0 \exp(Ebq - \phi)/kT \qquad (I)$$

Regardless of the validity of the model, the data may be fitted empirically to an equation of the form of (I) in either the high- or low-field regions of formation. Values of the parameters ϕ, bq, and i_0 depend on which region, as well as which crystal face, is being considered. As mentioned above, values of i_0 and the activation energy are determined unambiguously by the data in Table I, independent of the measurement of the absolute electric field. The absolute values of bq depend, however, on the measurements of the absolute field. Values of bq given in Table II were calculated using the value $E_0 = 5\times10^6$ v/cm. This value is derived from coulometric data on the (110) face and represents a minimum value for E_0 which may have to be revised upward when accurate measurements of the absolute field become available. The relative values of the bq product should be unaffected by more accurate evaluation of E_0.

The interpretation of the kinetic parameters which have been derived from the experimental data is difficult, since the detailed mathematical theory of the oxidation process in binary systems such as InSb has not yet been developed. Several novel features of mechanism are introduced by the binary nature of the system and others arise because of the strongly directional character of the surface bonding of the atoms; thus, the use of the Cabrera-Mott equation, (I), or even the complete equations of the space charge model, can hardly have more than qualitative validity. Nevertheless some interesting conclusions may be drawn.

Consider first the values of the bq product obtained from the low-field kinetic data. From Table II these are seen to vary appreciably from face to face, the (332) face exhibiting a value nearly 5/3 as large as the value observed on the other two faces. The variation of the (bq) product can hardly be ascribed to variations in the jump distance (b) since the geometry of the faces is so very similar and, as shown below, the "jump distances" so very large. Thus the variation of the bq product almost

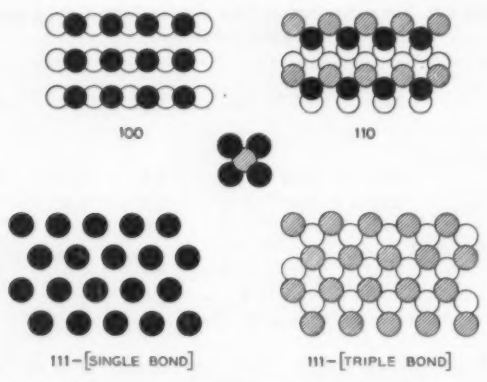

Fig. 6. Surface bonding on the (110), (100), and (111) faces of InSb. Black atoms are surface In, shaded atoms are Sb, unshaded atoms are below the surface atoms. The ($\bar{1}11$) face differs from the (111) only in the identity of the atoms.

certainly results from variations, from face to face, of the effective charge q.

The fact that the ratio of the bq products turns out to be very close to 5/3 implies that on the (332) face the removal of the Sb (+5) ions is rate-determining, while on the ($\bar{3}32$) and (110) faces, removal of the In (+3) ions is the slow step in the oxidation.

Since diffusion in the InSb lattice is very slow at room temperature, the oxidation of any face of an InSb crystal must, of course, involve the removal of both kinds of atoms. To say that, on a particular face, removal of the In ions is rate-determining simply means that at any given instant most of the surface atoms are indiums, the relative numbers of the two kinds of atoms being inversely proportional to their specific rates of removal.

At first glance it might seem strange that one face allows ready removal of one kind of atom while another face allows ready removal of the other kind of atom. Inspection of the type of surface bonding in zinc-blend structures makes this behavior quite clear. Fig. 6 shows the surface bonding of the (100), (110), and (111) faces. [The reasoning may be greatly simplified, with little loss in accuracy, by thinking of the (332) and ($\bar{3}32$) faces, respectively, as "stepped" (111) and ($\bar{1}11$) faces.] The antimony atoms on a (110) face are bonded to the crystal in exactly the same way as the In atoms; by virtue of their larger charge they will be acted on more strongly by the field and therefore the rate-limiting step from this face will presumably be the removal of In atoms.

On the ($\bar{1}11$) face two factors operate to make the In atoms the more tightly bound. There is the same effect of the field as on the (110) face, and in addition a surface In atom on the ($\bar{1}11$) face makes three bonds to the crystal while a surface Sb atom makes only one bond. On both counts the In atoms should be less easily removed than the Sb atoms.

A different behavior is expected on the (111) face; here the chemical and electrical effects act in opposite directions, a surface Sb atom being held to the crystal by three bonds, a surface In atom only by one bond. Thus, in spite of its smaller charge, the In atoms might well be less strongly held to this face than the antimonys and so, except perhaps at very high fields, the removal of antimonys could well be the rate-limiting step in oxidation.

The discussion above makes possible the evaluation of the jump distances themselves, from the bq products and the assumed values of q. These jump distances are shown in Table II. The values obtained (4.0-4.3Å) are roughly equal on the three faces as would be expected, and are quite comparable to those previously obtained on Al (3.5Å) (6) and on Ta at low fields (4.8Å) (8). These values are all surprisingly large, it being remembered that they are supposed to represent the distance from the potential energy minimum to the maximum.

The value of the bq product obtained at high fields is very much less than those obtained at low fields; the calculation of the value of b itself again depends on the value assumed for the effective charge. This has been taken as +3, the assumption being made that motion of the In ions through the film would, by virtue of its smaller charge and larger size, surely be the slower moving ion. Using this value of charge, the value 2.3Å for the jump distance at high fields was obtained. Again there is a surprising concordance with the results obtained on Ta; Vermilyea (8) finds a value of 2.4Å for the jump distance in Ta_2O_5 films at high fields. (He assumes +5 for the charge of the Ta ion.)

The activation energies (ϕ) and frequency factors (i_o) which have been calculated from the data show a definite dependence on crystal face at low fields. Differences are not very large, and the interpretation must therefore be largely speculative. Now the activation-energy-for-diffusion (ϕ) of a surface atom is determined by a whole complex of forces. The two largest factors would be presumably, (*a*) the chemical bonds which would hold the atoms to the crystal regardless of whether a film is present or not, and (*b*) the repulsive forces incident to squeezing past the first oxide ions in the film. Presumably the second of these factors will not vary significantly from one face to another if the activation process involves the same kind of ion on the faces considered. This is the case if the ($\bar{1}11$) and (110) faces are compared; thus the differences observed on the two faces probably arise from the nature of the bonding.

Fig. 6 shows that the In atoms make three bonds to the crystal on both the (110) and ($\bar{1}11$) faces. One might conclude from this that the bonding contribution to the activation energy would be the same on the two faces. This reasoning might be valid if one had a perfect crystal face with no edges or steps. However, it would not be true for any real crystal, since the (110) face has a structure which would "transmit" the edge or imperfection effects over the entire crystal face while the (111) does not. This can be seen quite simply by removing just one atom from each of the "perfect" planes of Fig. 6. On the (110) face the two neighboring atoms would then each be converted from a three-bonded to a two-bonded state. If these two-bonded atoms were in turn removed, the two adjacent atoms would be left

in a two-bonded state. Since two-bonded atoms would be expected to come off more readily, i.e., with lower activation energy, than three-bonded atoms, the (110) face would be expected to oxidize by a chain process of this sort. A similar chain process would not be anticipated on either the (111) or ($\bar{1}$11) faces, for on these faces the surface atoms are not bonded to one another; thus the removal of one surface atom does not change the bonding of the neighboring surface atoms.

This argument explains in a qualitative way the differences in activation energy observed between the (110) and ($\bar{3}$32) faces. It also explains the smaller i_0 value on the (110) face, for only a small fraction of the atoms on such a face are, at any given instant, subject to activation. In the simple Cabrera-Mott approximation, the frequency factor is given by

$$i_0 = m_s \nu \cdot V \qquad \text{(II)}$$

where m_s is the surface density of atoms susceptible to activation, ν is of the order of typical vibration frequencies ($\nu \sim 10^{12}$ sec^{-1}), and V is the atomic volume of the mixed oxide. Values of m_s calculated from the experimental data using (II) indicate that essentially all atoms on the ($\bar{3}$32) face are at all times subject to activation while only about 1 in 400 is subject to activation, at any given instant, on the (110) face. These values seem eminently reasonable, both in a relative and an absolute sense.

Summary

The kinetics of formation of anode films on InSb have been studied on three crystallographic faces and the composition of the resulting films has been determined as a function of the position in the film and the rate of formation. The kinetic data, both transient and steady-state, show striking similarities to those observed previously on the Ta_2O_5 system. The steady-state data may be understood, at least in qualitative fashion, in terms of the theories of Cabrera and Mott, and of Dewald. The pronounced crystallographic effects observed at low fields and the absence of such effects at high fields establish the location of the rate-limiting processes; at low fields, passage into the film is the difficult step; at high fields, passage through the film is the difficult step. Attempts are made to account for the various crystallographic effects in terms of the structure of InSb.

Films formed on InSb in 0.1*N* KOH are found to contain nearly equal quantities of In and Sb in spite of the fact that antimony oxide is strongly and readily soluble in the electrolyte. This result is taken to throw considerable doubt on the assumption of a simple interstitial-ion transport mechanism.

Manuscript received June 25, 1956. This paper was prepared for delivery before the Cincinnati Meeting, May 1-5, 1955.

Any discussion of this paper will appear in a Discussion Section to be published in the December 1957 JOURNAL.

REFERENCES

1. A. Gunterschultze and H. Betz, *Z. Phys.*, **92**, 367 (1934).
2. D. A. Vermilyea, *Acta Met.*, **1**, 282 (1953).
3. S. J. Basinka, J. J. Polling, and A. Charlesby, *ibid.*, **2**, 312 (1954).
4. D. A. Vermilyea, *This Journal*, **102**, 207 (1955).
5. L. Young, *Trans. Faraday Soc.*, **50**, 153 (1954).
6. N. Cabrera and N. F. Mott, *Repts. Progr. in Phys.*, **12**, 163 (1948-49).
7. J. F. Dewald, *This Journal*, **102**, 1, (1955).
8. D. A. Vermilyea, *ibid.*, **103**, 655 (1956).
9. D. A. Vermilyea, *Acta Met.*, **3**, 106 (1955).
10. Coster, Knolls, and Prins, *Z. Physik*, **63**, 345 (1930).
11. G. Wolff, paper delivered at the Chicago Meeting of the ECS, May (1954).
12. T. Moeller, *Ind. Eng. Chem. Anal. Ed.*, **15**, 272 (1943).
13. C. L. Luke and M. E. Campbell, *Anal. Chem.*, **25**, 1588 (1953).
14. G. B. Adams, Jr., Pierre Van Rysselberghe, and Mario Maraghini, *This Journal*, **102**, 502 (1955).
15. J. F. Dewald, *J. Phys. Chem. Solids*, In press.

Density and Electrical Conductance in the System KCl-$ZnCl_2$

Frederick R. Duke and Richard A. Fleming

Institute for Atomic Research and Department of Chemistry, Iowa State College, Ames, Iowa

ABSTRACT

The phase diagram of the system KCl-$ZnCl_2$ indicates the presence of the solid-state 2KCl·$ZnCl_2$. Density vs. composition isotherms in the range 475°-650°C are approximately linear. Isotherms of equivalent conductivity deviate negatively from additivity when plotted against composition, the maximum negative deviation being found near $X_{KCl} = 0.71$. The heat of activation for ionic migration falls rapidly from that of $ZnCl_2$ until X_{KCl} has reached 0.30, then slowly falls to the limiting value for pure KCl.

A knowledge of the electrical properties of fused salt systems has been found to be a powerful tool aiding the understanding of the physical nature of the systems. The work of Bloom and Heymann (1) in 1946 pointed out a possible relationship between the physical nature of the solid state and the electrical properties of the fused state. Their results indicated that isotherms of equivalent conductivity would be expected to exhibit moderate negative deviations from additivity in systems showing no

evidence of intermediate compound formation in the solid state. Strong negative deviations would be found to be associated with systems whose phase diagrams indicated the presence of congruently melting compounds, and could be explained on the basis of persistence to some extent in the liquid state of the complex known to be present in the solid state. Experimental heat of activation isotherms for ionic migration calculated on the basis of the Arrhenius equation would exhibit maxima near compositions corresponding to unstable liquid state complexes.

Data were found indicating the existence of the compound $2KCl \cdot ZnCl_2$ (2). A study of this system was undertaken to see whether or not the electrical properties would agree with the above generalizations. The information required included the phase diagram of the system and isotherms of specific conductivity and density at various concentrations.

Preparation and Analysis of Sample

"Bakers' Analyzed broken lump" $ZnCl_2$, meeting ACS specifications, was fused in a Pyrex test tube in the furnace at a temperature of about 400°C. The test tube was then transferred to an oven maintained at 110°C and the contents were allowed to solidify. A predetermined amount of Baker and Adamson reagent grade crystalline KCl was added and the mixture returned to the furnace. At this time hydrogen chloride gas was passed through the melt if any yellow ZnO was observed to be present, following which, in the case of conductivity measurements, the mixture was poured into a preheated cell. The cell was placed in the furnace and when the desired temperature was approached hydrogen chloride gas was passed through the cell, thus completing the preparation of the sample.

Bunker Hill brand electrolytic Zn with a minimum purity of 99.99% was dissolved in Baker and Adamson HCl (maximum heavy metal impurity of 0.0008%). The pure $ZnCl_2$ produced was used to standardize 1, 2-diaminocyclohexanetetraacetic acid from the Alrose Chemical Co. For analysis, some of the molten mixture was drawn up into a 5 mm diameter glass tube in which it was allowed to solidify. The mixture was quite hygroscopic, but by breaking the ends off the tube and quickly weighing the sample plus tube, the dry weight was determined. The solid sample was then dissolved from the tube and analyzed for Zn^{++} by the method of Loomis (3) following which the empty tube was reweighed. Knowing the weight of the sample and the weight of the $ZnCl_2$, the weight of the KCl was found by difference and the composition then calculated.

Apparatus

All the Pyrex conductivity cells used (Fig. 1) had cell constants in the range 400 ± 100 cm^{-1}. In the presence of water, $ZnCl_2$ may hydrolyze and form the oxide which is yellow at high temperatures. If the oxide is treated with hydrogen chloride gas, it is reconverted to the chloride and water vapor, and agitation will expell the latter from the melt. The long arm of the cell extended out of the furnace so that gas could be passed through it. The bulb on the short arm served two purposes. It prevented expulsion of the melt from the cell during passage of hydrogen chloride gas, and also allowed the use of larger samples, thus making chemical analysis of the composition of the melt easier and more accurate. The bubbling of the gas prior to a run also insured the homogeneity of the melt. Preliminary experiments indicated that the electrical conductivity of pure samples was unchanged following the passage of hydrogen chloride gas.

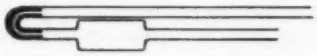

Fig. 1. Typical conductivity cell

The conductivity bridge was basically a L&N Wheatstone Bridge (Type S Test Set No. 5300). An audio-frequency vacuum tube oscillator served as the power source. No appreciable variation of resistance with frequency was noted and all measurements were made at 1000 cps. The waveform delivered by the oscillator was excellent as viewed on an oscilloscope. A variable condenser was used to balance capacity in the bridge. A cathode ray oscilloscope was used as a visual, null-point indicator [*see* ref. (4) for example]. All connecting leads were shielded and grounded.

The electrodes were open cylinders of Pt with a length of 3/8 in. and a diameter 3/16 in. They were connected to 10-in. Pt leads. The electrodes were kept well platinized.

The resistance furnace was operated by a Brown Indicating Controller operating through a proportioning motor. The chromel-alumel measuring thermocouple was connected to a L&N No. 8662 potentiometer with a reference junction compensator. The measuring thermocouple was calibrated at the melting points of Zn, Sb, and Al (5).

A slight modification of the method of Peake and Bothwell (6) was used in determining densities by the sinker method. The sinker was of Pt and weighed 16.815 g in air. Its volume at various temperatures was calculated from literature values of the density and the coefficient of expansion of platinum (7-9).

The phase diagram was constructed by the standard method of thermal analysis of cooling curve data. It was necessary to locate the position of the liquidus curve closely, since in the region on the temperature-composition diagram below this line, the composition in the melt is not the same as the over-all composition of the system.

Results

The phase diagram (Fig. 2) of the system indicates the formation of a solid phase compound corresponding to the composition $2KCl \cdot ZnCl_2$. Eutectics are found at about 433°C (mole fraction KCl of 0.69) and 230°C (mole fraction KCl of 0.51). The solid state compound has a melting point of about 450°C.

Density data were taken at five temperatures for each of eight compositions (Table I). Data at intermediate temperatures for each composition were determined graphically from the linear density-temperature graph. Densities at intermediate com-

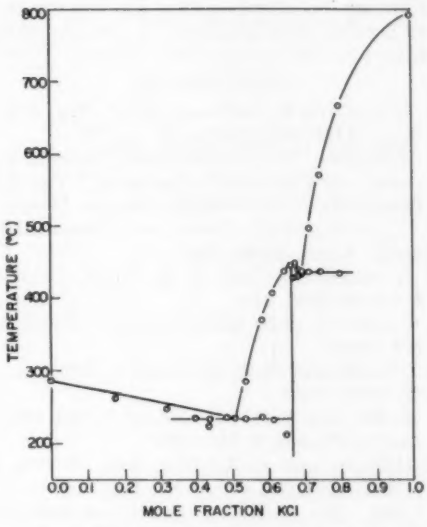

Fig. 2. Phase diagram of the system KCl-$ZnCl_2$

TABLE I. Density in the system KCl-$ZnCl_2$

X_{KCl}	t (°C)	d (g/cm³)	X_{KCl}	t (°C)	d (g/cm³)
0.000	450	2.457	0.452	453	2.150
	503	2.434		494	2.120
	555	2.405		540	2.094
	593	2.390		591	2.058
	637	2.360		645	2.022
0.094	462	2.399	0.639	442	2.007
	506	2.377		498	1.974
	548	2.351		554	1.939
	602	2.323		612	1.906
	674	2.283		658	1.876
0.158	454	2.369	0.698	447	1.950
	462	2.367		500	1.917
	486	2.349		547	1.888
	504	2.334		596	1.857
	554	2.304		649	1.830
	598	2.276			
	646	2.249	0.811	688	1.687
	660	2.242		715	1.672
0.313	451	2.261			
	500	2.228			
	548	2.201			
	603	2.170			
	661	2.131			

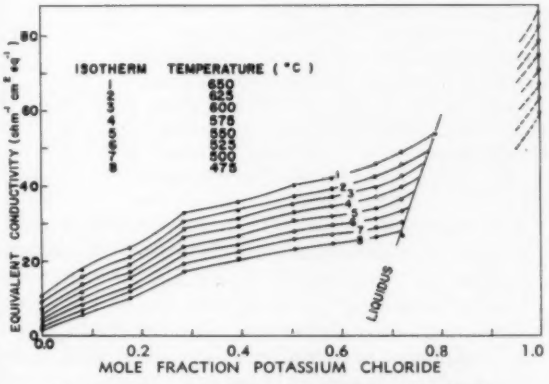

Fig. 3. Equivalent conductivity in the system KCl-$ZnCl_2$

TABLE II. Equivalent conductivity in the system KCl-$ZnCl_2$ equivalent conductivity at different temperatures (°C)

X_{KCl}	650°	625°	600°	575°	550°	525°	500°	475°
0.000	10.55	8.80	7.23	5.78	4.51	3.43	2.50	1.76
0.080	17.81	15.66	13.58	11.73	10.00	8.41	6.90	5.60
0.176	23.26	21.08	19.06	17.06	15.08	13.25	11.67	10.01
0.284	32.52	30.29	28.24	26.13	23.81	21.61	19.39	17.28
0.395	35.58	33.33	31.13	28.87	26.61	24.38	22.39	20.11
0.506	39.97	37.61	35.13	32.75	30.33	27.83	25.41	22.88
0.582	41.77	39.08	36.71	34.18	31.64	29.15	26.69	24.19
0.670	45.51	42.43	39.52	36.82	33.95	31.22	28.57	25.97
0.722	48.64	45.45	42.40	39.33	36.16	33.00	29.87	26.36
0.790	53.60	*	*	*	*	*	*	*

* This temperature is below the liquidus on a temperature-composition diagram.

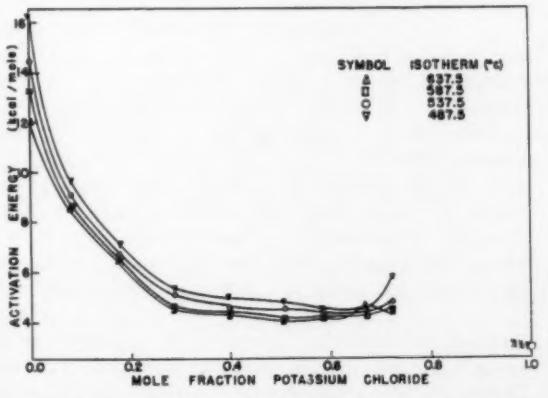

Fig. 4. Experimental heats of activation in the system KCl-$ZnCl_2$

positions were determined by interpolation on the graph of density vs. composition at constant temperature. The isotherms are somewhat "S" shaped. They deviate slightly from additivity in a positive direction at low KCl concentrations and have the suggestion of a negative deviation at low $ZnCl_2$ concentrations. The maximum relative error for the densities is $\pm 6 \times 10^{-4}$.

Isotherms of equivalent conductivity (Table II and Fig. 3) consequently look much like those of specific conductivity. Negative deviations become noticeable at a KCl mole fraction of about 0.30 and reach a maximum at about 0.71, corresponding closely to the composition $2KCl \cdot ZnCl_2$. The maximum relative error is $\pm$ 0.0054.

Experimental heats of activation for ionic migration computed from the Arrhenius equation, $\Omega = A \cdot \exp(-\Delta H^{\ddagger}/RT)$, change only slightly in the range of KCl mole fraction from 1.0 to 0.3, and do so in an approximately linear manner (Fig. 4). At the latter concentration, the activation energy begins a rapid rise to the limiting value for pure $ZnCl_2$. The maximum relative error is $\pm$0.025.

The large negative deviation from additivity exhibited by isotherms of equivalent conductivity and the maximum negative deviation occurring in the neighborhood of the composition corresponding to $2KCl \cdot ZnCl_2$ are both in agreement with the pro-

posals of Bloom and Heymann. Recent work by Duke and Laity (10) assigns ionic transport numbers t_+ and t_- of 0.25 and 0.75, respectively, in lead (II) chloride at 565°C. These results lend experimental support to earlier predictions of a number of authors that alkali halides are predominantly cationic conductors, while in the alkaline earth halides, the anions carry a larger share of the current. In the system KCl-$ZnCl_2$, K^+ dominates the equivalent conductivity and activation energy for pure KCl while Cl^- does the same for pure $ZnCl_2$. An interesting proposal is that K^+ dominates for the mixture in the KCl mole fraction range between 0.3 and 1.0, while Cl^- begins to become important at mole fraction 0.3, increasingly dominating these properties of the mixture from mole fraction 0.3 to 0.0. This proposal must be regarded as pure speculation, however, since a requisite for attempting any further significant discussion of the activation energy isotherms is the availability of data on the transport numbers of the ions at different compositions.

Manuscript received July 2, 1956. Contribution No. 502. Work was performed in the Ames Lab. of the A.E.C.

Any discussion of this paper will appear in a Discussion Section to be published in the December 1957 JOURNAL.

REFERENCES

1. H. Bloom and E. Heymann, *Proc. Roy. Soc. (London)*, **A188**, 392 (1946).
2. J. W. Mellor, "A Comprehensive Treatise on Inorganic and Theoretical Chemistry," Vol. 4, p. 551, Longmans, Green and Co., London (1947).
3. T. C. Loomis, Ph.D. Thesis, Iowa State College Library, Ames, Iowa (1953).
4. R. N. Haszeldine and A. A. Woolf, *Chemistry & Industry*, **1950**, 544.
5. H. F. Stimson, *J. Research Natl. Bur. Standards*, **42**, 209 (1949).
6. J. S. Peake and M. R. Bothwell, *J. Am. Chem. Soc.*, **76**, 2653 (1954).
7. R. Kieffer and W. Hotop, *Kolloid Z.*, **104**, 208 (1943).
8. J. Austin, *Physics*, **3**, 240 (1932).
9. L. Holborn and A. L. Day, *Ann. Physik*, **4**, 104 (1901), (original not seen). Referred to by R. F. Vines, "The Platinum Metals and their Alloys," The International Nickel Co., Inc., New York (1941).
10. F. R. Duke and R. W. Laity, *J. Phys. Chem.*, **59**, 549 (1955).

Technical Feature

The Potential of an Electrode of a Voltaic Cell; A New Definition with Justification for the Use of Two Sign Conventions

J. B. Ramsey

Department of Chemistry, University of California, Los Angeles, California

ABSTRACT

For orientation purposes a brief review of the meaning of the potential of an electrode, first proposed by Lewis and adopted by most American physical chemists, is given. A definition of the potential of an electrode, basically different from those of Lewis and of Gibbs, is developed on the basis of the thermodynamic analysis of conditions existing in an electrode system (half-cell) at equilibrium. It is shown that the partial molal free energy (chemical potential) of the electrons in the electrode of an electrode system at equilibrium provides a meaningful definition of the potential of an electrode. It is suggested that the potential of an electrode, so defined, be designated as the "electron chemical potential" of the electrode, in volts. The value of the electron chemical potential of an electrode, so defined, is shown (*a*) to be invariant in sign as is that of the Gibbs potential, and (*b*) to be equal in magnitude and opposite in sign to that of the Gibbs potential. A justification for the use of both of these definitions of an electrode potential, and therefore of two sign conventions, is presented.

It is well known that, at present, there is a lack of uniformity among chemists in the sign convention used in the designation of the values of the potentials of electrodes. Also the term "potential," as applied to electrodes, has, in general, been used somewhat indefinitely and with different meanings by different authors, and in some cases by the same author, in treating this subject. Even the terminology used, especially by American physical chemists, is quite varied. Reference to the most recent editions of American textbooks which treat this subject will substantiate this statement (1).

The new definition of the potential of an electrode developed in this paper, along with the derivation of its relation to the potential of an electrode (the Gibbs potential) as defined and used by electrochemists, most European chemists and many American biological and analytical chemists, may, it is hoped, be helpful in removing some of the confusion now existing among chemists regarding this subject. The basic thermodynamic and electrostatic principles involved are known, the latter less well than the former.

The meaning of electrode potentials as defined and used by Lewis and Randall (2) (referred to as the Lewis potential).—The definition of an "electrode potential," as given by these authors, is the one adopted and used by most American physical chemists. This usage has been more firmly established by its adoption in the well-known book by Latimer (3). The meaning of an "electrode potential" according to Lewis and Randall (to be symbolized by E) is given in the following quotation: "Thus if we are considering the junction at an electrode, we may represent this junction by the expression: electrode, electrolyte. We then say that the single potential measures the tendency for negative electricity to pass from right to left, that is from the electrolyte to the electrode. On the other hand, we may express the junction as: electrolyte, electrode. Here again the potential measures the tendency of the negative current to pass from right to left. It has the same magnitude as before, but the opposite sign."

The authors' interpretation of this statement (quoted above) may be most clearly given by a simple illustration. Consider the junction, Zn; solution containing Zn^{++}. The passage of negative electricity from right to left involves the change of Zn to Zn^{++}. The change in state (per faraday), which Lewis and Randall correlate with this junction, is formulated

$$\tfrac{1}{2}\ Zn \rightarrow \tfrac{1}{2}\ Zn^{++} + e^{-} \qquad (I)$$

It is understood that the thermodynamic state of the Zn is that of pure solid Zn and that of Zn^{++} is that determined by the composition of the solution. The state of the electron substance is that of the electrons in the electrode of the defined standard hydrogen electrode system at equilibrium. That this is

the state of electrons in all such formulations of half-reactions is a consequence of the fact that the authors assign arbitrarily the value, zero, for the ΔF (change in free energy) accompanying the change

$$\tfrac{1}{2}\ H_2\ (ss) \rightarrow H^+\ (ss) + e^-\ \text{(in the electrode at equilibrium)} \qquad \text{(II)}$$

where (ss) denotes the hypothetical standard state. The E of the Zn, Zn^{++} junction is then defined by the relation

$$E = -\Delta F/\mathbf{F} \qquad \text{(III)}$$

where ΔF is the change in free energy accompanying the change formulated in reaction (I) above and $\mathbf{F}$ represents the faraday. It should be noted that this ΔF is not the ΔF accompanying the change

$$\tfrac{1}{2}\ Zn \rightarrow \tfrac{1}{2}\ Zn^{++} + e^-\ \text{(in the Zn electrode after contact with the solution, i.e., at equilibrium)} \qquad \text{(IV)}$$

for the value of this latter ΔF would obviously be zero.

Now if the junction is written in the reverse direction, viz., solution containing Zn^{++}; Zn, the passage of negative electricity from right to left is correlated with a change in state which is the reverse of that of reaction (I). The E ascribed to this junction would therefore be equal in absolute value but opposite in sign to that of the junction, Zn; solution containing Zn^{++}.

According to the convention regarding the emf of a voltaic cell [first adopted by Lewis and Randall (1) and universally accepted] it follows that the value of E for the junction, Zn; solution containing Zn^{++}, is related to the ΔF accompanying the isothermal change

$$\tfrac{1}{2}\ Zn + H^+\ (ss) \rightarrow \tfrac{1}{2}\ Zn^{++}\ \text{(in the solution)} + \tfrac{1}{2}\ H_2\ (ss) \qquad \text{(V)}$$

by the equation

$$E = -\Delta F/\mathbf{F} \qquad \text{(III)}$$

The standard E-value of this junction, symbolized $E°$, refers to the E-value when the Zn and the Zn^{++} are also in their standard states and is equal to +0.76 v. The $E°$-values, tabulated by Lewis and Randall (2) and by Latimer (3) are given the sign corresponding to the junction: electrode, electrolyte.

The electromotive force of any voltaic cell, as formulated, is then equal to $E_{left} + E_{right}$, where E_{left} is that of the junction (electrode, electrolyte)$_{left}$, and E_{right} is that of the junction (electrolyte, electrode)$_{right}$.

Use of the term "junction" by these authors may be misleading since changes in state considered in defining E may be misinterpreted to pertain to those changes when all the substances in the half-reactions (including the electrons) are in the states existing after contact (junction) between the electrode and electrolyte is made, i.e., after equilibrium exists in the electrode system. This interpretation is obviously not correct. The E of Lewis and Randall (2) has been more fully discussed by de Béthune (4). He designates E as the "half-cell E.M.F.," a name which is generally well-accepted.

Use of the term "potential."—It seems probable that some of the confusion now existing regarding the potentials of electrodes arises from the fact that the term "potential" has been used ambiguously quite often in the treatment of this subject. It may be noted that Lewis and Randall (2) (*see* p. 402) consider "potential" to be synonymous with the "electromotive force," E, as they define it. This does not conform with the well-accepted use of these terms. For the term "potential" to have precise meaning it must apply to some definite point or phase, not to a junction between two phases. This is true whether it is defined in an electrostatic sense or in a thermodynamic sense.

Thermodynamic basis for a new definition of the potential of an electrode and its relation to the Gibbs electrode potential (4b).—According to generally accepted views, when two different uncharged media (phases), containing charged species, ions, and/or electrons, are brought into contact, a practically instantaneous flow (through the interface) of those charged species, which the two media have in common, will occur in the establishment of equilibrium between the two media. The resultant quantity of positive charge transferred in one direction (or of negative charge in the other) can be shown to be infinitesimal (5); so infinitesimal that the change in the composition of each of the two media due to this transfer is entirely negligible. As an illustration, consider a piece of uncharged Cu and one of uncharged Zn (both at the same temperature and pressure) each conceived to consist of uncharged metal atoms, positive ions, and electrons. On contact a spontaneous and practically instantaneous flow of electrons from the Zn to the Cu will occur in the attainment of equilibrium between the two metals. Thermodynamically it follows that the chemical potential, μ_{e^-}, or more specifically in this case, the partial molal free energy, $\overline{F}_{e^-}$, of the electrons [called the electrochemical potential of the electrons by Guggenheim (6), and the electron potential by Eastman and Rollefson (7)] is greater in the uncharged Zn than in the uncharged Cu. These two partial molal free energies become equal after contact, i.e., after equilibrium is attained. Briefly $(\overline{F}_{e^-})_{Zn} > (\overline{F}_{e^-})_{Cu}$ prior to contact and $(\overline{F}_{e^-})_{Zn} = (\overline{F}_{e^-})_{Cu}$ after contact. Restated in the terminology of Lewis (*see* Ref. 2, Chapter XVI) this means that the escaping tendency of electrons from uncharged Zn is greater than the escaping tendency of electrons from uncharged Cu, each at the same temperature and pressure.

In describing the equilibrium condition existing between Cu and Zn after contact, it is often said that the electrostatic potential of the Zn is greater than that of Cu, meaning by this statement that the electrostatic potential at any point within the Zn is greater than it is at any point within the Cu. [It should be noted that this potential difference should not be identified with the "Volta" or "contact potential difference" (*see* Ref. (5a), p. 336).] That this description has no physical significance has not been generally realized. A principal of electrostatics enunciated in 1899 by Gibbs (8) justifies this con-

clusion. He wrote, "Again, the consideration of the electrical potential in the electrolyte, and especially the consideration of the difference of potential in electrolyte and electrode, involve the consideration of quantities of which we have no apparent means of physical measurement, while the difference of potential in 'pieces of metal of the same kind attached to the electrodes' is exactly one of the things which we can and do measure." In 1929 Guggenheim (6) rediscovered this principle and brought it to the attention of physical scientists. He reformulated the principle as follows: "The electric potential-difference between two points in different media can never be measured and has not yet been defined in terms of physical realities. It is therefore a conception which has no physical significance." There is no doubt that the abandonment of the use of such a conception in discussing electrode systems and voltaic cells is imperative if confusion and misleading terminology are to be avoided. If one considers that one piece of the metal M (to be used in connecting the electrodes of a voltaic cell), is connected with one of the electrodes and another piece of M with the other, then it is physically meaningful to refer to the electrostatic potential difference between these two pieces of M. (The nature of M is immaterial.) This then is the only meaning that "the electrostatic difference in potential between two electrodes" can have.

Example of the two general types of electrode systems may now be analyzed. First, consider a piece of Zn and a solution containing a Zn salt. On dipping Zn into the solution, equilibrium is established between the Zn and the solution, and also within the metallic Zn. The following thermodynamic relations will then apply:

$$(\bar{F}_{Zn^{++}})_{\text{in the Zn}} = (\bar{F}_{Zn^{++}})_{\text{in the solution}} \qquad \text{(VI)}$$

and within the Zn

$$(\tilde{F}_{Zn}) = \bar{F}_{Zn^{++}})_{\text{in the Zn}} + 2(\bar{F}_{e^-})_{\text{in the Zn}} \qquad \text{(VII)}$$

where $\tilde{F}_{Zn}$ represents the molal free energy of pure Zn.

Since at a given temperature and pressure the value of the molal free energy of Zn, $\tilde{F}_{Zn}$, is fixed, and since the value of $\bar{F}_{Zn^{++}}$ in the metal is determined by (and equal to) the value of $\bar{F}_{Zn^{++}}$ in the solution, it follows that the value of $\bar{F}_{e^-}$ in the Zn is determined by the composition of the solution of the Zn salt.

It should be noted that even though the description of the equilibrium conditions has been given in terms of the fictitious electrochemical potentials, $\bar{F}_{Zn^{++}}$ and $\bar{F}_{e^-}$, nevertheless only linear combinations of these, which appear in the treatment of voltaic cells, are definable in terms of physical realities.

A second general type of electrode system is one in which the metallic electrode is not one of the chemical reactants or products of the half-reaction involved. The hydrogen electrode system is an example of this type. Another, more simply analyzable, is the ferrous-ferric electrode system. Consider a piece of Pt (or other suitable noble metal) dipping into a solution containing ferrous and ferric salts. In this case the equilibrium condition is described by the relation

$$(\bar{F}_{Fe^{++}}) = (\bar{F}_{Fe^{+++}}) + (\bar{F}_{e^-})_{\text{in the electrode}} \qquad \text{(VIII)}$$

It is seen that the electrochemical potential of the electrons, $\bar{F}_{e^-}$, in the metal electrode is determined by the composition of the solution, i.e., by the values of $F_{Fe^{+++}}$ and of $F_{Fe^{++}}$ in the solution.

It follows that, in general, the value of the partial molal free energy of the electrons, $\bar{F}_{e^-}$, in the electrode of any electrode system at equilibrium is determined by the tendency of the substances constituting the reduced state to change to the substances, constituting the oxidized state, and to electrons in the state in which they exist in the hydrogen electrode in the standard hydrogen electrode system at equilibrium. The greater the tendency for this change to occur, that is the greater the decrease in free energy $(-\Delta F)$ accompanying this change, the greater will be the value of $\bar{F}_{e^-}$ in the metal electrode of that electrode system at equilibrium. In terms commonly used, it may be said that the greater the strength of the reduced state, as a reducing agent, the greater will be the value of $\bar{F}_{e^-}$ in the electrode.

In order to give a value to the $\bar{F}_{e^-}$ in the electrode of any electrode system at equilibrium, it is necessary to assign arbitrarily the value zero to the $\bar{F}_{e^-}$ in the electrode of a specified electrode system at equilibrium. This is necessary since only differences in $\bar{F}_{e^-}$-values are physically measurable. It has been universally agreed to assign zero-value to the $\bar{F}_{e^-}$ of the electrons in the metal electrode (Pt generally used) when it is in equilibrium with hydrogen gas and hydrogen ion, each in their defined standard states, the latter in aqueous solution. This means that, according to the Lewis terminology, the fugacity of electrons in this electrode is taken as unity.

A voltaic cell in which the only significant changes in free energy accompanying the reversible isothermal flow of electricity through the cell are those occurring within the two electrode systems may be formulated

Electrode system (l), Electrode system (r) *(A)*

where l and r designate the system on the left and the one on the right, respectively. When referring to the potential (electrostatic) difference between the two electrodes, it is recalled that, to have meaning, this must refer to the potential difference between the two pieces of metal, M (usually Cu), which are considered to be attached to the two electrodes, respectively.

Consider a reversible transfer of electrons through M from the left electrode to the one on the right. This may or may not be the direction in which the transfer of electrons will occur spontaneously. Such a transfer will be accompanied by oxidation in the system on the left and reduction in the one on the right.

The resultant (total) chemical change in the cell per faraday passed is given by the general expression

$$Rd_l + Ox_r \rightarrow Rd_r + Ox_l \qquad (I)$$

where each of the four symbols represents one equivalent of each of the substances involved in the reduced and oxidized states of the respective electrode systems at equilibrium. This change in state is the resultant of the following three simultaneous changes in state:

(a) $Rd_l \rightarrow Ox_l + e^-$ (in left electrode) $\quad \Delta F_a = 0$

(b) e^- (in left electrode) $\rightarrow e^-$ (in right electrode) $\quad \Delta F_b = (\overline{F}_{e^-})_r - (\overline{F}_{e^-})_l$

(c) e^- (in right electrode) $+ Ox_r \rightarrow Rd_r \quad \Delta F_c = 0$

It is seen that $\Delta F_a + \Delta F_b + \Delta F_c$ is equal to the ΔF of the above resultant change in state, Eq. (I), which is thus given by

$$\Delta F = (\overline{F}_{e^-})_r - (\overline{F}_{e^-})_l \qquad (II)$$

Now the limiting (reversible) available work, $W'_{rev.}$, produced during this isothermal transfer of electrons from the piece of metal, M, connected with the left electrode, to the piece of metal, M, connected with the right electrode, is equal to that produced during the isothermal transfer of an equivalent quantity of positive electricity in the opposite direction, viz., from right to left through the external circuit. This quantity of work, in joules per faraday passed, is thus equal to $\mathbf{F}\,(V_r - V_l)$, where $\mathbf{F}$ is 96,491 coulombs and $V_r - V_l$ is expressed in volts. V_r and V_l are the electrostatic potentials of the pieces of metal, M, connected to the right and left electrodes, respectively. Therefore, the decrease in free energy accompanying the reaction, Eq. (I), is given by

$$-\Delta F = W'_{rev.} = \mathbf{F}\,(V_r - V_l) \qquad (III)$$

and, from the relation, Eq. (II)

$$-\Delta F = (\overline{F}_{e^-})_l - (\overline{F}_{e^-})_r = \mathbf{F}\,(V_r - V_l) \qquad (IV)$$

It is seen that if the process considered (electrons transferred from left to right through the external circuit) will occur spontaneously, i.e., $-\Delta F > 0$, then $(\overline{F}_{e^-})_l$ is greater than $(\overline{F}_{e^-})_r$ and V_r is greater than V_l. The electrostatic potential difference, $V_r - V_l$, the quantity directly measured experimentally, is equal in magnitude and sign to the electromotive force of Cell A. It should be noted, however, that $V_r - V_l$ is the difference in electrostatic potential existing between the two pieces of the metal, M, attached to the two electrodes, respectively, and not that between the two electrodes. The latter has no physical meaning.

The direct relation between the emf of any Cell A (symbolized by $E_{\text{Cell A}}$) and the value of ΔF accompanying the reaction, represented by Eq. (I), $[=(\overline{F}_{e^-})_r - (\overline{F}_{e^-})_l]$ is of primary interest to many chemists. This relation is obtained by rearranging Eq. (IV) to give

$$E_{\text{Cell A}} = -(V_l - V_r) = \frac{(\overline{F}_{e^-})_l}{\mathbf{F}} - \frac{(\overline{F}_{e^-})_r}{\mathbf{F}} = \frac{-\Delta F}{\mathbf{F}} \qquad (V)$$

From this relation, it is apparent that the quantity $\overline{F}_{e^-}/\mathbf{F}$ represents, for each electrode, an intensive-thermodynamic property, whose value is determined, as shown above, by the electrochemical equilibrium of the substances constituting the oxidized state, those constituting the reduced state, and the electrons in the electrode. Differences between the values of this thermodynamic property for different electrode systems determine the electromotive forces of cells made by combining any two electrode systems, as shown in Eq. (V). This thermodynamic property is a potential, in volts, and should be designated by an appropriate name and symbol. The symbol adopted here is the script capital $\mathcal{E}$, and it is suggested that the quantity $\mathcal{E}_i$, to be defined by the equation

$$\mathcal{E}_i = (\overline{F}_{e^-})_i/\mathbf{F} \qquad (VI)$$

should be designated as the "electron chemical potential" of the *ith* electrode (in volts). This designation seems meaningful and unambiguous.

The electron chemical potential $\mathcal{E}$ coincides in sign (and magnitude) with a quantity to which MacDougall (1c) gave the name, "electrode E.M.F." However, in definition, the two quantities are fundamentally different, since nothing is said in the definition of $\mathcal{E}$ about the "potential difference between two phases" [Ref. (1c), page 580], and the latter phrase has been shown above to be devoid of physical significance. On the other hand, the designations "electrode emf" and "half-cell emf" have been much more commonly applied to the E of Lewis and Randall (2), a quantity which (as shown above) changes its sign when the half-cell diagram and half-cell reaction are reversed, viz., from electrode, electrolyte to electrolyte, electrode. Thus there is justification for the new name "electron chemical potential" and for the new symbol $\mathcal{E}$ for the potential defined here.

The emf of Cell A is then given by

$$E_{\text{Cell A}} = \mathcal{E}_l - \mathcal{E}_r = -(V_l - V_r) \qquad (VII)$$

It may be noted that the sign of the value of $E_{\text{Cell A}}$ thus obtained conforms to the convention regarding the sign to be given to the emf of a cell which has been recommended by the Commission on Physico-Chemical Symbols and Terminology and the Commission on Electrochemistry of the International Union of Pure and Applied Chemistry (9) meeting in Stockholm in 1953. As previously mentioned this convention was originally adopted by Lewis [*see* Ref. (2), p. 390]. de Béthune (4b) has given a thorough discussion of the recommendations of these Commissions, and a valuable synthesis of the electrochemical thermodynamic conventions of Nernst, Lewis and Randall, together with those of the Stockholm Commissions, and with the thermodynamic treatment of Gibbs. Also certain important historical facts pertinent to the development of this subject are to be found in this paper.

The electron chemical potential of the electrode of any electrode system at equilibrium may now be defined by the relation

Electron chemical potential of the *ith* electrode

$$= \mathcal{E}_i - \mathcal{E}^\circ_{H_2} \qquad \text{(VIII)}$$

where $\mathcal{E}^\circ_{H_2}$ refers to the electron chemical potential of the electrode (Pt) in equilibrium with $H_2(g)$ and $H^+ \cdot Aq$, each in their defined standard states. The Gibbs electrode potential, V, is defined by the relation

Gibbs electrode potential of the *ith* electrode

$$= V_i - V^\circ_{H_2} \qquad \text{(IX)}$$

where the V's represent the electrostatic potentials of the two pieces of the metal, M (to be used in connecting the electrodes), attached to each of the two metal electrodes of the two electrode systems at equilibrium.

If now the electrode system on the left in the Cell A (formulated above) is considered to be any electrode system and the one on the right to be the standard hydrogen electrode system, it follows from Eq. (VII) that

$$E_{cell} = \mathcal{E}_i - \mathcal{E}^\circ_{H_2} = -(V_i - V^\circ_{H_2}) \qquad \text{(X)}$$

Since $\mathcal{E}^\circ_{H_2}$ is arbitrarily taken as zero, as is also $V^\circ_{H_2}$, it follows that

$$\mathcal{E}_i = -V_i \qquad \text{(XI)}$$

It is therefore evident that when the potential of an electrode is given its $\mathcal{E}$-value, the word, "potential," is used in a thermodynamic sense in that it refers to the electron chemical potential of the electrode. When given its V-value, "potential" is defined in its electrostatic sense and refers to the piece of connecting metal, M, attached to the electrode. It is the latter which is referred to by de Béthune (4*b*) as "the Gibbs electrode potential." For example, $\mathcal{E}^\circ(Zn, Zn^{++}) = +0.76$ and $V^\circ(Zn, Zn^{++}) = -0.76$.

It should be noted that the sign of the value of $\mathcal{E}_i$, as defined above, is independent of the direction of the reversible flow of electrons (through the connecting wire), as is also the sign of V_i. In other words, its sign (and value) is the same whether the reversible process considered makes the electrode in question the cathode or the anode, that is the sign of $\mathcal{E}$ is invariant. Thus $\mathcal{E}$ differs fundamentally from the E as defined by Lewis and Randall and as used by most American physical chemists. The sign of E is bivariant. Both $\mathcal{E}_i$ and V_i may be properly considered to be intensive properties of any electrode system, i, at equilibrium at a certain temperature and pressure, and their signs and values are consequently independent of the direction of the reversible process under consideration. The V-values (the Gibbs electrode potentials) of electrodes are used by electrochemists, most European chemists, and many biological and analytical chemists. It is important to note that the "potential" of an electrode as defined by its $\mathcal{E}$-value is fundamentally different from "potential" as defined by its V-value even though the two values are very simply related ($\mathcal{E}_i = -V_i$). The value of $\mathcal{E}_i$, that is of $\mathcal{E}_i - \mathcal{E}^\circ_{H_2}$, is correctly described as a measure of the difference between the escaping tendency of the electrons in the electrode of the *ith* electrode system at equilibrium and that of the electrons in the electrode of the standard hydrogen electrode system at equilibrium. The escaping tendency of the electrons in an electrode, as defined here, is measured by the partial free energy per coulomb of the electrons in that electrode.

Justification for the use of two sign conventions.—Valid reasons can be given for the designation of the potentials of electrodes by their V-values as is done by electrochemists, most European chemists, and many biological and analytical chemists. The V-values have the practical advantage, namely, that the electrode of a voltaic cell which has the larger V-value, that is, the larger electrostatic potential of the piece of connecting metal attached to it, is designated "the positive pole." The relative polarity of the two electrodes of a cell follows directly from the relative V-values of the two pieces of the same metal connected with the two electrodes. Also, it is the difference, $V_r - V_l$, which is experimentally measured in determining the emf of a cell, that is $(emf)_{cell} = V_r - V_l$.

Those chemists who, along with the author, choose to designate the potentials of electrodes by their $\mathcal{E}$-values (as defined in this paper and named "electron chemical potentials") can find justification for their choice in the fact that the emf of a cell follows in a more direct thermodynamic way from the two $\mathcal{E}$-values. The $\mathcal{E}$-value of an electrode is directly proportional (proportionality constant = $1/\mathbf{F}$) to the value of the partial molal free energy (chemical potential) of the electrons in the electrode of the electrode system at equilibrium. It is the difference between the two $\overline{F}_{e^-}$-values which gives directly the value of ΔF (per faraday) accompanying the isothermal change in state in the cell. The basis for these statements is shown by the following relations applicable to any voltaic cell, as symbolized by Cell A, per faraday of electrons passed reversibly through the outer circuit from the left-hand electrode to the right-hand electrode.

$$(emf)_{cell} = \frac{(\overline{F}_{e^-})_l}{\mathbf{F}} - \frac{(\overline{F}_{e^-})_r}{\mathbf{F}} = \mathcal{E}_l - \mathcal{E}_r$$

and

$$\Delta F \text{ (per faraday passed)} = (\overline{F}_{e^-})_r - (\overline{F}_{e^-})_l$$
$$= \mathbf{F}(\mathcal{E}_r - \mathcal{E}_l) = -\mathbf{F}(\mathcal{E}_l - \mathcal{E}_r) = -\mathbf{F}(emf)_{cell}$$

It may be recalled that the value of the so-called "potential," E, as defined by Lewis and Randall (2), is such that the emf of a voltaic cell, as formulated, is given by the relation

$$(emf)_{cell} = E_l + E_r = E(\text{electrode, electrolyte}) + E(\text{electrolyte, electrode})$$

The value of the emf of a voltaic cell in terms of V, $\mathcal{E}$, and E is thus given by

$$(emf)_{cell} = V_r - V_l = E_l + E_r = \mathcal{E}_l - \mathcal{E}_r$$

where the meaning of the Lewis and Randall expression, $E_l + E_r$, is that given above.

Continued use by some chemists of the V-values for the potentials of electrodes (with one sign con-

vention) and of the $\mathcal{E}$-values by other chemists (with the opposite sign convention) seems completely justifiable.

In phraseology commonly used in the discussion of half-cells, it may be of value to reiterate that in any electrode system the greater the tendency of the substances in the reduced state to change to the substances in the oxidized state, and to electrons, in the thermodynamic state in which they exist in the electrode of the standard hydrogen electrode system at equilibrium, the greater will be the value of $\mathcal{E}$ (as defined in this paper) and the less will be the value of V, both on an algebraic scale.

Acknowledgment

The author wishes to thank Professor André J. de Béthune for his generous assistance in the clarification and organization of this presentation.

Manuscript received Jan. 3, 1956.

Any discussion of this paper will appear in a Discussion Section to be published in the December 1957 JOURNAL.

REFERENCES

1. As examples, *see* (*a*) F. Daniels and R. A. Alberty, "Physical Chemistry," pp. 422-431, John Wiley & Sons, Inc., New York (1955); (*b*) Linus Pauling, "General Chemistry," 2nd ed., pp. 652-654, W. H. Freeman and Co., San Francisco (1953); (*c*) F. H. MacDougall, "Physical Chemistry," 3rd ed., pp. 609-610, The Macmillan Co., New York (1952); (*d*) C. F. Prutton and S. H. Maron, "Fundamental Principles of Physical Chemistry," Revised Ed., p. 531, The Macmillan Co., New York; (*e*) A. A. Noyes and M. S. Sherrill, "A Course of Study in Chemical Principles," 2nd ed., pp. 366-370, The Macmillan Co., New York (1938).
2. G. N. Lewis and M. Randall, "Thermodynamics and the Free Energy of Chemical Substances," pp. 402-404, McGraw-Hill Book Co., Inc., New York (1923).
3. W. M. Latimer, "Oxidation Potentials," 2nd ed., Prentice-Hall, Inc., New York (1952); *see* also Latimer, *J. Am. Chem. Soc.*, **76**, 1200 (1954).
4. A. J. de Béthune, (*a*) *This Journal*, **101**, 252*C* (1954); (*b*) *ibid.*, **102**, 288*C* (1955).
5. (*a*) E. A. Guggenheim, "Thermodynamics," Chap. X, p. 331, Interscience Publishers, Inc., New York (1949); (*b*) A. A. Noyes and M. S. Sherrill, "Chemical Principles," 1st ed., p. 255, The Macmillan Co., New York (1929).
6. E. A. Guggenheim, *J. Phys. Chem.*, **33**, 842 (1929); also E. A. Guggenheim, ref. (5*a*), pp. 331-332.
7. E. D. Eastman and G. K. Rollefson, "Physical Chemistry," pp. 438-440, McGraw-Hill Book Co., Inc., New York (1947).
8. "The Collected Works of J. Willard Gibbs," Vol. 1, p. 429, Longmans, Green and Co., New York (1928).
9. J. A. Christiansen and M. Pourbaix, *Compt. rend. XVII Conf. Inter. Union Pure and Appl. Chem.*, held in Stockholm in 1953, pp. 82-84, Maison de la Chimie, Paris (1954).

FUTURE MEETINGS OF
The Electrochemical Society

Washington, D. C., May 12, 13, 14, 15, and 16, 1957

Headquarters at the Statler Hotel

Sessions will be scheduled on

Electric Insulation, Electronics (including Luminescence, Semiconductors, Thermionic Cathodes, Instrumentation, and Screen Applications), Electrothermics and Metallurgy, Industrial Electrolytics, and Theoretical Electrochemistry (including a special symposium on electrolytes)

★ ★ ★

Buffalo, October 6, 7, 8, 9, and 10, 1957

Headquarters at the Statler Hotel

Sessions will be scheduled on

Batteries, Corrosion, Electrodeposition (symposium on "Metal Powders"), Electrodeposition—Corrosion (Joint Symposium on "Corrosion of Electrodeposited Metals"), Electronics (Semiconductors), Electro-Organics, Electro-Organics—Theoretical Electrochemistry (Joint Symposium), and Electrothermics and Metallurgy

★ ★ ★

New York, April 27, 28, 29, 30, and May 1, 1958

Headquarters at the Statler Hotel

★ ★ ★

Ottawa, September 28, 29, 30, October 1, and 2, 1958

Headquarters at the Chateau Laurier

★ ★ ★

Papers are now being solicited for the meeting to be held in Buffalo, N. Y. Triplicate copies of each abstract (*not exceeding 75 words in length*) are due at the Secretary's Office, 216 West 102nd St., New York 25, N. Y., *not later than June 1, 1957* in order to be included in the program. *Please indicate on abstract for which Division's symposium the paper is to be scheduled.* Complete manuscripts should be sent in triplicate to the Managing Editor of the JOURNAL at the same address.

Current Affairs

Hackerman and Schaefer to Take Office in Washington

Norman Hackerman

R. A. Schaefer

As a result of the recent annual election, in which the voting is by mail ballot, Norman Hackerman has been elected the new President of the Society, and Ralph A. Schaefer, Third Vice-President. The new officers will take office at 8:00 A.M. on Thursday, May 16, 1957, in Washington, D. C.

Dr. Hackerman, professor of chemistry, chairman of the department, and director of the Corrosion Research Lab., University of Texas, Austin, Texas, replaces Hans Thurnauer, Head of the Inorganic Section of the Central Research Lab., Minnesota Mining and Manufacturing Co., St. Paul, Minn. Mr. Thurnauer, as Past President, will continue as a member of the Board of Directors.

Ralph A. Schaefer, Technical Advisor to the President of the Cleveland Graphite Bronze Division of the Clevite Corp., Cleveland, Ohio, will start his first term as Society Vice-President and will serve with the two previously elected Vice-Presidents, Sherlock Swann, Jr., and William C. Gardiner.

Lyle I. Gilbertson begins the last year of his three-year term as Treasurer.

Plans Now Complete for Washington Meeting

Arrangements for the Spring Meeting of the Society to be held at the Hotel Statler, Washington, D. C., May 12-16, 1957, have been completed. Preliminary information appeared in the January and February JOURNALS.

Be sure to mail your hotel reservation card to the Hotel Statler (Headquarters hotel), or to the hotel of your own selection, at least two weeks before the meeting and, preferably, even before April 26. Please be sure to mention The Electrochemical Society prominently when making reservations.

Technical Sessions

The full program appeared in the March JOURNAL. Technical sessions will be conducted by the Electric Insulation, Electronics, Electrothermics and Metallurgy, Industrial Electrolytic, and Theoretical Electrochemistry Divisions.

The Theoretical Electrochemistry Division of the Society, with the support of the National Science Foundation, is sponsoring a Symposium on the Structure of Electrolytic Solutions. In addition to many prominent individuals from this country, the following invited guests from other countries will speak: J. N. Agar, Cambridge University, Cambridge, England; J. M. Austin, R. A. Matheson, and H. N. Parton, University of Otago, Dunedin, New Zealand; R. P. Bell, Balliol College, Oxford, England; A. N. Campbell, The University of Manitoba, Winnipeg, Canada; C. W. Davies, University College of Wales, Aberstwyth, Wales, Great Britain; J. F. Duncan and D. L. Kepert, The University of Melbourne, Victoria, Australia; M. Eigen, The University of Göttingen, Göttingen, Germany; E. Glueckauf, Atomic Energy Research Establishment, Harwell, Berks., England; E. A. Guggenheim, The University of Reading, Reading, England; J. J. Hermans, Ryks University, Leiden, The Netherlands; E. Lange, University of Erlangen, Erlangen, Germany;

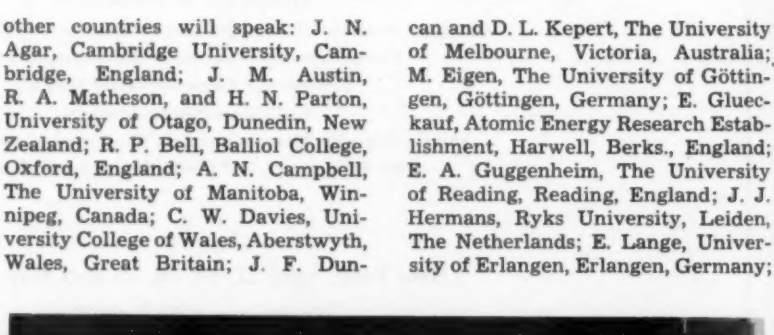

Nuclear reactor to be shown on Naval Research Lab. visit

R. A. Robinson, University of Malaya, Singapore, Malaya; R. H. Stokes, The University of New England, Armidale, N.S.W., Australia; A. R. Ubbelhohde, Imperial College of Science and Technology, London, England.

Peter Debye will be the guest speaker at the Annual Luncheon of the Theoretical Electrochemistry Division.

The Electric Insulation Division is sponsoring symposia on New Material Developments, Thermal Aging and Classification of Materials, Insulation Life, and Prefabricated Circuitry. Several prominent men have been invited to participate in a panel discussion on High Temperature Capacitors.

K. N. Mathes will be the guest speaker at the Annual Luncheon of the Electric Insulation Division. His subject will be, "Europe—Another Dimension in Technical Growth."

The Electrothermics and Metallurgy Division will hold a symposium on "Columbium (Niobium)" and will co-sponsor a joint symposium with the Corrosion Division on "Role of Metal and Oxide Structure in Oxidation and Corrosion."

The Electronics Division will hold symposia on Luminescence, Semiconductors, Thermionic Cathodes, Instrumentation, and Screen Applications.

The Industrial Electrolytic Division is sponsoring symposia on Fused Salt Electrolytes, and Chlor-Alkali Processes.

Laboratory Visits

Arrangements have been made for visits to the Naval Research Lab., the Naval Ordnance Lab., and the National Bureau of Standards. U. S. citizens wishing to visit the Naval Research Lab. should register for the trip before 10:00 A.M., Monday, May 13, so that the required passes may be prepared.

Highlights of the Board of Directors' Meeting

(Held January 4, 1957)

The minutes of the last meeting were approved after minor corrections.

Report of Tellers of Election

For President: Norman Hackerman, 915; total ballots, 945. For Vice-President: R. A. Schaefer, 420; I. E. Campbell, 308; A. L. Smith, 177; total ballots, 945.

It was voted to accept the Report of the Tellers. President Thurnauer then declared that Norman Hackerman had been elected President for the forthcoming year, and Ralph A. Schaefer Vice-President.

Communications from the President

The President reported regretfully that Dr. R. M. Burns had resigned as Chairman of the Publication Committee due to the fact that he will be out of the country for a few years.

The President reported that The Asia Foundation has granted support to our Indian members to the extent of $135. This is a continuation of last year's contribution.

Communications from the Treasurer

The report published here is a summary of the sales of Society monographs since their inception.

Sales and Royalties Received from Monographs Published by The Electrochemical Society, Inc.

Monograph	Period of time From	To	Domestic Copies sold	Domestic Royalties	Foreign Copies sold	Foreign Royalties	Total Copies sold	Total Royalties	Advanced for expenses
Abstracts of Literature on Semiconducting and Luminescent Materials									
1953 Issue	1/1/55	6/30/56	686	$343.00	326	$81.50	1,012	$424.50	$857.90
1954 Issue	7/1/55	6/30/56	562	281.00	360	90.00	922	371.00	
Corrosion Handbook	1/1/48	6/30/56	11,064	20,886.31	3,832	3,710.62	14,896	24,596.93	
Electrochemistry in Biology and Medicine	1/1/55	6/30/56	640	1,008.01	663	522.12	1,303	1,530.13	258.00
Gray's Modern Electroplating	7/1/53	6/30/56	3,086	4,017.31	1,681	1,101.57	4,767	5,118.88	175.00
High Temperature Technology	1/1/56	6/30/56	786	1,768.50	470	528.75	1,256	2,297.25	
Vapor Plating ..	1/1/55	6/30/56	1,021	842.34	727	299.89	1,748	1,142.23	
Vacuum Metallurgy	5/1/55	9/30/56					790	*3,324.28	1,877.31
			17,845	$29,146.47	8,059	$6,334.45	26,694	$38,805.18	$3,168.21

* Total sales.

The Treasurer explained the new method of presenting our Balance Sheet and pointed out that Mr. Robert Shannon, Assistant Secretary, has streamlined our accounting so that greater efficiency is being attained in our office.

Communications from Dr. Uhlig

Dr. Uhlig requested reconsideration of the method of handling royalties from Corrosion Division monograph funds. After considerable discussion, this was referred back to the Corrosion Division.

Communications from the Secretary

The Secretary reported that the Editor had requested that Dr. Donald H. Baird of Sylvania Electric Products Inc. in Flushing, N. Y., be appointed as Semiconductor Editor for the JOURNAL, replacing Dr. H. Bandes. It was voted that Dr. Baird be appointed. Dr. Middleton suggested to the Board that as a matter of procedure the Chairmen of the Society's Divisions should be informed of impending changes and consulted with respect to new appointees. It was voted that our By-laws should be amended in this regard.

There was considerable discussion on publication of material previously distributed as "Naval Research Laboratory Reports." The Editor was asked to contact the Naval Research Lab. with respect to arriving at an equitable decision on this matter.

Future Meetings

The program for the Washington Meeting was reviewed briefly. Dr. Fielding Ogburn, General Chairman of the Washington Meeting, reported that they are planning to get reprints of the printed program and distribute them to Division officers for circulation to nonmembers who might be interested.

The Board approved a motion made by Dr. Swann that there should be no exchange of money at any formal function at a national meeting, and that this should be standard policy for all future meetings.

Dr. Swann further recommended that introductions of speakers at meetings should not be a lengthy biography but a short statement of the title of the paper, the authors and their company affiliation, and the name of the person presenting the paper.

Report of the Ways and Means Committee

Dr. Swann, as Chairman of the Ways and Means Committee, recommended several changes in our Con-

stitution and Bylaws. Changes in the Constitution will be presented for ratification at the Washington Meeting. The revised Constitution and Bylaws will then be published in the JOURNAL in their entirety.

The Ways and Means Committee reported further on their study of the suggestion of Dr. Burns to give an annual award for conspicuous research and progress. There had been some thought of changing the Young Author's Prize along these lines. The Committee asked the President to appoint a committee to study this problem further. H. H. Uhlig, Chairman, R. A. Woofter, and U. B. Thomas were appointed to serve on this committee.

The problem of selection of a new printer for the JOURNAL was discussed. This matter had been brought to the attention of the Ways and Means Committee by the Secretary since Waverly Press has announced an increase in printing costs up to 12%. Mrs. Sterns has received two bids from other sources. The Lew A. Cummings Co., Inc. submitted the lowest bid and, since they do a very good job on the *Journal of Metals*, it was felt that a change in printers should be made since the increase in costs announced by Waverly Press would materially reduce the amount of technical material that we could publish next year. This change will be made, effective April 1, 1957.

Finance Committee

The proposed revised budget for the fiscal year Janary 1, 1956–March 31, 1957 was distributed to the Board. The budget, as approved at the Cleveland Meeting, contained an error which has been corrected; further, we have found it necessary to increase the budget for Bound Volumes, since in this 15-month period we must provide for binding two volumes. (These being minor revisions, the entire revised budget is not being reproduced here.) It was voted that the revised budget be approved.

The Secretary distributed two proposed budgets to the Board for the fiscal year April 1, 1957–March 31, 1958. One provides the Society Reserve Fund with the entire amount that the Board has, by its previous action, set aside for Reserves. The budget anticipates a total income of $117,220, of which $14,520, or about 12.4% of our total income, would be placed in Reserves. Proposed budget No. 1 is practically in balance before providing for Contingencies. This was done on the basis that Contingencies are not generally considered to be expendable. On the recommendation of the Editor, Dr. King, and the former Chairman of the Publication Committee, Dr. Burns, a second proposed budget was submitted. This budget provides for an increased appropriation of $4,000 for printing and mailing of the JOURNAL, and an additional $2,000 for hiring part-time editorial assistance. In this proposal, the amount budgeted to Reserves would be decreased by a

Proposed Revised Budget for the Fiscal Year 4/1/57–3/31/58

	1956 Budget—4/5 current approved budget	Proposed revised budget #1	Proposed revised budget #2
Income			
Membership Dues	$35,400	$39,200	$39,200
Patron & Sustaining Memberships	15,900	16,000	16,000
Reprints	4,000	4,700	4,700
Nonmember Journal Subscriptions	25,900	22,000	22,000
Office Sale Publications & Journal	1,000	500	500
Advertising	12,800	12,500	12,500
Bound Volumes	2,000*	2,500	2,500
Conventions	5,000*	5,300	5,300
Total Income to General Funds	$102,000	$102,700	$102,700
Nonmember Journal Subscriptions	4,070	4,200	4,200
Nonmember Convention Registration	1,200	2,520	2,520
Monograph Royalties	4,400	6,000	6,000
Income on Investments	400	1,800	1,800
Total Income to Reserve Funds	10,070	14,520	14,520
Total Income	$112,070	$117,220	$117,220
Expenses			
Printing & Mailing Journal	$36,000	$36,000	$40,000
Reprints	2,500	2,500	2,500
Publication Committee	350	350	350
Advertising Commission	5,200	5,200	5,200
Salaries, Social Security, & Insurance	39,000	40,000	42,000
Rent & Moving	2,400	4,000	4,000
Postage, Supplies, & Miscellaneous	6,200	6,200	6,200
Local Sections & Divisions	1,000	1,000	1,000
Young Author's Prize	100*	100	100
Reserve New Office Equipment	585	585	585
Bound Volumes	2,000*	3,000	3,000
Convention Expenses Less Salary Charges:			
Program Booklet	1,580*	1,580	1,580
Travel N.Y. Personnel	1,700*	1,400	1,400
Materials & Supplies	320*	320	320
Postage & Express	500*	500	500
Total Estimated Expenses	$ 99,435	$102,735	$108,735
Contingency 1% of Estimated Income	1,020	1,027	1,027
Total Expenses	$100,455	$103,762	$109,762
Excess Income Over Expenses, General Fund	+1,545	−1,062	−7,062
Income Credited to Society Reserve Fund	+10,070	+14,520	+14,520
Net Excess Income Over Expenses	+11,615	+13,458	+7,458

* The items starred in the first column have not been reduced by 4/5 as indicated in the column heading. The reason for this is that they have not appeared an extra time due to the length of the fiscal year.

total of $6,000. The second revised budget, published here, was approved by the Board.

Report of Publication Committee

Dr. King distributed to the Board statistics on the JOURNAL. It was voted to accept this report.

The possibility of increasing income in order that more papers might be printed in the JOURNAL, thereby cutting down the backlog, was discussed from many angles. No action was taken.

The President then submitted a report from Hans Neumark recommending that our Society no longer be represented on the ASA Chemical Industry Advisory Board. It was voted that we discontinue representation on this committee.

Palladium Medal Committee

Dr. Hackerman reported that the Palladium Medal Committee recommends that Dr. K. F. Bonhoeffer be awarded the Palladium Medal for 1957, subject to his being able to accept in person. It was voted that this nomination be accepted.

Membership Committee

The Membership Committee Report was submitted, indicating the biggest gain in membership of any year in the Society's history. It was voted that Frank Biondi and William Faust be congratulated for their efforts in increasing the membership of The Electrochemical Society, and that the Membership Committee Report be accepted.

New Business

Dr. Hackerman asked members of the Board to give consideration to nominees for the Perkin Medal.

Dr. Middleton brought up the matter of taking pictures at meetings and recommended that the Board rescind its former action; it was voted that the previous action be rescinded. The previous action is as follows: "On motion of Mr. McKay, it was voted that the Board does not favor indiscriminate photographing of slides during technical sessions. It was recommended that the program booklet contain a request that no such pictures be taken and that the chairmen of the technical sessions should administer this rule."

Henry B. Linford, *Secretary*

Gordon Research Conferences

The 1957 Gordon Research Conferences will be held from June 10 to August 30 at Colby Junior College, New London, N. H., New Hampton School, New Hampton, N. H., and Kimball Union Academy, Meriden, N. H.

The Conferences were established to stimulate research in universities, research foundations, and industrial laboratories, by means of scheduled lectures and free discussion groups. Sufficient time is available to stimulate informal discussions among the members of a Conference. Meetings are held in the morning and in the evening, Monday through Friday, with the exception of Friday evening. The afternoons are available for recreation, reading, or participation in discussion groups as the individual desires. This type of meeting is a valuable means of disseminating information and ideas which otherwise would not be realized through the normal channels of publication and scientific meetings, and scientists in related fields form valuable associations which result in collaboration and cooperative effort between different laboratories.

It is hoped that each Conference will extend the frontiers of science by fostering a free and informal exchange of ideas. The purpose of the program is not to review the known fields of chemistry, but primarily to bring experts up to date as to the latest developments. In order to protect individual rights and to promote discussion, it is an established rule of each Conference that no information presented is to be used without specific authorization of the individual making the contribution, whether in formal presentation or in discussion. No publications are prepared as emanating from the Conferences.

The first meeting of each Conference is held Monday morning at 9:00 A.M., Eastern Daylight Saving Time. The morning sessions, through Friday, are scheduled from 9:00 A.M. to 12.00 Noon. The second session of each day is held in the evening from 7:30 to 10:00 P.M., Monday through Thursday. There are no Friday evening meetings.

Accommodations are available for a limited number of women to attend each Conference, also for wives who wish to accompany their husbands. All such requests should be made at the time of the request for attendance because these limited accommodations will be assigned in the order that specific requests are received.

Individuals interested in attending the Conference should request an application form from the office of the Director. Attendance at each Conference is limited to 100.

Requests for attendance at the Conferences, or for any additional information, should be addressed to W. George Parks, Director, Dept. of Chemistry, University of Rhode Island, Kingston, R. I. From June 10 to August 30, 1957 mail should be addressed to Colby Junior College, New London, N. H.

Chemistry and Physics of Metals

Kimball Union Academy
Meriden, N. H.
A. S. Nowick, *Chairman*
E. S. Machlin, *Vice-Chairman*

July 8

Visual Observation of Dislocations
B. Chalmers, *Chairman*

P. Hirsch—Electron Optical Studies of the Arrangement and Movement of Dislocations in Thin Films.

J. J. Gilman—Visual Measurements of the Mobility of Dislocations in Lithium Fluoride Crystals.

Panel Discussion on Observation of Dislocations. J. C. Fisher, *Chairman*; W. C. Dash, F. W. Young, Jr., M. Abrahams, J. Washburn, Panel Members.

July 9

Irradiation Effects I
H. B. Huntington, *Chairman*

G. H. Vineyard—Theory of Irradiation Displacements.

R. Smoluchowski—Irradiation Effects in the Alkali Halides.

Irradiation Effects II
K. G. McKay, *Chairman*

K. Lark-Horovitz—Irradiation Effects in Semiconductors.

J. H. Crawford, Jr.—Irradiation Effects in Non-Metallic Crystals.

July 10

Irradiation Effects III
C. Wert, *Chairman*

J. A. Brinkman—Comparison of Existing Models for Defect Production and Migration in Metals.

A. Sosin and C. J. Meechan—Electron Irradiation of Metals.

M. D. Fiske—Electron Irradiation of Metals.

Irradiation Effects IV
G. J. Dienes, *Chairman*

T. H. Blewitt—Recent Irradiation Experiments on Metals at Oak Ridge.

R. W. Balluffi—Recent Irradiation Experiments on Metals at Illinois.

July 11

Properties of Dislocations
W. T. Read, Jr., *Chairman*

A. Seeger—Some Recent Developments in Dislocation Theory.

K. Lücke—To be announced.
D. O. Thompson—Irradiation Effects on Young's Modulus and Internal Friction of Copper Crystals.
A. S. Nowick, *Chairman.*
W. Dekeyser—Recent Work on Lattice Imperfections at Gent.

July 12

Panel Discussion on Interaction Between Point Defects and Dislocations. R. Thomson, *Chairman;* J. E. Bauerle, A. E. Roswell, R. Maddin, R. R. Coltman, Panel Members.

Corrosion

Colby Junior College
New London, N. H.
W. D. Robertson, *Chairman*
J. E. Draley, *Vice-Chairman*

July 15

Hydrogen Absorption and Embrittlement
J. J. Harwood, *Chairman*

M. L. Hill—The Solubility and Diffusion of Hydrogen in Steel.
J. O'M. Bockris—Adsorption of Hydrogen on Metals with Reference to Corrosion and Embrittlement.
F. de Kazinczy—Hydrogen Absorption and Embrittlement.
B. F. Brown—Delayed Fracture and Hydrogen Absorption.

July 16

Structure—Dependent Corrosion and Oxidation

N. Cabrera—Subject to be announced.
W. E. Tragert—The Structural Factors Associated with the Oxidation of High Purity Aluminum in Water.
A. T. Gwathmey—Subject to be announced.
T. N. Rhodin—Oxidation of Niobium Binary Alloys.

July 17

Effects of Radiation on Corrosion
J. E. Draley, *Chairman*

M. T. Simnad—The Effects of Nuclear Irradiation on Metal Surface Reactions.
G. H. Jenks—The Effect of Radiation on the Corrosion of Zirconium.

Corrosion in Water at High Temperatures
E. C. W. Perryman, *Chairman*

R. A. U. Huddle—Atomic Energy Research Establishment, Harwell, England.
J. E. Draley—Behavior of Aluminum and Uranium in Water at High Temperatures.

July 18

Corrosion in Water at High Temperatures (cont'd)
E. C. W. Perryman, *Chairman*

M. W. Burkart—Corrosion of Uranium Alloys in High Temperature Water.
F. H. Krenz—Intergranular Corrosion of Aluminum in High Temperature Water.

Stress Corrosion Cracking of Stainless Steel
M. A. Streicher, *Chairman*

J. J. Harwood—Current Research and Problems Associated with Cracking Failures of Stainless Steel.
H. H. Uhlig—New Research on Austenitic Stainless Steels.

July 19

Stress Corrosion Cracking of Stainless Steel (cont'd)
M. A. Streicher, *Chairman*

Hugh L. Logan—Research at the National Bureau of Standards on Cracking of Stainless Steels.
A. W. Dana—Corrosion Cracking of Stainless Steels.

Division News

Electrodeposition Division Symposia

The Electrodeposition Division is planning two symposia for the 1957 fall meeting of the Society in Buffalo, to be held October 6-10.

Dr. Cloyd Snavely, Battelle Memorial Institute, Columbus, Ohio, is arranging for a series of papers on "Metal Powders," covering the production, use, and properties of electrolytic powders.

"Corrosion of Electrodeposited Metals" is being organized by Dr. F. A. Lowenheim, Metal & Thermit Corp., P. O. Box 471, Rahway, N. J., and Dr. Harry Copson, International Nickel Co., P. O. Box U, Bergen Point Station, Bayonne, N. J., as a joint symposium with the Corrosion Division.

Authors who wish to present papers on either or both subjects are invited to contact the respective chairmen promptly. Abstracts (*not exceeding 75 words in length*) must be submitted to the Society Headquarters Office *not later than June 1, 1957.*

Electronics Division

The Nominating Committee (C. W. Jerome, Chairman, F. J. Biondi, and H. C. Froelich) has selected the following nominees for officers during the 1957-59 term (2 years).

Chairman—H. Bandes, Sylvania Electric Products Inc., Woburn, Mass.
Vice-Chairman (Luminescence)—R. J. Ginther, Naval Research Lab., Washington 25, D. C.
Vice-Chairman (General Electronics)—C. T. Lattimer, RCA Tube Div., Chemical & Physical Lab., Marion, Ind.
Vice-Chairman (Semiconductors)—J. W. Faust, Jr., Westinghouse Research Labs., Churchill Borough, Pittsburgh 35, Pa.
Secretary-Treasurer—M. F. Quaely, Lamp Div., Research Dept., Westinghouse Electric Corp., Bloomfield, N. J.

Although the term of office of Secretary-Treasurer had one more year to run he has agreed to have his term end at the next business meeting of the Division, so as to permit the terms of all elective officers to begin and end together.

Each nominee has given assurance of his willingness to serve if elected.

The Bylaws of the Division provide that additional nominations may be made by petition signed by five members of the Division. Such petitions must be in the hands of the Chairman of the Nominating Committee before the election, and the nominees must have given assurance of their willingness to serve if elected.

The election will be held at the business meeting of the Electronics Division during the spring meeting of the Society in Washington, D. C., May 12-16, 1957.

M. F. Quaely, *Secretary-Treasurer*

Electro-Organic—Theoretical Electrochemistry Symposium

A joint symposium sponsored by the Electro-Organic and the Theoretical Electrochemistry Divisions is to be held at the Buffalo Meeting of The Electrochemical Society, October 6-10, 1957. Among the topics selected for discussion are:

(*A*) Mechanism of organic reactions at electrodes.

(*B*) Mass transport in organic electrochemical systems.

(*C*) Polarization, adsorption, and double layer theory in organic systems.

(*D*) Round table—subject to be announced.

The program is to include invited and contributed papers. All abstracts of papers should be submitted in triplicate to the Secretary's Office, 216 W. 102nd St., New York 25, N. Y., *not later than June 1, 1957.*

Electro-Organic Symposia

Papers are being solicited for presentation at the ECS Meeting to be held in Buffalo, October 6-10, 1957. The major topics to be presented are:

(*A*) Electrochemical methods in organic analysis.

(*B*) Electrolytic oxidation or reduction in organic synthesis.

(*C*) Organic polarography.

(*D*) Arc electrolysis.

(*E*) Mechanism of the Kolbe reaction.

(*F*) Anodic substitution reactions.

All abstracts of papers (*not exceeding 75 words in length*) should be submitted in triplicate to the Secretary's Office, 216 W. 102nd St., New York 25, N. Y., *not later than June 1, 1957.*

M. J. Allen, *Secretary-Treasurer*

E & M—Corrosion Joint Symposium

A feature of the forthcoming Spring Meeting of the Society will be a symposium entitled "The Role of Metal and Oxide Structure in Oxidation and Corrosion Processes." The program, which will be jointly sponsored by the Electrothermics and Metallurgy and the Corrosion Divisions, is scheduled to take place on Tuesday, May 14, at the Hotel Statler, Washington, D. C.

The morning session, under the chairmanship of W. E. Tragert, will feature papers by W. D. Robertson, M. A. Streicher, and A. T. Gwathmey. The emphasis in these papers will be on the effects of metal structure in oxidation and corrosion with specific attention given to crystallographic orientation, grain boundaries, dislocations, and second phase particles. D. A. Vermilyea will serve as chairman for the afternoon session which will include presentations by C. E. Birchenall, N. Cabrera, and J. T. Waber. Emphasis will center on the properties of surface oxides and the effects of composition, structure, imperfections, and epitaxy on the mode and rate of oxidation.

It is expected that each paper will take 40-45 minutes in presentation and that ample time for questions and discussion will be available. Prepared discussions have been solicited from several investigators who are active in the field and will be presented if time permits.

E & M Division Columbium Symposium

The spotlight of technical inquiry is to be turned on columbium (niobium), a refractory metal of increasing economic importance, during the four sessions of a symposium arranged by the Electrothermics and Metallurgy Division for the Washington Spring Meeting of the Society.

In former years an addition to stainless steel and stainless welding rod, columbium now has several new and important applications. Among these are its use in nuclear reactors as a material of construction, as a major constituent of new high-temperature alloys, and in fabrication of special corrosion-resistant equipment. Discovery of a number of substantial ore bodies in recent years has assured an adequate future supply of this metal which, in nature, usually is found keeping company with tantalum, a metal it resembles greatly in chemical properties.

Papers describing the supply situation, extraction of the metal from its ores, preparation in a state of high purity, its mechanical, chemical, and physical properties, and its alloys and their characteristics are to be discussed. If sufficient interest develops, it is probable that the proceedings of this symposium will be published.

Originally suggested as a symposium subject by Dr. I. E. Campbell, Chief, Division of Inorganic Chemistry and Chemical Engineering, Battelle Memorial Institute, the columbium program was formulated by Drs. Campbell and B. W. Gonser, Technical Director, and E. M. Sherwood, Assistant Chief, Division of Inorganic Chemistry and Chemical Engineering, all of Battelle.

Extended Abstracts Booklets

The Electronics Division will again publish an "Enlarged Abstracts" booklet for the Spring 1957 convention of the Society at Washington. The booklet will have 1000-word abstracts of the papers to be presented before the Electronics Division in its symposia on

Luminescence
Semiconductors
Instrumentation
Thermionic Cathodes
Screen Application

The abstracts will contain pertinent information and experimental data given in the papers, and will provide these details before publication, thus aiding workers in the field. The abstracts will be "printed but not published."

The booklet should be available by about April 15; the price will be $2.00.

Copies of the 1956 "Enlarged Abstracts" booklet of the San Francisco Meeting are still available at $2.00 per copy.

Checks should be made payable to: Electronics Division, The Electrochemical Society.

Orders should be sent to:
Martin F. Quaely
c/o Westinghouse Electric Corp.
Research Dept., Lamp Div.
Bloomfield, N. J.

★ ★ ★

The Theoretical Electrochemistry Division is making available extended abstracts of the symposium sponsored by the Division and the National Science Foundation on the Structure of Electrolytic Solutions (Electrolytes), as well as the two general symposia, for the Spring 1957 Washington Meeting.

Copies of the booklet can be obtained, at $3.00 each, from:
Dr. Ralph Roberts
3308 Camalier Drive
Washington 15, D. C.

Copies of the extended abstracts booklet of the 1956 San Francisco Meeting are still available at $2.00 each.

Theoretical Electrochemistry Division

The Nominating Committee (Norman Hackerman, Chairman, H. H. Uhlig, and Ernest Yeager) has selected the following nominees for officers of the Theoretical Division for the coming term:

Chairman—Paul Delahay, Louisiana State University, Baton Rouge, La.

Vice-Chairman—Charles Tobias, University of California, Berkeley, Calif.

Secretary-Treasurer—Ralph Roberts, 3308 Camalier Drive, Washington, D. C.

Members-at-Large on Executive Committee—J. O'M. Bockris and Sigmund Schuldiner

Each nominee has given assurance of his willingness to serve if elected.

The election will be held at the business meeting of the Theoretical Division, May 16, during the Spring Meeting of the Society in Washington, D. C.

Section News

Boston Section

The fifth meeting of the Boston Section was held on January 9, 1957 in the Graduate House at the Massachusetts Institute of Technology,

where Mr. Robert C. Wade of Metal Hydrides, Inc. presented a paper on the subject "Metal Hydrides—New Compounds for Industry."

These new compounds, formed between hydrogen and other elements, may be classified into four general categories: (*a*) *ionic* which includes the LiH, NaH, CaH_2, $NaBH_4$, and $LiAlH_4$; (*b*) *covalent* of which SnH_4, SiH_4, GeH_4, NH_3, AlH_3, B_2H_6, HCl are typical examples; (*c*) *alloy* as exemplified by TiH_2 and ZrH_2; and (*d*) *borderline* of which Cu-H and Zn-H are examples.

The current and potential uses of a number of commercially available hydrides were reviewed.

Charles Levy, *Secretary*

Chicago Section

The Chicago Section had its annual President's Night December 7, 1956 at the Chicago Engineers Club. Dr. Sherlock Swann introduced President Hans Thurnauer who reported a record attendance at Cleveland and other interesting news of the Society. He urged Local Sections to give aid to high schools to increase student interest in the field of electrochemistry.

The technical subject of the evening was "High Temperature Materials." One of the principal needs for these materials is in military applications. As speeds of missiles and planes increase, so do the high temperature strength requirements. At mach 3 and higher the frictional heat increases rapidly. Ceramics offer very good high temperature strength but are sensitive to thermal shock. Designers are, however, thinking in terms of a ceramic airplane. In electronics, entire circuits have been built and operated at red heats. Vacuum tubes, resistors, and capacitors were constructed from ceramics. Mr. Thurnauer emphasized the great need for ceramic structures of less brittleness, and suggested that the obstacle might be circumvented by design. The new development of "flame ceramics" may be helpful as a solution to the brittleness problem. President Thurnauer pointed out that greater efficiency could be obtained by operating atomic reactors at higher temperatures and in this regard he suggested the use of ceramic fuel elements.

William H. Colner, *Secretary*

New York Metropolitan Section

A meeting of the Metropolitan Section was held at Schwartz Restaurant, New York, on November 14, 1956, featuring an address by Dr. Henry F. Ivey of Westinghouse Electric Corp. on "Electroluminescence."

Dr. Ivey defined electroluminescence as the process whereby visible light is emitted directly when an electric field is applied to a phosphor.

Being an area source of light, electroluminescent lighting gives shadowless illumination. Since the color of the light from many phosphors can be changed by varying the voltage or frequency, the color of the light can be varied to fit any mood. Possible applications include electronic devices such as light amplifiers and television.

Dr. Ivey concluded with a demonstration of various electroluminescent cells.

Frances S. Lang,
Secretary-Treasurer

Battery Life Symposium Papers

The life of lead-acid batteries was discussed at the 1956 Cleveland Meeting in a symposium sponsored by the Battery Division. A booklet, "Life Testing of Automobile Batteries and Related Subjects," has been prepared containing the complete text and illustrations along with a summary of the discussion which followed.

This booklet can be obtained by sending $2.00 to E. J. Ritchie, Secretary, Battery Division, Eagle Picher Co., Joplin, Mo.

Papers included in this 96-page booklet are:

"Appearance of Battery Components at the End of Life Under Laboratory Test" by B. Agruss.

"Effect of Normal Car Service on the Intermediate and Final Periods of Lead Storage Battery Performance" by D. Haskell.

"The Correlation of Laboratory Life Tests with Automotive Service Tests of Lead-Acid Batteries" by J. F. Schaefer.

"The Effect of Temperature on the Cycling Life of Lead-Acid Storage Batteries" by J. F. Macholl and A. G. Koch.

"The Effect of Arsenic and Silver in Grid Alloy on Storage Battery Life in Field Tests and Fleet Service" by Howard Stoertz.

"Pulse Maintaining of Storage Batteries" by J. B. Godshalk.

"Positive Post Corrosion in Lead-Acid Cells" by Otto H. Bauer.

Philadelphia Section

In an attempt to elucidate all facets of the technical manpower problem, four Philadelphia chapters of national technical and scientific organizations, the American Chemical Society, American Institute of Chemists, American Institute of Chemical Engineers, and The Electrochemical Society cooperated in presenting a symposium entitled "Scientific Manpower—Its Meaning to the Scientist and the Nation." The meeting was held December 6, 1956 in the University of Pennsylvania Museum Auditorium.

Dr. Norman A. Shepard, consultant to the Dept. of Defense and other government departments, outlined the technical manpower problem.

Dr. Christopher L. Wilson, President of Hudson Chemical Co., speaking on the supply and demand question, deplored the frantic recruiting practices of industry.

Dr. Eli Ginzberg, Professor Economics and Director of Staff Studies of the National Manpower Council at Columbia University, next spoke on the utilization problem, pointing out that industry must do a better job in utilizing those whom it attracts.

The third speaker of the afternoon, Dr. Harry C. Kelly, Assistant Director for Scientific Personnel and Education of the National Science Foundation, spoke on the education problem, emphasizing the necessity of insuring a sufficient number of highly qualified scientists and engineers to advance and develop frontiers of knowledge.

The fourth speaker, Dr. David H. Dawson, Vice-President, member of the Board of Directors, and member of the Executive Committee of E. I. du Pont de Nemours & Co., delivered his address at dinner. He discussed the relationship between the manpower problem and attempts to solve it.

H. C. Mandell, Jr.

San Francisco Section

A regular Section meeting was held on January 30, 1957 at the Faculty Club of the University of California, in Berkeley. The speaker was Mr. J. D. Buhler, Manager of Process Control and Development for the Reduction Operations Division, Kaiser Aluminum & Chemical Corp. His topic was the "Practical Aspects of the Electrolytic Production of Aluminum."

Aluminum production in the United States has quadrupled in the last ten years and now consumes about 6% of the total electric power pro-

duced in this country. Lately fossil fuels (natural gas, coal, lignite) have become an increasingly important source of power for the industry, although hydroelectric power is still predominant.

However, progress in the electrolytic process itself has not kept pace with the growth of the industry. The operation of an aluminum cell is still very much an art; very few instruments are used, and means of control are often rudimentary. For example, one of the most useful and versatile tools is an ordinary steel rod: it is used to check depth of molten aluminum and bath; to feel the condition of the cell bottom (if alumina is fed at an excessive rate, the bottom will become "mushy"); to feel the "ledge" (i.e., frozen bath on the sides of the cell cavity) in order to gain information on the heat balance of the cell. The color of the "pot flame" (i.e., the burning anode gases) is another criterion of cell operation. Many other examples of available controls were given. A number of typical operating data were also presented.

The second Local Section meeting of the season was held on November 28, 1956 at the University of California Faculty Club, in Berkeley. The guest speaker was Dr. Morris Eisenberg, Vice-President of Thermo Materials, Inc., in charge of Research and Development. The subject he presented was "The Electrochemical Behavior of Titanium as an Anode Material."

The study of the anodic behavior of titanium stemmed from a practical problem, i.e., the necessity of subjecting the metal to an anodic etch prior to electroplating. This etch is carried out in nonaqueous or semi-aqueous solutions containing HF and organic liquids such as ethylene glycol.

The anodic polarization curve of titanium in the above solutions is not continuous: discrete jumps are often observed, and the nature of the anodic phenomena may change from one region of the curve to the next one. The situation is complicated by the fact that, even in the absence of current, some chemical etching will take place, with hydrogen evolution. As increasing anodic current is applied, the rate of dissolution of the titanium first decreases and goes through a minimum near the "critical current density" at which gassing ceases. From then on, the rate of anodic dissolution increases almost linearly with current, and the titanium appears to be going into solution at an apparent valence slightly in excess of 3.

Morris Feinleib

Washington-Baltimore Section

Johns Hopkins University, Baltimore, Md., was the site of the January meeting of the Section. The program included two speakers, Dr. Ralph J. Brodd of the National Bureau of Standards and Dr. Gilbert W. Castellan of the Catholic University of America.

Dr. Brodd's topic was "Polarization and Surface Area." The polarization capacities of Pt, Ni, Cr, Ta, Fe, Al, Cu, and Pb in 1M Na_2SO_4 were evaluated from charging and decay curves obtained by imposing a 2 cps signal on a cell containing one of these metals and a large nonpolarizable electrode. These values were compared to surface areas for the metals determined by Kr adsorption. For some of the metals the electrochemical method is suitable for routine surface measurements.

Dr. Castellan spoke on "A Thermodynamic Discussion of the Palladium-Hydrogen System." He reported on work he had done with Dr. Schuldiner and Dr. Hoare at the Naval Research Lab. concerning the potential differences between a palladium-hydrogen electrode and a platinum-hydrogen electrode in the same acid solution. The measurements showed that the potential on the palladium-hydrogen electrode was independent of the partial pressure of hydrogen and had the same dependence on pH as the platinum-hydrogen electrode. The half-reaction on palladium is: $H^+ + e^- \rightarrow H$ (in alpha palladium). The Nernst equation for the half-cell reaction is then $E = E^\circ - 0.06014 \log(a_H/a_{H^+})$ (at 30°F). From the known pressure-composition data for the palladium-hydrogen alloys in the alpha-solution range, E° was computed and found to be −0.06243 v. The potential corresponding to the saturated alpha-phase was then computed to be +0.048 v, in good agreement with the 0.050 v which has been observed by various investigators using pure palladium electrodes with hydrogen.

Gwendolyn B. Wood, *Secretary*

New Members

In February 1957 the following were approved for membership in The Electrochemical Society by the Admissions Committee:

Active Members Sponsored by a Sustaining Member

Walter R. Hibbard, Jr., General Electric Research Lab.; Mail add: 2213 Almeria Rd., Schenectady 9, N. Y. (Electrothermics & Metallurgy)

Francis W. MacMullen, Merck & Co., Inc., Rahway, N. J. (Electronics)

Robert E. Maizell, Olin Mathieson Chemical Corp., Niagara Falls, N. Y. (Industrial Electrolytic)

By action of the Board of Directors of the Society, all prospective members must include first year's dues with their applications for membership.

Also, please note that, if sponsors sign the application form itself, processing can be expedited considerably.

Active Members

Dimitri Argyriades, Carnegie Institute of Technology; Mail add: 5742 Northumberland, Pittsburgh 17, Pa. (Theoretical Electrochemistry)

Malcolm A. Buell, Bridgeport Brass Co., 30 Grand St., Bridgeport, Conn. (Corrosion, Electrodeposition)

Kuang L. Cheng, Materials Engineering Dept., CL-20, Westinghouse Electric Corp., East Pittsburgh, Pa. (Electrodeposition, Electronics, Electro-Organic, Electrothermics & Metallurgy)

Milton Eaton, Shawinigan Chemicals Ltd.; Mail add: 363 9th St., Shawinigan Falls, Que., Canada (Electrothermics & Metallurgy)

Irving Feinberg, Electronics Division, Sylvania Electric Products Inc., 100 Sylvan Rd., Woburn, Mass. (Electronics)

Demmar R. Gardner, Northrop Aircraft Inc.; Mail add: 1325 N. Occidental, Los Angeles 26, Calif. (Corrosion, Electrodeposition, Theoretical Electrochemistry)

Charles P. Giannarakos, Raytheon Manufacturing Co.; Mail add: 229 Andover St., Lowell, Mass. (Electrothermics & Metallurgy)

Joseph Glickstein, Adelphi College; Mail add: 435 E. 14th St., New York 9, N. Y. (Theoretical Electrochemistry)

Luis L. Grunbaum, Kaiser Aluminum & Chemical Corp.; Mail add: 1325 Cowper St., Palo Alto, Calif. (Industrial Electrolytic, Theoretical Electrochemistry)

Jerrold O. Hinshaw, North American Aviation; Mail add: 12353 So. Richeon Ave., Downey, Calif. (Electrodeposition)

John N. Hornak, U. S. Steel Research Center, P. O. Box 38, Monroeville, Pa. (Electrothermics & Metallurgy)

Akiya Kozawa, Dept. of Chemistry, Duke University, Durham, N. C. (Battery)

James J. Leddy, Electrochemical Lab., Dow Chemical Co., Midland, Mich. (Electrodeposition, Electrothermics & Metallurgy, Theoretical Electrochemistry)

J. Adrien M. Le Duc, Diamond Alkali Co.; Mail add: 54 Hayes St., Painesville, Ohio (Electrodeposition, Electrothermics & Metallurgy, Industrial Electrolytic, Theoretical Electrochemistry)

Eugene A. Maduk, ALCOA Research Labs.; Mail add: 560 Longvue Rd., New Kensington, Pa. (Industrial Electrolytic)

Thomas J. Manns, Philco Corp., Church Rd., Lansdale, Pa. (Electronics)

George W. Mao, Chemical Research Lab., Kaiser Aluminum & Chemical Corp., Permanente, Calif. (Corrosion, Electrodeposition, Electrothermics & Metallurgy, Theoretical Electrochemistry)

Gregory P. Martusevich, American Metal Co., Ltd.; Mail add: 11 Augustus St., Bloomfield, N. J. (Industrial Electrolytic, Theoretical Electrochemistry)

James O. McCaldin, Hughes Aircraft Co.; Mail add: 19024 Pacific Coast, Malibu, Calif. (Electronics)

Henry T. Minden, Sylvania Electric Products Inc., 208-20 Willets Pt. Blvd., Bayside, N. Y. (Electronics)

Bertrand G. Morissette, Central Research Lab., Canadian Industries Ltd., McMasterville, Que., Canada (Industrial Electrolytic)

George F. Nordblom, Foote Mineral Co.; Mail add: 807 Pitt Rd., Cheltenham, Pa. (Theoretical Electrochemistry)

John P. Olatta, Chemical Products Plant, General Electric Co., 1099 Ivanhoe Rd., Cleveland 10, Ohio (Electronics)

Leslie R. Prout, Messrs. Oldham & Son Ltd.; Mail add: 2, Sunnyside Grove, Ashton-Under-Lyne, Lancs., England (Battery)

Edward J. Richards, General Motors Corp.; Mail add: 45614 Hecker Dr., Utica, Mich. (Electrodeposition)

Ralph M. Saria, Metals Research Labs., 4625 Royal Ave., Box 580, Niagara Falls, N. Y. (Industrial Electrolytic)

Milton Schneider, Sperry Semiconductor Division; Mail add: 254-15 82nd Ave., Floral Park, N. Y. (Electronics)

William G. Scholz, Climax Molybdenum Co. of Michigan; Mail add: 14410 Woodrow Wilson, Detroit 38, Mich. (Electrothermics & Metallurgy)

Herbert P. Silverman, Research Labs., Kaiser Aluminum & Chemical Corp., Permanente, Calif. (Theoretical Electrochemistry)

A. Stuart Tulk, Sylvania Electric Products Inc.; Mail add: 302 Third St., Towanda, Pa. (Electronics)

Glenn F. Zellhoefer, Eureka Williams Corp., 1201 East Bell St., Bloomington, Ill. (Battery)

Helmut Winterhager, Institut fur Metalluhuttenwesen und Elektrometallurgie, Intzestrasse 3, Aachen Rhld., Germany (Electrodeposition, Electrothermics & Metallurgy, Industrial Electrolytic, Theoretical Electrochemistry)

Student Associate Member

John C. Banter, Western Reserve University; Mail add: 2572 J East 110 St., Cleveland 4, Ohio (Theoretical Electrochemistry)

Reinstatements to Active Membership

George C. Allen, Wyandotte Chemical Corp.; Mail add: 2319 Second St., Wyandotte, Mich. (Industrial Electrolytic)

James R. Newberry, Olin Mathieson Chemical Corp.; Mail add: 4829 University Ct., Niagara Falls, N.Y. Electrothermics & Metallurgy, Industrial Electrolytic)

Chester N. Richardson, Carborundum Metals Co.; Mail add: East Ave., Youngstown, N.Y. (Electrothermics & Metallurgy, Industrial Electrolytic)

Transfer from Student Associate to Associate Membership

Robert W. Gardner, Curtiss-Wright Corp.; Mail add: 420 E. Foster Ave., State College, Pa. (Electrothermics & Metallurgy)

Transfer from Associate to Active Membership

Boris Levy, Engineering Center, Westinghouse Electric Corp., East Pittsburgh, Pa. (Corrosion, Electronics, Theoretical Electrochemistry)

Personals

Gerald V. Kingsley has been appointed Director of Research of Bohn Aluminum and Brass Corp., Detroit, Mich. Dr. Kingsley was Chief Metallurgist before his promotion.

Edwin T. Goodridge has resigned as President of Horizons Inc., process and material research organization of Cleveland, Ohio, and Princeton, N. J. Mr. Goodridge has made this decision in order to devote his full time to other business activities. He is being retained by Horizons in

Manuscripts and Abstracts for Fall Meeting

Papers are now being solicited for the Fall Meeting of the Society, to be held at the Statler Hotel in Buffalo, N. Y., October 6, 7, 8, 9, and 10, 1957. Technical Sessions will be scheduled on Batteries, Corrosion, Electrodeposition (symposium on "Metal Powders"), Electrodeposition—Corrosion (Joint Symposium on "Corrosion of Electrodeposited Metals"), Electronics (Semiconductors), Electro-Organics, Electro-Organics—Theoretical Electrochemistry (Joint Symposium), and Electrothermics and Metallurgy.

To be considered for this meeting, triplicate copies of abstracts (*not to exceed 75 words in length*) must be received at Society Headquarters, 216 West 102nd St., New York 25, N. Y., *not later than June 1, 1957. Please indicate on abstract for which Division's symposium the paper is to be scheduled.* Complete manuscripts should be sent in triplicate to the Managing Editor of the JOURNAL at the same address.

* * *

The Spring 1958 Meeting will be held in New York City, April 27, 28, 29, 30, and May 1, 1958, at the Statler Hotel. Sessions will be announced in a later issue.

a consulting capacity. Mr. Goodridge, along with Dr. Eugene Wainer, co-founded the company in 1946.

Frank W. Hurd has been named Director of Research of Union Carbide Nuclear Co., a Div. of Union Carbide and Carbon Corp., New York City. Previously he was Superintendent of Research and Development, Industrial Applications. Dr. Hurd has been identified with Union Carbide's activities in the atomic energy field since 1943.

John W. Winslow, Jr., formerly of Cincinnati, Ohio, is now at the U. S. Naval Radiological Defense Lab., Nuclear Radiation Branch, San Francisco, Calif.

Paul T. Woodberry, who had been with Battelle Memorial Institute, Columbus, Ohio, is now associated with Avco in Wilmington, Mass.

Hendrik Van Der Horst, previously at the Van Der Horst Corp. of America, Olean, N. Y., is currently in Hilversum, Holland, with Lemet Chromium.

R. S. Margeson has become affiliated with the Crescent Carbon Corp., Lancaster, Calif., as Vice-President of Manufacturing. He had been Manager of Application and Development for the International Graphite Div. of Speer Carbon Co., Niagara Falls, N. Y.

Arthur J. Sherburne, previously with the General Electric Co. in Coshocton, Ohio, has been transferred to the company's newly organized section on insulating materials, Schenectady, N. Y., as a specialist on insulation systems in the Chemical and Metallurgical Dept.

Earnest E. Nelson has left the Naval Research Lab., Washington, D. C., to join the Socony Mobile Lab. in Brooklyn, N. Y.

William von Fischer, formerly with Case Institute of Technology, is now Co-Ordinator of Research and Development of The Glidden Co., Cleveland, Ohio.

Spotswood D. Bowers, Jr., has taken a position with the Atomic Power Development Association, Detroit, Mich. He had been with the Detroit Edison Co.

Mervin E. Runner, who had been at the Illinois Institute of Technology, is now at the Armour Research Foundation, Chicago, Ill.

Thomas L. Kendall is now with the United Motors Div. of General Motors Corp., Detroit, Mich. Previously he was with the company's Delco-Battery Operations in Muncie, Ind.

Earle S. Bidgood, formerly employed by the Superior Tube Co. in the Photoforming Div., Stamford, Conn., has been transferred to the Phoenixville, Pa., plant which is devoted to the manufacture of aperture masks for color television tubes.

John A. Colquhoun, who had been Superintendent of the Carbide Div., is now Superintendent of the Shawinigan East Div., Shawinigan Chemicals Ltd., Shawinigan Falls, Que.

Paul A. Weidle recently joined Gannon College, Erie, Pa., as an instructor in physics. He had been associated with the Ronson Corp. of Pennsylvania as supervisor of electroplating.

Robert J. Good, previously at the University of Cincinnati in Ohio, is now with the Convair Scientific Research Lab., San Diego, Calif.

H. Robert Schoenfeldt, with the General Electric Co. in Cleveland, has been transferred from the Cuyahoga Lamp Plant to Product Testing and Evaluation.

1956 Directory

The 1956 Directory of Members of The Electrochemical Society is now available. The Directory contains an alphabetical and geographical list of members of the Society as of March 1, 1956, and a list of Patron and Sustaining Members, Past Presidents, and winners of Society prizes and awards.

Members who wish to receive the Directory are requested to fill in and return the order form below, accompanied by check, to Society Headquarters, 216 West 102 St., New York 25, N. Y.

Please send.....copy(ies) of the 1956 Membership Directory to:

Name .....

Company .....

Street .....

City ..... Zone..... State.....

Attached is check for $..... for Directory. (Single copies cost $2.00.)

News Items

University Professor and Oil Co. Chemist Get 1957 NACE Awards

At the NACE's 13th Annual Conference and Exhibition on March 13 in St. Louis, the 1957 Willis Rodney Whitney Award for corrosion research was presented to Carl Wagner, Professor of Metallurgy at Massachusetts Institute of Technology, Cambridge. Walter F. Rogers, Chief Chemist, Houston Production Division Chemical Lab., Gulf Oil Corp., Houston, received the Frank Newman Speller Award for achievements in corrosion engineering.

Dr. Wagner, a native of Leipzig, Germany, attended universities in Munich and Leipzig and received a Ph.D. in physical chemistry from the latter school in 1924. He has been a teacher at universities in Germany and was professor of physical chemistry, Darmstadt Institute of Technology, 1940-45. From 1945 to 1949, when he became affiliated with M. I. T., he was Scientific Advisor, Ordnance Research and Development Division Suboffice (Rocket), Fort Bliss, Texas. He was named professor at M. I. T. in 1955. Dr. Wagner received the first Palladium Medal Award of The Electrochemical Society in 1951 for "outstanding achievements in the study of corrosion of metals and its control."

Free Radicals Symposium

A three-day Symposium on the Formation and Stabilization of Free Radicals will be held at the National Bureau of Standards September 18-20, 1957. The meeting will be sponsored jointly by the Applied Physics Laboratory of the Johns Hopkins University, the Catholic University of America, and the National Bureau of Standards.

Recent advances in low-temperature physics, high polymer research, and other fields have stimulated much scientific interest in the isolation and study of free radicals. A

number of industrial, Government, and university laboratories are now conducting free radical research programs which should yield results of broad significance in basic chemistry and physics. The September conference is expected to provide a valuable medium for exchange of information in this rapidly growing field.

Further information on the program may be obtained from Dr. A. M. Bass, Free Radicals Research Section, National Bureau of Standards, Washington 25, D. C.

Metal Finishing Competition Being Organized

The Midland Branch is organizing a competition for the Institute of Metal Finishing, London, to encourage its younger members to take an interest in productivity in the metal finishing industry. The subject of the competition is plating shop layout. Candidates will be supplied with an outline of the plating shop and a list of process tanks and plant which they will have to incorporate in the design.

They will have to lay out the shop so that it would be capable of handling the normal variety of work encountered in a jobbing shop with the maximum efficiency possible. Full details of the competition will shortly be published by the I.M.F., and entry forms may be obtained from the offices of the Institute, 32 Gt. Ormond St., London, W.C. 1, England. Three main prizes will be awarded: First £30, Second £20, Third £10.

College Teacher Awards Program Announced by MCA

The Manufacturing Chemists' Association has announced that this June it will present six medals and cash awards for outstanding teaching of chemistry at the undergraduate level in American colleges and universities.

Nominations can be offered through April 15 by presidents of colleges or universities offering four-year bachelor degrees. Winners will be announced about May 1 and will be presented their awards at the annual meeting of the MCA at White Sulphur Springs, W. Va., June 6.

To be eligible for nomination a teacher must have had at least 15 years' service in undergraduate teaching in the field of chemistry, with a minimum of five years of such service at the institution from which he is named. Professors emeritus are among those eligible.

In reviewing a nomination the judges will consider evidence that the nominee has been personally responsible over a period of years for holding and inspiring the interest of students in the field of chemistry. Accompanying this should be supporting information such as: (a) the percentage of the student body electing one or more courses in chemistry; (b) the percentage of the graduating class electing majors in the general field of chemistry; and (c) the percentage of graduates selecting postgraduate courses related to chemistry.

E. G. Clarke Vice-President and Director of European Operations for Acheson Industries

Because of the rapid expansion of European industrial production, which has greatly increased the demand for its products abroad, Acheson Industries, Inc., New York, has created a new position, Vice-President in charge of European operations. Edwin G. Clarke, formerly managing director of Acheson's British affiliate, Acheson Colloids, Ltd., has been elected to the new post, Howard A. Acheson, President, has announced. Mr. Clarke, who has played an important part in the growth of the British and European business, has also been elected a director of Acheson Industries, Inc.

Mr. Clarke, who has been with the Acheson organizations for 35 years, will continue to make his headquarters in London, at 18 Pall Mall, S.W. 1.

First West Coast Plant to Make Carbon and Graphite Products

Crescent Carbon Corp., a subsidiary of Crescent Corp., has announced that its carbon and synthetic graphite plant under construction between Rosamond and Lancaster, Calif., is nearing the time of initial testing and operation.

This plant will produce carbon and graphite electrodes, anodes, electrolytic anodes, and other carbon and graphite products. The principal raw materials used in the manufacturing of carbon and graphite products are petroleum coke and pitch.

The multimillion dollar plant, completely equipped, will be the most modern in the world, and will utilize the most modern techniques in production of synthetic graphite and carbon. A technical staff with modern laboratory facilities will be equipped to work with Western industry on production, development, and research problems.

This is the first such plant to be constructed in the West and, as this is a basic industry, will contribute to further stabilization of Western industry. Location of this plant in the West is also a desirable decentralization measure from the standpoint of the national defense program. It will further be encouraging to other basic industries which may be contemplating construction of plants in the West.

New Location for Kosmos Electro-Finishing

Kosmos Electro-Finishing Research, Inc. announces an extended program of research in metal finishing in its new location at 140 Liberty St., Hackensack, N. J. A complete line of plating room supplies and equipment will be carried by the firm.

Kosmos offers Ker-Chro-Mite AL (a chromate conversion coating for aluminum and its alloys). The process imparts a yellowish protective coating on high purity aluminum as well as on high silicon bearing alloys. The solution is a chromate type, which will attack the most stubborn oxides and impart a protective coating. Supplied in concentrated solution form, it is diluted up to 100 volumes for processing. The attractive yellowish finish is an excellent base for paint or as a corrosion resistance final finish.

Sylvania Forms Semiconductor Division

Reflecting its rapidly expanding activities in the development and production of transistors and diodes, Sylvania Electric Products Inc. has formed a Semiconductor Division.

Charles W. Hosterman, who headed the former Electronics Division, has been appointed general manager of the new Semiconductor Division, whose headquarters are in the company's 150,000-square-foot plant at Woburn, Mass.

Union Carbide Announces Plans for Park Ave. Building

Plans for a 52-story office building of stainless steel and glass, to house the home offices of Union Carbide and Carbon Corp., were announced recently by Morse G. Dial, President of Union Carbide. The building will occupy the block between Madison and Park Aves., from 47th to 48th Sts.

The structure, to be known as the Union Carbide Building, will consist of an ultramodern, single-block tower facing Park Ave. and a 12-story section fronting on Madison Ave. The estimated construction cost is $46,000,000. Towering some 750

ft above street level, the new Union Carbide headquarters will be the tallest building on fast-changing Park Ave. It will contain approximately 1,500,000 square feet of space, making it one of New York's largest office buildings.

American Potash Opens Addition to Research Laboratory

A $200,000 addition to American Potash & Chemical Corp.'s Whittier (Calif.) Research Lab. was opened recently as part of the company's expanding research program.

The new addition, which doubles previous workroom space, consists of three four-man labs, two three-man labs, a small lab for microanalytical work, two large labs for process development, and other rooms for allied uses.

In line with AP&CC's expanding research activities, personnel at the company's Whittier facility has more than doubled since the lab was opened three years ago. With less than 30 employees in 1953, the lab now has a staff of 65 under the direction of Dr. William Emerson.

Important among research programs conducted by the company have been those in connection with lithium carbonate, lithium hydroxide, boric oxide, elemental boron, borate esters, phosphoroborine compounds, parathion, various electrochemicals, and others.

Du Pont Hyper-Pure Silicon Plant

The nation's first full-scale plant for the production of hyper-pure silicon, a vital part of many electronic and electrical devices, will be constructed on a large tract of rolling timberland near Brevard, N. C., by the Du Pont Co. of Wilmington, Del. Construction was to have begun in February, and the plant is expected to be ready for operation early in 1958.

Located in Transylvania County at the western tip of North Carolina, the 10,500-acre plant site offers protection against airborne contamination from industry or agriculture. Since impurities in silicon are measured in parts per billion, extremely pure air is essential in its manufacture.

Initially, the plant will employ about 200 persons in its operating force, though future plans call for a still larger unit.

The plant is expected to produce about 50,000 lb of semiconductor grade silicon annually. This is the material used in the manufacture of such devices as transistors, diodes, and power rectifiers.

The Du Pont Co., which pioneered the commercial production of hyper-pure silicon and is the nation's only producer today, does not make electronic devices; it makes only the silicon.

Because of its extreme purity, and the difficulty of purification, the material sells at $320 a lb. However, a small sliver of the material, worth from five to ten cents, makes up the heart of the new electronic devices.

The Brevard Plant will also have an annual capacity of 20,000 lb of "solar-cell" grade silicon. This grade, introduced about eight months ago, selling today at $150 a lb, was developed by Du Pont for use in the so-called "solar batteries" which convert the direct rays of the sun into electrical energy.

At present, silicon is produced in a unit at Du Pont's Newport, Del., plant. This unit will continue to produce the material during the period of construction at Brevard and will be used subsequently for research and product development.

Carpenter Expanding Corrosion Research Lab.

The Carpenter Steel Co., Reading, Pa., has announced that it is expanding its corrosion research laboratory to broaden its work on corrosion problems in the atomic energy and guided missile fields.

Norman D. Groves has been appointed to direct both this specialized and over-all corrosion research activity for Carpenter. Groves recently joined the company after five years as corrosion engineer at the Hanford Atomic Products Operation conducted by General Electric at Richland, Wash.

Better work, less waste with "Plus-4" Anodes

TYPICAL TREEING that occurs when using ordinary electrolytic tough pitch copper anodes.

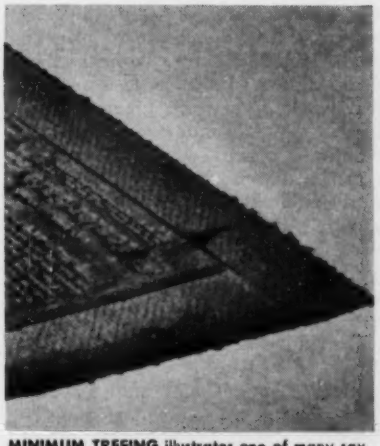

MINIMUM TREEING illustrates one of many savings with "Plus-4" (Phosphorized Copper) Anodes.

The Cincinnati Electrotype Co., of Cincinnati, Ohio, switched to Anaconda "Plus-4" Anodes and now tells its customers on its advertising blotters:

"We use PHOSPHORIZED COPPER because it has . . .

1. Finer, smoother *Grain Structure*. Retains the true value of modern type faces, dot formations of halftone, and tone value of multicolor engravings.
2. Over-all *Uniformity* of shell thickness, longer plate life, reduces replacement costs.
3. Greater *Tensile Strength*, maximum resistance to abrasive and chemical action of colored inks.
4. Sturdy *Backup* for Nickeltypes.
5. Better *Adhesion* for chrome."

From an operating standpoint, Cincinnati Electrotype is also enthusiastic. "Plus-4" Anodes cut waste from treeing (shown above), from solution correction and from sludge. With electrolytic tough pitch copper anodes, they used to clean sludge from tanks 3 times a year. Tanks filled exclusively with "Plus-4" Anodes will run a year or more without cleaning. They also report a time saving of 30% or more in a normal plating cycle when using "Plus-4" Anodes.

It will pay you to see for yourself how Anaconda "Plus-4" (Phosphorized Copper) Anodes can save you time and money—give you better work. Send the coupon today.

87141

"PLUS-4" ANODES

(Phosphorized Copper)

A product of

ANACONDA

Made by The American Brass Company

The American Brass Co., Waterbury 20, Conn.
In Canada: Anaconda American Brass Ltd., New Toronto, Ont.
Give me details on how I can get a test quantity of "Plus-4" Anodes sufficient to supply one tank.

NAME.....

COMPANY.....

ADDRESS.....

CITY.....ZONE....STATE.....

The expanded laboratory facilities, to be completed early this year, are being set up to study and solve corrosion problems in these growing new fields that are "more complex and different from those generally encountered in ordinary chemical corrosion."

While the enlargement applies mostly to the atomic energy and guided missile industries, the laboratory will also expand its activities in all other phases of corrosion research.

Book Review

Transport Processes in Applied Chemistry by R. C. L. Bosworth. Published by John Wiley & Sons, Inc., New York, 1956. X + 387 pages, $12.00.

This is an interesting and important book. It attempts to give a unifying treatment of all transport phenomena in the fields of interest to the chemist and chemical engineer. The significance of transport processes in chemical kinetics is illustrated by an exothermic catalytic reaction which offers difficulties when scaled up from a laboratory experiment. A scale up of the size of a cylindrical reactor by a factor of two increases the volume eightfold while the wall area available for heat transfer increases only fourfold with the result that the catalyst temperature may exceed optimum limits, thus leading to a loss of its activity. Dimensional analysis and the theory of models so successfully used in mechanics of solids and fluids have been found, according to the author, to be of limited value in chemical kinetics. Fundamentally, a proper understanding of the role of transport processes is absolutely necessary for the design of a large scale reactor from performance data of a small model. This fact has already been recognized, in general, by chemical engineers. Chemists, on the other hand, frequently fail to appreciate the role of many transfer processes in the over-all chemical reaction.

Following the chapter on the basic mechanisms of transport processes covering such concepts as mean free path, Brownian movements, stochastic processes, and diffusion processes with and without activation, a phenomenological description of potential differences, fields, fluxes, and flow circuitry follows. Special attention is given to coupled transport processes involving combinations of vector, tensor, and scalar fluxes. Transfer by molecular motion, by radiation, by convection, and by turbulent motion is dealt with in separate chapters. Following a review of irreversibility concepts, the so-called grand transport process, as a combination of small, individual transport processes, is discussed, and the generalized Bernouilli equation is used as an example of grand transport process.

An interes.ing discussion is devoted to chemical similarity (similitude), a problem so frequently ignored in scaling up chemical reactions. Dimensionless numbers are discussed only briefly. It would have been desirable to put more emphasis and devote more space to such a discussion.

Chapters on the efficiency of transport processes and their wider aspects complete the volume. A rather philosophical discussion on the driving force in industrial operations concludes with an interesting formula for a measure of the prosperity of a country as related to its power generation, efficiency of utilization, and population.

This book will, no doubt, cause a lot of discussion, and perhaps controversy. It certainly fills a definite need, and may be briefly described as a general treatise on the role of transport processes in chemistry.

Morris Eisenberg

Announcements from Publishers

Alkaline Storage Batteries: The Self-Discharge of the Positively Charged Nickel Oxide Electrode. Part 1—The Role of Water in the Process, A. L. Pitman and G. W. Work, Naval Research Lab., Oct. 1956. Report PB 121430,* 7 pages, 50 cents.

Solubility and the Products of Reaction between Iron and Water at 26°C and 300°C, V. J. Linnenbom, J. I. Hoover, and H. S. Dreyer, Naval Research Lab., Sept. 1956. Report PB 121409,* 15 pages, 50 cents.

Platinum Metals Review, a quarterly journal, is published by Johnson, Matthey & Co., Limited, Hatton Garden, London, E.C. 1, the sole refiners and distributors of platinum metals from the Rustenburg Platinum Mines in South Africa. Copies are obtainable from Johnson Matthey & Co., Inc., 608 Fifth Ave., New York, N. Y., or from J. Bishop & Co., Platinum Works, Malvern, Pa.

* Order from Office of Technical Services, U. S. Dept. of Commerce, Washington 25, D. C.

Advertisers' Index

American Brass Company 103C
Dow Chemical Company 90C
Enthone, Incorporated ..... Cover 4
Great Lakes Carbon Corporation ..... Cover 2
E. H. Sargent & Company 88C

Meetings of Other Organizations

April 7-12—American Chemical Society, National Meeting, Municipal Auditorium, Miami, Fla.

April 8-11—National Electrical Industries Show, 71st Regiment Armory, New York, N. Y.

April 22-24—Canadian Institute of Mining and Metallurgy, Annual General Meeting, Chateau Laurier Hotel, Ottawa, Ont., Canada.

April 24—Association of Consulting Chemists and Chemical Engineers, Banquet and Symposium, Belmont Plaza Hotel, New York, N. Y.

April 24-25—Armour Research Foundation, National Industrial Research Conference, Conrad Hilton Hotel, Chicago, Ill.

April 25-27—American Physical Society, Regional Meeting, Washington, D. C.

May 20-22—National Association of Corrosion Engineers, Northeast Regional Meeting, Syracuse, N. Y.

May 22-24—American Institute of Chemists, Annual Meeting, Sheraton-Mayflower Hotel, Akron, Ohio.

June 9-12—American Institute of Chemical Engineers, Regional Meeting, Olympic Hotel, Seattle, Wash.

June 17-21—American Society for Engineering Education, Annual Meeting, Cornell University, Ithaca, N. Y.

June 20-22—American Physical Society, Regional Meeting, Notre Dame, Ind.